FACULTY 3 – MATHEMATICS AND COMPUTER SCIENCE

MONOGRAPH DISSERTATION

DESIGN ENHANCEMENTS AND CONTROL OF A LOWER EXTREMITY EXOSKELETON

IBRAHIM TIJJANI

Supervisors:

Reviewer 1: Prof. Dr. Dr. h.c. Frank Kirchner
Faculty 3 – Mathematics and Computer Science
Universität Bremen

Reviewer 2: Asst. Prof. Dr. Shivesh Kumar
Department of Mechanics & Maritime Sciences
Chalmers University of Technology, Gothenburg, Sweden

Date of Submission: August 27, 2024

Date of Defense: September 23, 2024

Printed with the support of the German Academic Exchange Service (DAAD).

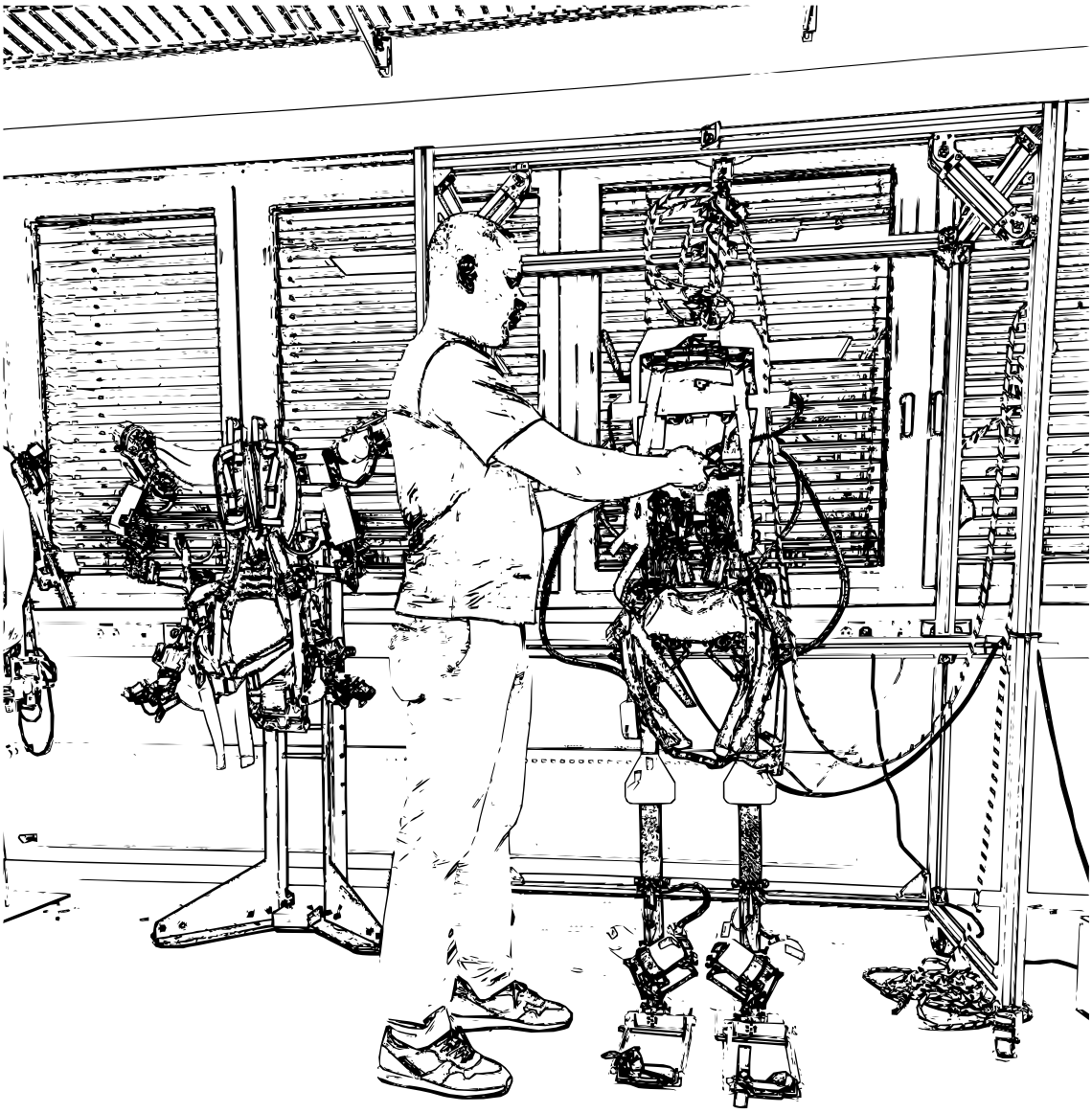

Design Enhancements and Control of a Lower Extremity Exoskeleton

von Ibrahim Tijjani

Dissertation

zur Erlangung des Grades eines Doktors der
Ingenieurwissenschaften
- Dr.-Ing. -

Vorgelegt im Fachbereich 3 (Mathematik & Informatik)
der Universität Bremen
im August 2024

Datum des Promotionskolloquiums: September 23, 2024

Gutachter: Prof. Dr. Dr. h.c. Frank Kirchner (Universität Bremen)
Asst. Prof. Dr. Shivesh Kumar (Chalmers University of Technology)

ABSTRACT

Exoskeleton robots, powered by electric, pneumatic, or hydraulic actuators, support human bones and muscles externally, enhancing movement and strength. They are indispensable in fields such as medical, industrial, military, and safety, aiding both healthy and disabled individuals. Full-body exoskeletons support the entire body, while lower-body exoskeletons target the hip, knee, and ankle joints to assist with locomotion and reduce physical stress. The goal of enabling independent walking with exoskeletons has significant potential for neurological dysfunction rehabilitation and could improve the quality of life of people with disabilities. Over the last two decades, exoskeleton research and development have grown substantially, and some prototypes are now commercially available. However, significant challenges in design, modeling, and control persist. Some of these challenges include managing complex kinematics and dynamics, dealing with intricate geometries, addressing holonomic loop constraints, and overcoming workspace limitations inherent in parallel or series-parallel hybrid mechanisms. The robotics research community employs model-based and model-free control methods to enhance performance, aiming to develop robust, safe, and reliable exoskeletons for assistive, rehabilitative, and power augmentation purposes. Despite these efforts, achieving the desired levels of adaptability, user comfort, and seamless integration remains an ongoing challenge, requiring continuous innovation and interdisciplinary collaboration.

This thesis addresses key challenges inherent in the Almost Spherical Parallel Mechanism (ASPM) device, which are crucial to exoskeleton research and development. The ASPM is a 3-DOF module representing the ankle and hip joint modules of the Recupera-Reha full-body exoskeleton. It has three principal movements: dorsiflexion-plantarflexion (DF-PF), eversion-inversion (EV-IN), and adduction-abduction (AD-AB). However, the joint modules are faced with workspace limitations due to inadequate alignment in the exoskeleton leg. We address these problems using the rotative inverse geometric method to align the principal human joint axes with the axes that optimize the ASPM device's range of motion in the exoskeleton leg. The study demonstrated that rotating the mechanism along the AD-AB yaw axis and selecting appropriate ball and socket joints for the actuators can significantly enhance the usable workspace for the exoskeleton wearer. Furthermore, we present advancements in the functionality of the Recupera-Reha lower extremity exoskeleton robot, which features a series-parallel hybrid design with multiple kinematic loops, resulting in 148 degrees of freedom for all the spanning tree joints and 102 independent loop closure constraints. These complexities pose significant challenges for modeling and control. We tackled these challenges by utilizing the Hybrid Robot Dynamic (HyRoDyn) software framework to address the kinematic loop constraints. We then employed an optimal control approach to generate feasible trajectories for movements such as sitting, standing, and static walking, which are tested on the exoskeleton robot. To generate initial trajectories, the method efficiently solves the optimal control problem using a serial abstraction of the model. We then use the full series-parallel hybrid model, which accounts for all kinematic loop constraints, to generate the final actuator commands. Finally, experimental results confirm

the effectiveness of this approach in achieving the desired motions for the exoskeleton and advancing its functional capabilities.

ZUSAMMENFASSUNG

Exoskelett-Roboter, die durch elektrische, pneumatische oder hydraulische Aktuatoren angetrieben werden, unterstützen die menschlichen Knochen und Muskeln von außen und verbessern so die Bewegungsfähigkeit und Kraft. Sie sind in Bereichen wie Medizin, Industrie, Militär und Sicherheit unverzichtbar und helfen sowohl gesunden als auch behinderten Menschen. Ganzkörperexoskelette unterstützen den gesamten Körper, während Exoskelette für den Unterkörper auf die Hüft-, Knie- und Fußgelenke abzielen, um die Fortbewegung zu erleichtern und die körperliche Belastung zu verringern. Das Ziel, mit Exoskeletten unabhängiges Gehen zu ermöglichen, birgt ein erhebliches Potenzial für die Rehabilitation neurologischer Funktionsstörungen und könnte die Lebensqualität von Menschen mit Behinderungen verbessern. In den letzten zwei Jahrzehnten hat die Forschung und Entwicklung von Exoskeletten erheblich zugenommen, und einige Prototypen sind inzwischen im Handel erhältlich. Dennoch gibt es nach wie vor erhebliche Herausforderungen bei Design, Modellierung und Steuerung. Zu diesen Herausforderungen gehören die Beherrschung komplexer Kinematik und Dynamik, die Bewältigung komplizierter Geometrien, die Berücksichtigung holonomer Schleifen und die Überwindung von Arbeitsraumbeschränkungen, die mit parallelen oder seriell-parallelen Hybridmechanismen einhergehen. Die Robotik-Forschungsgemeinschaft setzt modellbasierte und modellfreie Steuerungsmethoden ein, um die Leistung zu verbessern und robuste, sichere und zuverlässige Exoskelette für Hilfs- und Rehabilitationszwecke sowie zur Leistungssteigerung zu entwickeln. Trotz dieser Bemühungen bleibt das Erreichen des gewünschten Niveaus der Anpassungsfähigkeit, des Benutzerkomforts und der nahtlosen Integration eine ständige Herausforderung, die kontinuierliche Innovation und interdisziplinäre Zusammenarbeit erfordert.

Diese Arbeit befasst sich mit den zentralen Herausforderungen des Almost Spherical Parallel Mechanism (ASPM), die für die Forschung und Entwicklung von Exoskeletten entscheidend sind. Der ASPM ist ein 3-DOF-Modul, das die Knöchel- und Hüftgelenksmodule des Recupera-Reha-Ganzkörperexoskeletts darstellt. Es verfügt über drei Hauptbewegungen: Dorsalflexion-Plantarflexion (DF-PF), Eversion-Inversion (EV-IN) und Adduktion-Abduktion (AD-AB). Allerdings stoßen die Gelenkmodule aufgrund der unzureichenden Ausrichtung des Exoskelettbeins an ihre Grenzen. Wir lösen diese Probleme mit Hilfe der rotativen inversen geometrischen Methode, um die wichtigsten menschlichen Gelenkachsen mit den Achsen auszurichten, die den Bewegungsbereich des ASPM-Geräts im Exoskelettbein optimieren. Die Studie hat gezeigt, dass die Drehung des Mechanismus entlang der AD-AB-Gierachse und die Auswahl geeigneter Kugelgelenke für die Aktuatoren den nutzbaren Arbeitsbereich für den Exoskelett-Träger erheblich erweitern kann. Darüber hinaus präsentieren wir Fortschritte in der Funktionalität des Recupera-Reha-Roboters mit Exoskelett für die unteren Extremitäten, der sich

durch ein seriell-paralleles Hybriddesign mit mehreren kinematischen Schleifen auszeichnet, was zu 148 Freiheitsgraden für alle überspannenden Baumgelenke und 102 unabhängigen Schleifenschließungsbeschränkungen führt. Diese Komplexität stellt eine große Herausforderung für die Modellierung und Steuerung dar. Wir gingen diese Herausforderungen an, indem wir das Software-Framework Hybrid Robot Dynamic (HyRoDyn) einsetzten, um die kinematischen Schleifenbeschränkungen zu berücksichtigen. Anschließend haben wir einen Ansatz zur optimalen Steuerung verwendet, um machbare Trajektorien für Bewegungen wie Sitzen, Stehen und statisches Gehen zu erzeugen, die auf dem Exoskelett-Roboter getestet wurden. Zur Erzeugung von Anfangstrajektorien löst die Methode das Problem der optimalen Steuerung effizient mit Hilfe einer seriellen Abstraktion des Modells. Anschließend verwenden wir das vollständige seriell-parallele Hybridmodell, das alle kinematischen Schleifenbeschränkungen berücksichtigt, um die endgültigen Aktuatorbefehle zu erzeugen. Schließlich bestätigen experimentelle Ergebnisse die Wirksamkeit dieses Ansatzes bei der Erzielung der gewünschten Bewegungen für das Exoskelett und der Verbesserung seiner funktionellen Fähigkeiten.

ACKNOWLEDGMENTS

The successful completion of this doctoral thesis is attributed to the invaluable contributions of numerous individuals who have guided, taught, and supported me. I would like to express my sincere gratitude to everyone who has encouraged and motivated me throughout this journey of pursuing my PhD.

First and foremost, I am profoundly grateful to my first supervisor, Professor Dr. Frank Kirchner, for granting me this golden opportunity and for believing in my potential, allowing me to join the Robotics Innovation Center at DFKI Bremen—a place I have come to consider my second home. Reflecting on our first meeting, he asked me, "What can you do to improve the quality of life of one physically disabled person in Nigeria?" This was an extremely rare motivation that kept me going throughout my PhD journey. His invaluable guidance, encouragement, and unwavering support throughout the course of my research. The insightful feedback received during the PhD retreats have been instrumental in shaping my reasoning and professional growth. I would also like to thank the Nigerian-Petroleum Technology Development Fund (PTDF) and the German Academic Exchange Service (DAAD) for their support and funding the first three years of this journey.

My deepest and heartfelt appreciation goes to Assistant Professor Shivesh Kumar who started as my first mentor and is now my second supervisor. In our first meeting with him in the office we shared, I addressed him as Dr. Shivesh, but he insisted I call him Shivesh. Coming from an electrical engineering background, he quickly grasped my capabilities in robotics within a few hours. He said, "Ibrahim, you need to start from the basics of robotics, but I will be your guide." Indeed, he has been a guide. He consistently assigned me tasks and provided constructive feedback, offering unconditional support and guidance throughout my research journey. Thank you Dr. Nina Hoyer for your moral support, advice and motivation in my early research stage. Special thanks also go to my second mentor, Dr. Melya Boukheddimi. The Recupera-Reha exoskeleton was my nightmare until she said, "We will make the robot walk," and indeed, it walked. When I encountered difficulties, Melya was always prompt in her responses. To me, she is never sleeping all day, offering steadfast guidance, encouragement, and support that continues to this day.

I am indebted to many DFKI Wissenschaftliche Mitarbeiter, including Martin Mallwitz, Rohit Kumar, Ivan Bergonzani, Tobias Stark, Daniel Pizzutilo, Pierre Willenbrock, Vinzenz Bargsten, Heiner Peters, Sankaranarayanan Natarajan, Mahdi Javadi, Dirk Heimann, Amrita Suresh, Haider Khan Lodhi, Dr. Mehmed Yüksel, the members of the Intelligent Healthcare System (IHS) team, the entire staff and students of the Mechanical Workshop and Electronics Lab, the Software Backbone team, ISG team and my fellow researchers Christoph Stoeffler, Felix Wiebe, Mihaela Popescu, Sara Khan, Shubham Vyas, Bingbin Yu, for their fellowship, stimulating discussions, and support have been invaluable in creating a nurturing academic community.

In October 2023, I transitioned from a guest researcher to a scientific researcher and employee of DFKI under the lead of Dr. Dennis Mronga, whose charismatic and transformational leadership in the M-ROCK project within the Mechanics and Control team was instrumental in helping me achieve my set goals.

I am grateful to the DFKI for providing the necessary resources, facilities, and environment conducive to research and learning. Special thanks to Dr. Sirko Staube, Frau Petra Gerdes, Frau Verena Menge, and Dr. Daniel Kühn for their administrative support and assistance at the outset and during my PhD journey.

My heartfelt gratitude goes to my parents and siblings for their unwavering support. And to my lovely wife Khadija Abdulazeez, I am sincerely grateful for your unconditional love, unending support, patience, and understanding throughout this journey. Lastly, I dedicate this thesis to my wife and our amazing children Faiza and Fadil.

DECLARATION

I affirm that this thesis is the result of my own original work. Regarding the conference paper where i am the sole author, i independently conducted the research. In the other publications where i am the first author, i played a crucial role in literature review, conceptualization, modeling and control, simulation and experimentation, and the final formalization of results. In the published book chapter, I also made a significant impact by modeling the Recupera-Reha full-body exoskeleton.

Ibrahim Tijjani

"We are facinated with robots because they are reflections of ourselves"

— Ken Goldberg

Contents

1 General Introduction 1
1.1 Introduction . . . 1
1.2 Motivation . . . 1
1.3 Problem Statement . . . 3
1.4 Goal of this Thesis . . . 5
1.5 Thesis Contributions . . . 5
1.6 Organization . . . 6
1.7 Related Publications . . . 8
2 State of the Art 9
2.1 Introduction . . . 9
2.2 History of Bipedal Walking Exoskeleton Robots . . . 9
2.2.1 Challenges in Bipedal Walking Exoskeleton Robots . . . 11
2.3 Classification of Wearable LEE's on Application Domain . . . 12
2.3.1 Medical Application of LEE . . . 12
2.3.2 Industrial Application of LEE . . . 16
2.3.3 Military Application of LEE . . . 18
2.3.4 Distinctions in the Exoskeleton Classifications . . . 19
2.4 Design Concept for Lower Extremity Exoskeletons . . . 23
2.4.1 Human and Exoskeleton Lower Extremity Joints . . . 23
2.4.2 Actuator Design for Exoskeleton Robots . . . 29
2.5 Modeling and Control of Exoskeleton Robots . . . 30
2.5.1 Modeling . . . 30
2.5.2 Control Methods . . . 31
2.6 Discussion and Future Research Directions . . . 35
2.6.1 Discussion . . . 35
2.6.2 Future Research Directions . . . 37
2.7 Conclusion . . . 39
3 Design Enhancement of the ASPM 40
3.1 Introduction . . . 40
3.2 Problem Description . . . 41
3.3 Kinematic Analysis of the Ankle and Hip Joint Modules . . . 42
3.4 Optimal Placement for the Hip and Ankle Mechanisms in the Leg . . . 45
3.4.1 Parameterization Procedure . . . 45
3.5 Preliminary Simulation Result . . . 47
3.6 Design Modification of the Recupera-Reha Foot Base . . . 53

3.7 Discussion . . . 54
3.8 Conclusion . . . 54
4 Modeling and Control Strategy 55
4.1 Introduction . . . 55
4.1.1 Background of the Study . . . 55
4.1.2 Related Works . . . 56
4.2 Modeling of Recupera-Reha Exoskeleton Robot . . . 57
4.2.1 Modeling of Closed Loops as Explicit Constraints . . . 58
4.2.2 System Description . . . 58
4.2.3 Tree Abstraction Model . . . 60
4.3 Motion Generation Defined As An Optimization Problem . . . 61
4.3.1 Whole-body dynamics under constraints . . . 61
4.3.2 Optimal Control Problem Definition . . . 62
4.3.3 Desired Motions Formulated As Cost Models . . . 63
4.4 Discussion . . . 64
4.5 Conclusion . . . 65
5 Results and Application Scenario 66
5.1 Introduction . . . 66
5.2 Low-level Control Architecture . . . 66
5.2.1 Integrating the Low-level Architecture with a Software Framework . . . 67
5.3 Simulation and Experimental Pipeline . . . 69
5.4 Results . . . 71
5.4.1 Leg joints ROM verification . . . 72
5.4.2 Sitting and standing motion . . . 74
5.4.3 Static walk motion . . . 77
5.5 Application in Human-Robot Interaction . . . 79
5.5.1 Experiments with a human wearing the robot for sitting motion . . . 79
5.5.2 Experiments with a human wearing the exoskeleton robot for static walking 81
5.5.3 Explicit feedback assessments from human interaction with the Recupera-Reha exoskeleton . . . 84
5.6 Discussion . . . 84
5.7 Conclusion . . . 85
6 Conclusion and Outlook 86
6.1 Summary of Contributions . . . 86
6.2 Outlook . . . 87

I Appendix
A Kinematic and Dynamic Analysis of a 2R1P Robotic Leg 90
A.1 Spherical Manipulator and its Topological Scheme . . . 90
A.1.1 The 2R1P Robotic Leg . . . 91
A.2 Geometric model formulation for a 2R1P robotic leg . . . 91
A.2.1 Velocity Analysis . . . 93

A.2.2 Acceleration Analysis 94
A.3 Dynamic Model for a 2R1P Robotic Leg 95
B Symbolic Computation of 2R1P Robotic Leg using Matlab Snipet 98
List of Figures 105
List of Tables 107
List of Acronyms 108

Bibliography 111

1

GENERAL INTRODUCTION

"The evolutionary journey has equipped humans with remarkable adaptability, but it also accounts for our susceptibility to instability, as we balance on the delicate edge of our bipedal nature."

— Inspired by evolutionary theory

1.1 INTRODUCTION

This chapter serves as the general introduction to the thesis and fulfills three key purposes: 1) It explains the motivation behind the research and demonstrates its significance in addressing challenges related to exoskeleton robots and improving human locomotion; 2) it outlines the primary goal of the thesis and contextualizes it within the broader field; and 3) it provides a brief overview of the adopted methodology and highlights the main contributions. Additionally, it outlines the structure of the thesis, offering a summary of each chapter to assist readers in navigating the document.

1.2 MOTIVATION

Individuals with musculoskeletal disabilities affecting their lower extremities, primarily caused by aging, strenuous jobs, road accidents, physical exercise, or neurological conditions such as stroke, spinal cord injury (SCI), and osteoarthritis (OA), frequently experience mobility issues that diminish their quality of life. The World Health Organization (WHO) reports that 16% of the global population experiences significant disabilities, including mobility impairments, and expects this figure to increase due to the increasing prevalence of non-communicable diseases and an aging population [64, 152]. Stroke, for example, is a leading cause of disability in the United States, particularly among those aged 65 and older, often resulting in long-term or permanent impairment [63]. Experts estimate that the annual incidence of SCI will be between 40 and 80 cases per million people. Ambulatory support devices such as crutches, canes, walkers, mobility carts, and wheelchairs (see Figure 1.1) can greatly enhance the self-esteem, confidence, and independence of individuals with disabilities. These devices help them gain control over their lives and reduce reliance on others, which is vital for their psychological well-being. Nevertheless, these individuals most often still require assistance from caregivers and therapists to perform daily activities. While crutches and walkers help maintain physical activity, which is beneficial for overall health, prolonged crutches can cause skin abrasions and additional spinal pain due to the constant bending of the vertebral column.

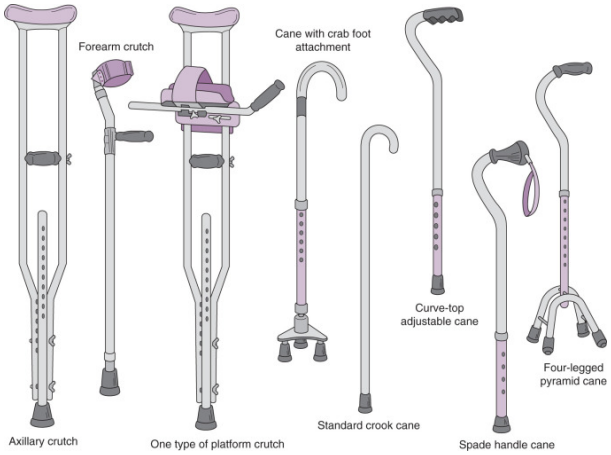

(a) Crutches and cane types [42]

(b) Walker

(c) Recupera-reha wheelchair: (credit: DFKI GmbH)

Figure 1.1: Various mobility aids for individuals with mobility disorder

Similarly, extended periods of sitting in a wheelchair can lead to various health complications [119, 121, 167]. Recent advancements in assistive and rehabilitative technology, particularly wearable exoskeleton robots, have significantly improved mobility and physical support for people with disabilities. These mobility-supporting devices offer physical comfort and safety, enhance social interactions and psychological well-being, and promote long-term health benefits. These devices can significantly improve the quality of life for individuals with lower-limb disabilities by improving mobility and independence. Using exoskeleton robots and adjustable orthotic devices for the lower limbs is emerging as a promising solution for managing these health conditions.

The Lower Extremity Exoskeleton (LEE) is an orthotic device that achieves fixation to the lower limbs, providing artificial support to one or more of the three main joints in the human

leg: the hip, knee, and ankle. Its primary purpose is to aid in gait rehabilitation by enhancing locomotion strength, augmenting power for industrial and military applications, and ensuring safety in all ramifications. Exoskeleton robots for bipedal walking are designed to mimic the biological structure of the human gait or to be strapped to the body to support the limb joints. Modern exoskeleton robots, used in various application domains, come in either wearable or platform-based designs. Wearable exoskeletons, as shown in (Figure 1.2a and Figure 1.2b), are robotic devices strapped to the human body, providing active or passive support to the lower limbs. These devices are widely used in industrial logistics, clinical gait training, military operations, and other fields. A platform-based exoskeleton, as depicted in Figure 1.2c , is placed on level ground surface and to facilitate gait training. They are used primarily for rehabilitation or exercise on a treadmill.

(a) ReWalk^{TM} Personal 6.0: (copyright: ReWalk Robotics GmbH)

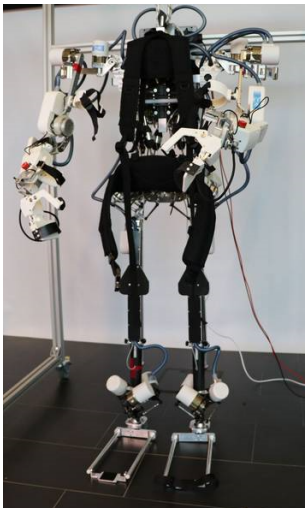

(b) Recupera-reha: (credit: DFKI GmbH)

(c) ReoAmbulator (copyright: Motorika Ltd., USA)

Figure 1.2: Wearable and platform-based exoskeleton

1.3 PROBLEM STATEMENT

The Recupera-Reha is a full-body exoskeleton with a modular lower extremity unit that is primarily designed to support upper body weight during robot-assisted upper-limb rehabilitation from neurological conditions. While it provides support for the wearer during sitting and standing, it has not been adapted for walking due to several significant challenges. Overcoming the challenges are essential for enhancing the effectiveness and user acceptance of the LEE. This subsection identifies the specific problems and limitations in the design, control, and application of the Recupera-Reha LEE depicted in Figure 1.2b, emphasizing areas where further research and development are necessary. The challenges and limitations are detailed as follows:

- `Ergonomic Design`: Several key issues impact the effectiveness of the Recupera-Reha exoskeleton's ergonomic design for natural walking motions. The exoskeleton's knee joint functions as a linear translation motion, devoid of a suitable fixation that would allow it to seamlessly connect with the human knee. This design choice fails to replicate the natural bending and flexing of the knee during movement. Similarly, the footplate is rigid and lacks a flexible connection to the ankle, allowing only plantar flexion (toe-down motion) but not accommodating natural dorsiflexion (toe-up motion). This rigidity hinders the natural walking gait, making movement less intuitive and more mechanical from a mechanical point of view. Additionally, the foot base of the exoskeleton has a small surface area, which acts like a point of contact with the ground. In natural walking, humans use the middle of the foot (metatarsus) as a pivot point, but in the current design, the ankle joint serves as the pivot. This limited pivoting action can reduce stability and make walking feel unnatural. Addressing these ergonomic issues is crucial for improving the user experience and ensuring that the exoskeleton can support natural and stable walking motions.

  The open question is whether to modify and adapt the existing design or to build new knee joint module and foot base unit for the exoskeleton. The recommended approach involves specific modifications: adding straps to the knee joint to ensure a secure connection with the human body; replacing the foot base with a wider surface area to create a support polygon at the four edges or separating the foot plate into two pieces connected by a hinge joint to enable greater flexibility in the flexion angle motion. These enhancements aim to improve overall stability but will not replicate a more natural walking motion due to the design structure of the knee joint.

- `Optimal Placement of the Ankle and Hip Joint Modules in the Leg`: The complex design structure makes it challenging to find an optimum mounting configuration for the ankle and hip joint modules that is properly aligned with the human joint axis complex. So, it's important to get these modules aligned properly with the axes of human joints. To test and improve the exoskeleton's walking performance, a full kinematic analysis of these modules is necessary.

- `Methodology for Exoskeleton Modeling and Motion Control`: Since the Recupera-Reha lower body exoskeleton was initially not designed to support walking, its complete lower body model was not integrated into the in-house software database that stores analytical solutions for complex modular sub-mechanisms with multiple closed loops. Consequently, it is necessary to resolve the kinematic loop constraints for the sub-mechanisms not yet in the database and integrate them accordingly. As a result, a control method for generating desired motions, such as static walking, has not been implemented before. To establish an effective control method for the exoskeleton's static walking motion, a comprehensive understanding of the robot's model is essential, including knowledge of its actuator constraints such as joint limits, velocity, and torque limits. This understanding is crucial for identifying the appropriate control algorithm to use.

- `Application in Human-Robot Interaction`: Before implementing human-robot interaction, it is necessary to confirm the robot's robustness. To establish effective

robot interaction with a human in the loop, a thorough understanding of the robot's capabilities is essential, along with insights into its sensor integration, communication protocols, and the robot's adaptive response. This understanding is crucial for integrating appropriate interaction methods.

1.4 GOAL OF THIS THESIS

The goal of this thesis is to advance the functionality of the Recupera-Reha LEE by enhancing the design as necessary, integrating its complete model, and implementing an optimal control (OC) method to generate feasible motions for sitting, standing, and static walking. To accomplish this, two sub-goals have been outlined.

1. Perform a thorough kinematic and dynamic analysis of the almost spherical parallel mechanism (ASPM) representing the hip and ankle joint modules. Optimize the placement of the ASPM in the leg of the exoskeleton to improve the working range for key movements. Use the Hybrid Robot Dynamics (HyRoDyn) software framework to resolve all closed loops inherent in the model and ensure comprehensive model accuracy and functionality using a hybrid control approach.

2. Develop an optimal control problem (OCP) using the Differential Dynamics Programming (DDP) method to generate feasible motion trajectories for sitting, standing, and static walking. These motion trajectories are tailored to suit the capabilities of the Recupera-Reha exoskeleton, aiming to maximize its operational effectiveness.

1.5 THESIS CONTRIBUTIONS

This thesis makes significant contributions to the field of exoskeleton robots, particularly focusing on the lower extremity. We conducted a thorough survey [201] in Chapter 2 to gain a comprehensive understanding of the current state of exoskeleton technology. This survey examines the challenges and limitations in the design and control of existing LEEs and suggests pathways for future development and improvement. The survey reveals that most reported exoskeletons emphasize kinematics and dynamics modeling, with a strong focus on lightweight actuation and sensor technology. These efforts address concerns about limited workspace and misalignment with the human joint complex. In terms of control, the primary challenge is achieving stability during walking motions without the need for additional supporting devices. This thesis's contributions are summarized below:

- This study's first significant contribution is the enhancement of the ankle and hip joint modules positioning and orientation within the Recupera-Reha exoskeleton leg. The kinematics of the ASPMs are evaluated by exploiting the rotative inverse geometric method (*RIGM*) and adjusting motor constraints on the hardware side. This approach expands the mechanism's workspace for principal movements such as the dorsiflexion-plantarflexion (DF-PF), eversion-inversion (EV-IN), and adduction-abduction (AD-AB) of

the hip and ankle joints to accommodate a broader range of motion. This evaluation enables extensive movement and alignment with the leg joint complex, laying the groundwork for advanced dynamic modeling. Furthermore, this evaluation demonstrates its potential for integrating functional rehabilitation exercises.

- The second significant contribution to this thesis is advancing the capabilities of the Recupera-Reha LEE, which is primarily designed to support upper body weight during upper-limb rehabilitation. It demonstrates a successful formulation and execution of an OCP for sitting, standing, and static walking using a DDP-based method. The study also highlights the efficient handling of loop closure constraints with the HyRoDyn software framework, which includes 102 constraints, making it possible to exploit the full capabilities of the complex series-parallel hybrid exoskeleton.
- As an outlook, the thesis explored the possibility of partially integrating human-robot interaction, which would allow human users to provide explicit feedback by rating or assessing different speed limits of the generated trajectories during the transition from standing to sitting while wearing the exoskeleton. However, the thesis does not include the results of this exploration because the data analysis is still ongoing.

1.6 ORGANIZATION

This thesis is structured into seven chapters. Figure 1.3 provides a graphical overview to guide the reader through the following chapters.

- **Chapter 2** presents a survey on the design and control of LEE. This survey provides a comprehensive overview of the latest developments in the design and control of LEEs. The survey offers an in-depth exploration of current advancements in the design and control of LEE. It includes a historical analysis of exoskeleton robotics, an examination of challenges specific to exoskeleton walking, and a categorization of exoskeletons based on diverse application areas. Furthermore, it focuses on actuator design concepts, modeling techniques, and control strategies, concluding with insights into potential future research avenues.
- **Chapter 3** presents the kinematic analysis of the ASPM (hip and ankle joint) modules with the aim of determining the optimal placement of the mechanisms in the Recupera-Reha exoskeleton leg and improving its workspace for principal joint movements.
- **Chapter 4** demonstrates the implementation of an OC approach using a DDP-based method to generate feasible trajectories for sitting, standing, and walking. It also effectively utilizes the HyRoDyn software framework to explore numerical-analytical hybrid solutions for resolving closed loop formations, and provides a mapping between independent joint space and actuator joint space.

- **Chapter 5** presents simulation and experimental results for the Recupera-Reha exoskeleton's range of motion joint tracking, sitting, standing, and static walking motions, highlighting the enhanced capabilities of the exoskeleton and its potential for assistive and rehabilitation applications.
- **Chapter 6** concludes by summarizing this thesis and outlining future research directions.

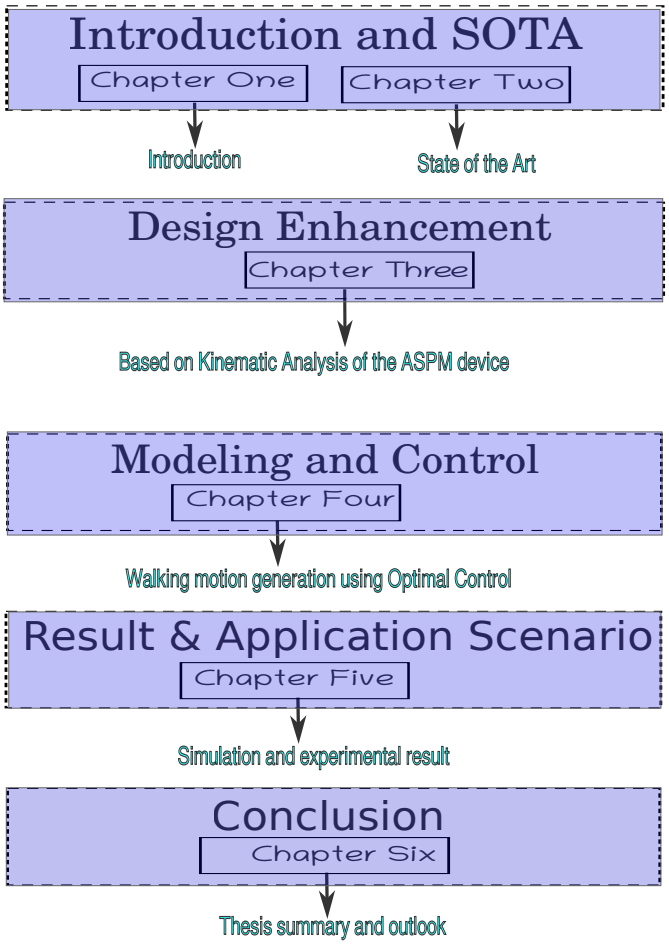

(a)

Figure 1.3: Thesis Organization

1.7 RELATED PUBLICATIONS

Tijjani, I., Kumar, S. and Boukheddimi, M. (2022). "A Survey on Design and Control of Lower Extremity Exoskeletons for Bipedal Walking" Applied Sciences 12, no. 5: 2395.

Tijjani, I. (2022). Finding Optimal Placement of the Almost Spherical Parallel Mechanism in the Recupera-Reha Lower Extremity Exoskeleton for Enhanced Workspace. In: Müller, A., Brandstötter, M. (eds) Advances in Service and Industrial Robotics. RAAD 2022. Mechanisms and Machine Science, vol 120. Springer, Cham.

Tijjani, I., Kumar, R. and Boukheddimi, M. and Trampler, M. and Kumar, S. and Kirchner, F. (2024). Sitting, Standing and Walking Control of the Series-Parallel Hybrid Recupera-Reha Exoskeleton. The 2024 IEEE-RAS International Conference on Humanoid Robots, Nancy, France, November 22-24

Mallwitz, M. and Maurus, M. and Kumar, S. and Trampler, M. and Tabie, M. and Wöhrle, H. and Kirchner, A. E. and Wiedemann, H. and Peters, H. and Schulz, C. and Chari, K. and **Tijjani, I.** and Kirchner, F. (2024). Recupera Exoskeletons, In: Biologically Inspired Series-Parallel Hybrid Robots: Design, Analysis, and Control. Elservier 2024

2

STATE OF THE ART

"It is comparatively easy to make computers exhibit adult level performance on intelligence tests or playing checkers, and difficult or impossible to give them the skills of a one-year-old when it comes to perception and mobility."

— Moravec Hans

Tijjani, I., Kumar, S. and Boukheddimi, M. (2022). "A Survey on Design and Control of Lower Extremity Exoskeletons for Bipedal Walking". Applied Sciences 12, no. 5: 2395.

2.1 INTRODUCTION

This chapter presents the state of the art in the design and control of exoskeleton robots as documented in [201]. The chapter is organized as follows: Section 2.2 delves into the history of bipedal walking robots and exoskeletons, emphasizing the challenging aspects researchers must overcome to achieve better bipedal locomotion. Section 2.3 categorizes wearable exoskeleton robots across various application domains and offers overviews of their sub-categories. Section 2.4 elaborates on the design concepts and technical features of the highlighted lower extremity exoskeletons, drawing connections to the biomechanical structure of human lower extremity joints. Section 2.5 focuses on the modeling tools and control methods utilized for exoskeleton robot models, highlighting the strengths and weaknesses of various control strategies. Section 2.6 provides a summary of existing design and control methods for biped walking exoskeletons and proposes a future research direction aimed at a paradigm shift.

2.2 HISTORY OF BIPEDAL WALKING EXOSKELETON ROBOTS

In the research history of bipedal walking robots with two telescopic legs, way back in 1960, there were designs, but these were limited to two dimensions (2D) [206]. In 1992, the Massachusetts Institute of Technology (MIT) laboratory developed and controlled a three-dimensional (3D) biped robot walking and running on grass and flat surfaces, performing somersaults [158]. Subsequently, a more complex design called the Meltran V [78] bears an interesting similarity to the 3D biped robot with a prismatic joint at the knee. The M2V2 [162] is also a 3D bipedal walking robot designed to walk on rough terrain. Recently, Oregon State University unveiled the CASSIE robot [184], a bipedal walking robot that could traverse 5 km of outdoor terrain in less than an hour. In an effort to replicate the anatomical structures and locomotion of humans, early researchers devised bipedal walking robots. We refer to these modernized bipedal

walking robots as "humanoid robots." They are designed either for entertainment, logistics, collaborative maintenance in the industries, or teleoperation [46, 72, 118, 124, 154, 188]. To this end, researchers have drawn inspiration from 2D designs, 3D bipedal robots, and humanoid robots to design exoskeleton robots for bipedal walking. The development of exoskeleton robots for bipedal walking began in the second half of the 20th century. In 1965, General Electric initiated the development of Hardiman [143], a giant full-body exoskeleton intended to lift heavy objects. However, this endeavor ultimately proved unsuccessful because the exoskeleton exhibited uncontrolled motions when powered on, posing a risk of injury to its human wearer. The first exoskeleton for gait assistance was developed towards the end of the 1960s and early 1970s at Mihajlo Pupin Institute Serbia [141] and similarly at the University of Wisconsin-Madison USA [180], respectively, but due to their technical limitations, absence of clinical support, and lack of experience and knowledge, it took several decades until the technology became mature and available to the market community.

Robots that mimic human walking patterns inspire people in the 21st century. Consequently, exoskeleton designs have experienced a progressive evolution, garnering considerable market interest. Among these designs, BLEEX is one [203]. The United States (US) Army designed BLEEX, the first functional, energetically autonomous exoskeleton. The XOS 2 exoskeleton [168], a second generation robotics suit designed by Raytheon and unveiled in 2008, was used for a military operation to support locomotion and the wearer's backpack. In medical applications, there have been quite a few exciting designs. Lokomat [30] was released in 2001 for gait rehabilitation on a treadmill. A leading-edge design in cybernetics evolved in 2007 with the development of the robot suit HAL (hybrid assistive limb), used to improve support for human locomotion ability, as reported in [175]. ReWalk Company develops powered solutions that provide gait training and mobility support to lower limb disability patients with crutches. In 2012, the safety and tolerance of the ReWalk exoskeleton on people with SCI were evaluated in [221], with prospects channeled towards walking disabilities. Walk Again [207] is a consortium project. Researchers from the consortium tested their first robotic exoskeleton using brain-machine interaction. Delft University of Technology and the University of Twente (the Netherlands) recently developed the Symbitron exoskeleton, a modular lower limb exoskeleton. Patients with partial and complete SCI test the Symbitron exoskeleton's control effect to assess its adaptation to velocity changes during walking. Additionally, the exoskeleton can be adjusted to accommodate a broad range of disability levels [136]. REX Bionics is a New Zealand-based exoskeleton company. The REX clinical analysis evaluation for Food and Drug Administration (FDA) approval in the United States was carried out in 2016 on two variant designs of the exoskeleton: one intended for clinical use and the other for personal use [18]. In 2017, the German Research Center for Artificial Intelligence (DFKI) at its Robotics Innovation Center Bremen developed the Recupera-Reha [101] full-body exoskeleton. It is a modular and self-supporting system for the robot-assisted upper-body rehabilitation of neurological diseases. In 2018, Wandercraft unveiled ATALANTE [69], their first hands-free lower limb exoskeleton, giving individuals with paralysis the ability to walk independently without crutches or additional support. The enhanced Atalante X prototype obtained FDA clearance in December 2023, allowing its use by individuals with SCI from levels T5 to L5. This approval builds upon its previous clearance

for stroke patients, distinguishing it as one of the few FDA-cleared exoskeletons and the only one with a powered ankle mechanism replicating natural human gait. Exoskeleton development for industrial purposes has also advanced over the last decade, in contrast to the advancements observed in medical applications. The Guardian XO Alpha [176], a powered exoskeleton primarily utilized in industrial logistics and other physically demanding tasks, was introduced in 2019. In 2017, Ekso Bionics launched the evolution of EksoEvo, EksoVest, and EksoZeroG [43]. The EksoVest, a strapped upper-body suit, enhances power and relieves pain during industrially motivated tasks. The latter variant is the EksoZeroG, and it helps construction workers in the automobile industry work faster and reduce fatigue while lifting and working with heavy-weight tools. In 2017, Hyundai, a South Korean company, introduced its chairless exoskeleton (H-CEX), reducing musculoskeletal injuries caused by pressure on the body, particularly the knee joint. For tasks requiring frequent squatting, the H-CEX seat plate alleviates the discomfort experienced by construction workers [114].

2.2.1 *Challenges in Bipedal Walking Exoskeleton Robots*

Despite recent progress with various humanoid robots, bipedal walking remains a challenging control problem. Walking exoskeletons should provide assistance to humans in an comfortable way while taking care of the underactuated dynamics of the combined human and exoskeleton systems. Moreover, the alignment of the exoskeleton device with the human joint complex may not be precise. Hence, the structure may not be sufficient to support the human torso in providing an efficient, stable gait [215]. Stability involves maintaining balance and posture, and it has been a central focus in the earliest studies of bipedal robots. Researchers initially aimed to achieve stability, recognizing it as a challenging factor. Over time, significant progress has been made, with robots now capable of static and dynamic walking, jumping, and running [166, 206]. However, maintaining balance and posture while multi-tasking with an exoskeleton device strapped to the legs and navigating through uneven terrain is a difficult problem to solve. When standing on a sloped surface, a bipedal exoskeleton cannot guarantee stability for its human wearer; even a slight change in foot position can put the wearer at risk of falling. To maintain balance, humans intuitively and actively control their nerves, tendons, and muscles, using body compliance and active muscles as support. During motion, muscle flexion and extension can alter movement patterns to help maintain stability. Moreover, ensuring the safety of a human wearing an exoskeleton without additional support is a significant concern, especially for physically disabled users. Therefore, meeting legal requirements often takes a considerable amount of time before deploying such exoskeletons for commercial use. Stability, safety, and human-motion intentions are all critical to achieving efficient control of an exoskeleton robot for bipedal walking. Some researchers have used the zero moment point (ZMP) criteria to control humanoid robots that walk with two legs [86, 206]. Others have used the center of pressure (COP) or center of mass (COM) criteria to move the center of gravity in exoskeletons to their support polygon during walking [113]. Existing reviews of bipedal walking exoskeletons have focused on their medical applications. In the last ten years, a lot of research has focused on modular rehabilitation of ankle or knee joints [38, 81, 139, 179]. Other research has looked at

the composition of the leg with an extra support device [11, 28, 171, 183, 193, 223]. In recent decades, there have been numerous reviews, designs, and clinical gait evaluations. However, no comprehensive meta-analysis has integrated various analyses, evaluations, design approaches, and control methods into a validated model, serving as a proof of concept for the development of efficient, affordable, and safe bipedal walking exoskeleton robots that do not require additional crutch support. To underscore the necessity of such an analysis, the subsequent sections will delve into the technological gaps and challenges encountered in the design, modeling, and control of bipedal walking exoskeletons, proposing feasible solutions to address these issues.

2.3 CLASSIFICATION OF WEARABLE LEE'S ON APPLICATION DOMAIN

In this section, the LEE robots for bipedal walking are classified into three application domains: medical, industrial, and military. Additionally, the variations among the application domain with regards to dominance in the existing designs are highlighted. The medical application LEEs are designed to assist humans with lower limb disabilities towards enhancing locomotion and gait training while physically reducing demanding tasks by therapists. It will enable older humans with weaker muscles and also the disabled to regain locomotion and walk again [155, 175]. It also focuses on mobility compensation for paralyzed and aged persons, and it is used in the healthcare facilities to enhance the physical performance of the wearer and augment strength to stroke patients, SCI, and other forms of paralysis of the lower limb. The medical application is further categorized into three areas: rehabilitation, paraplegic assistance, and power augmentation. In an industrial application, LEE's are used for power augmentation, i.e., to enhance the human muscle strength in tasks that require more energy in manipulation at a faster rate or for carrying heavy loads in factories [176]. Military application exoskeleton robots play a pivotal role as a tactical and operational tool for military armed forces [225], e.g., for carrying heavy loads on the war field.

2.3.1 *Medical Application of LEE*

Accidents, aging, and diseases related to the nervous system such as stroke, SCI, and OA can lead to weak muscles and total loss of the lower limb parts. There has hardly been any progress in reducing the number of road traffic incidents, leading to SCI and loss of limbs in many low-income countries between 2013 and 2016, according to the World Health Organization (WHO) [58]. The WHO's Global Status Report on Road Safety 2023 estimates that over 1.19 million people die each year as a result of road traffic accidents. Aging is a significant risk factor that casuses a disability such as stroke. Over time, the anatomy and physiology of the human body becomes weak, as growth depreciates. It is a natural phenomenon where the tissues, cartilages, and muscles are too weak to support the body joints actively, and locomotion becomes difficult. Stroke and SCI are significant causes of paralysis, leading to impairment in the motor or sensory function of the limbs. OA is a disease that affects the human body joints. The foot is the most used part of the human body, especially in locomotion; therefore, the ankle and the knee joint are majorly affected by OA, resulting in breakdown of the joint cartilage and underlying bone over

time. In addition, strenuous exercises and high-impact sports such as basketball, rugby, squash, and outdoor cycling can also cause OA. The authors of [7] suggest that athletes are more prone to this disease than the general population, while most former footballers suffer chronic knee joint damages, unlike running, cycling at the gym, and swimming, which is less risky for joint injuries. In addition, medical application exoskeletons have been developed for rehabilitation to assist patients with limb impairments due to neurological disorders like SCI. The walking assistance of the HAL exoskeleton has been evaluated for safety with support on a treadmill for therapy training [177]. Furthermore, the Bergmannsheil University Hospital in Bochum has intensified its cooperation with the Japanese robotics company Cyberdyne using HAL for robot-assisted therapy procedures. With EksoGT [50] (formerly eLEGS) as shown in Figure 2.1a, various analysis evaluations and training for the lower limb in neurorehabilitation on paraplegic subjects [27, 50, 151] were carried out, using the active powered exoskeleton as a test bench. The clinical trials yielded positive results that are safe, practical, and with minimal risk to secondary injuries and patients with incomplete SCI. However, a limitation of the design is the lack of experimental methods for demonstrating the relative effectiveness of the exoskeleton in comparison with other rehabilitative techniques and technologies. An improved version of the EksoGT is the EksoNR [44], which assists in regaining natural gait patterns by re-teaching the human brain and muscles how to walk again after healing. It means the variant has been integrated with sensors to monitor the movement intent of the leg continuously. Phoenix as shown in Figure 2.1b is the world's lightest wearable powered LEE developed by SuitX. It is designed to assist people with impairment disabilities and has enabled many individuals to stand upright and walk around. It is adjustable for different sized users with only two actuators at the hip joint. In addition, the knee joints are designed to allow support with a pair of crutches during stance and ground clearance during swing [155]. The Recupera-Reha shown in Figure 2.1c is a modular full-body exoskeleton for healthcare applications [95, 101, 108]. The upper-body is used to assist and rehabilitate weak upper limbs, while the lower body has two modes; sitting and standing. The goal of Recupera-Reha is to develop an innovative and mobile whole-body exoskeleton that combines online evaluation of electroencephalography (EEG) and electromyography (EMG) signals [90, 94], to enable an assessment of the condition of the operator and multi-level support via embedded multimodal multisensor interfaces [45, 91, 211]. However, the prototype requires optimization towards application as a full-body exoskeleton for rehabilitation of gait [101]. Recently, a modular full-body exoskeleton for physical assistance called AXO-SUIT as shown in Figure 2.1d has been designed for medical applications to assist elderly persons. The exoskeleton enhances full-body motions such as walking, standing, and bending, as well as performing lifting and carrying tasks to assist older users to perform tasks of daily living [29]. ATALANTE is a lower limb exoskeleton that allows stable walking for paraplegic people without any additional stabilization tools, such as crutches. The mechanical design supports the entire weight of the patient, with the exoskeleton firmly strapped from the feet to the abdomen. Experimental results on paraplegic patients presented in [69] show a slow gait of 0.1 m/s as shown in Figure 2.1e and a simulated stable gait of 0.4 m/s. The medical application of exoskeletons for bipedal walking is further sub-categorized into three. The first category, for rehabilitation or recovery from injuries like fracture, joint sprain, OA, SCI, stroke, surgery, and other accidents, may require

physical therapy to strengthen and heal the injured leg towards normal locomotion activities. The second category is assistive, and this is mainly offered to mentally healthy and aged individuals whose lower limb muscles are too weak to stand alone and actively walk without support. They require some aid, which could improve the quality of their lives by removing crutches and wheelchairs that serve as external support to enhance walking. A third category is a form of full power augmentation offered to completely paralyzed patients and amputees who are completely physically disabled. The exoskeletons are further categorized into: partial support (minimal force exerted by the exoskeleton) and full support (all the force exerted by the exoskeleton) types.

(a) EksoGT™by ©Ekso Bionics

(b) Phoenix (credit: SuitX)

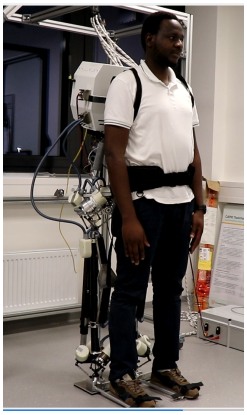

(c) Recupera-Reha (Photo credit: Annemarie P., DFKI)

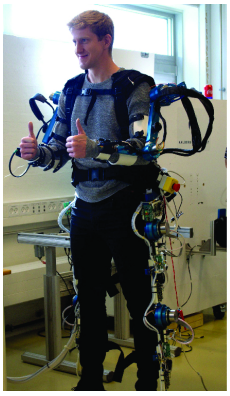

(d) AXO-SUIT (copyright: Shaoping B.,)

(e) ATALANTE lower limb exoskeleton with free hands during walking experiments with a paraplegic patient (photo credit: Wandercraft)

Figure 2.1: Medical application exoskeletons

Various LEEs developed from the last two decades for medical applications are summarized and categorized into three; Table 2.1 for rehabilitation, Table 2.2 for assistance and Table 2.3 for power augmentation.

Table 2.1: Overview on medically-based biped exoskeleton robots for rehabilitation purposes.

Name / Institution	**Exoskeleton Type**	**Full / Partial Support**
ATALANTE X, (2023) [22]	wearable	full
ReWalk Personal 6.0, (2015) [198]	"	partial
University of Goce Delcev,	platform	"
Macedonia, (2013) [97]	"	"
Vrije University Brussel, (2009) [12]	"	"
eLEGS, (2010) [14]	wearable	"
H-MEX, (2017) [41]	"	"
WalkBot, (2020) [170]	platform	"
LOKOMAT, (2013) [30]	"	"
Recupera-Reha (2018) [95, 101]	wearable	"

Table 2.2: Overview on medically-based biped exoskeleton robots assistive purposes.

Name / Institution	**Exoskeleton Type**	**Partial / Full Support**
HAL, (2017) [75]	platform	full
KEEOGO, (2017) [8]	wearable	"
University of Elect. Sci. and Tech., China, (2015) [65]	wearable	"
Korea Adv. Inst. of Sci. and Tech. (KAIST), (2021) [212]	"	"
Istituto Italiano di Tecnologia, Genoa, Italy, (2020) [36]	"	"
Axo-Suit, (2019) [1]	"	"
Exosuit, (2013) [210]	"	partial

Table 2.3: Overview on medically-based biped exoskeleton robots for power augmentation.

Name / Institution	**Exoskeleton Type**	**Partial / Full Support**
XoMotion (2022) [182]	wearable	full
EksoGT (2015) [50]	"	"
Yonsei University China, (2013) [87]	"	"
Phoenix, (2018) [155]	"	"
ATALANTE, (2018) [66, 80]	"	"
MINDWALKER, (2014) [209]	"	"

2.3.2 *Industrial Application of LEE*

Exoskeletons have widely been used in industrial applications and are still in progressive development. They are used to enhance human power during locomotion and transportation of heavy loads. The Guardian Alpha XO as shown in Figure 2.2a is an industrial application full-body exoskeleton used for logistics. It represents the cutting edge of physical human augmentation and wearable robots to enhance power [176]. It is designed and operated to perform manual handling tasks with four limbs simultaneously, and the two exoskeleton limbs can suspend the weight of an object to themselves while the human upper limbs are stationary. Thus, during locomotion, the wearer feels little or no weight that restricts movements with the lower limbs. The LegX [192] as shown in Figure 2.2b, a product from SuitX company is an industrial application exoskeleton suit strapped below the torso to relieve pain and fatigue while squatting. It can be combined with the earlier variant modules V3 ShoulderX and BackX to perform human movement motions [156]. The chairless chair [163], as shown in Figure 2.2c, has a unique feature that could be transformed from standing to sitting. It enables industry workers to actively work, either standing or comfortably sitting, while also relieving stress and fatigue. Task coordination is one of the fundamental activities in industries that require the movement of both production equipment and manufactured products. The German Bionics company developed the CrayX [17]. It is capable of manual handling tasks and can be integrated into digital logistic workflow devices. Ottobock industrials, also a German-based company, developed a passive exoskeleton (PAEXO) robot to relieve logistic workers from energy-demanding tasks. The six variant design modules are: PaexoBack, PaexoShoulder, PaexoThumb, PaexoWrist, PaexoNeck, and Paexo softback [153], which support individual tasks for the upper-body in the logistic industries, and some modules can be combined. Evaluation tests with the PAEXO exoskeleton strapped to the body in [135] have been carried out in the laboratory and on the field. Overhead tool lifting tasks were performed with whole-body inertial motions of some healthy students. Their reaction force exerted on the ground, oxygen consumption, heart rate, and muscle motions of the upper limbs were captured using EMG sensors. The lab experiment revealed reduced

heart rate and oxygen consumption while performing the tasks with the exoskeleton worn on the body, compared to manually handling the tasks without the exoskeleton.

(a) Guardian® XO Alpha (photo credit: Sarcos Robotics).

(b) LegX (photo credit: SuitX)

(c) Chairless Chair 2.0 [59] (Credit: Noonee)

Figure 2.2: Industrial application exoskeleton

An overview of the industry-based exoskeleton with full-body and lower-body design configuration is presented in Table 2.4 in walking assistance, load handling, and relief from pain and fatigue. First, we can discern the difference between the two design configurations. The former has the capabilities of the average human functionalities, while the latter case may have one or more functionalities. It means that designing a full-body exoskeleton device capable of accommodating different functionalities could assist humans in multi-tasking while applying less strength. However, no available table of overview for the military application of exoskeleton in this research work exists, because similar functionalities are exhibited by their industrial counterpart. A majority of the already existing military application exoskeletons enhance muscle power or load handling while walking.

Table 2.4: Overview on industrially-based biped exoskeleton robots (for walking assistance, load handling, pain or fatigue relief assistance)

Name	**Body Part**	**Walking Assistance**	**Load Handling**	**Pain/Fatigue Relief**
Guardian Alpha XO, [176]	Full-body	✓	✓	✓
Power Assist Suit (PAS), [142]	"	✓	✓	✓
FORTIS, [131]	"	✓	✓	✓
CrayX, [17]	-	✗	✗	✓
H-CEX, [114]	Lower-body	✗	✗	✓
LegX, [192]	"	✗	✗	✓
Chairless chair, [59]	"	✓	✗	✓
BoostX, [191]	"	✓	✗	✗
ONYX, [123]	"	✗	✓	✓

2.3.3 *Military Application of LEE*

The military application of biped exoskeleton robots is designed to augment the muscle power of humans during military operations in demanding terrain. The electrically actuated LEE BLEEX, as shown in Figure 2.3a successfully demonstrated autonomous walking while supporting its weight with an extra payload [225]. The wearable LEE used for military operation focused more on actuator design, each leg with seven DOFs representing three DOFs each for the hip and ankle joints and a single DOF on the rotary joint of the knee. Apart from grounding its weight, the BLEEX architectural design decreased the complexity of power consumption while clinical gait analysis (CGA) data were obtained to measure approximate torque, motion angles, and power required by the joints to determine actuation selection. On the other hand, not all the joints are aligned in conformity with the human leg. It is not power-efficient, as it cannot actuate all DOF at the same time. Instead, it offers only a substantial positive power to actuate the joints during desired gait movement. Another biomechanical design is a variant of BLEEX powered by linear hydraulic actuators and capable of carrying its weight with an extra payload. Despite approximating the BLEEX kinematics and dynamics similar to the human leg, the motion curves obtained from CGA data did not match the human leg [224]. Other BLEEX military application exoskeleton variants are the ExoHiker for load augmentation on a long-distance mission, ExoClimber carrying heavy loads while ascending/descending stairs/slopes, and Human Universal Load Carrier (HULC). The HULC exoskeleton shown in Figure 2.3b is a third-generation exoskeleton designed to incorporate features of both ExoHiker and ExoClimber, carrying heavy loads on uneven terrain without the wearer applying much strength [67]. The

HULC was originally developed by Berkeley Bionics (now Ekso Bionics) in 2008, and in 2009 Lockheed Martin acquired the design license to provide soldiers with a decisive advantage in ground operations.

(a) BLEEX (credit: Berkeley Bionics).

(b) HULC (photo credit: Lockheed Martin).

Figure 2.3: Military application exoskeleton

2.3.4 *Distinctions in the Exoskeleton Classifications*

The bipedal walking exoskeleton robot design is significant to human life due to daily activities requiring extra strength to perform specific tasks. Over time, aged persons experience weak muscles, while joint disorders such as sprain, OA, and paralysis could be sustained by athletes or even during physically demanding tasks by physically able persons. Though exoskeleton robots for medical purposes have been in geometric progression over the past years, most designs today compensate for mobility loss or lower limb joint disorders. Researchers have focused on kinematic optimization of the exoskeleton [99, 101], multimode rehabilitation [45, 91, 94], and others have evaluated the motion intention of the wearer as evidence of support for general use [92, 98, 216], but the designs are still not sustainable safety-wise for personal use. It can be seen that the adoption of an exoskeleton for bipedal walking has indeed become evident in the last two decades in the three application areas; medical, industrial, and military. The pie-chart representation shown in Figure 2.4 shows the percentage variations of exoskeletons designed based on their application in the last two decades. A large proportion of about 50%, which accounts for 60 selected papers either as a modular LEE joint or a LEE leg, has dominated the medical applications design field. These powered exoskeletons can improve the quality of life of people who have lost the active use of their legs by enabling system-assisted walking. However, before they can be commercially available in the United States, the FDA must approve them. In Europe, however, the new Medical Device Regulation (MDR), which replaced the

previous regulations; Medical Device Directive (MDD) and Active Implantable Medical Devices Directive (AIMDD) [116] ensures that legal requirements, regulations, and standards are also met before they are commercially accepted. In the industrial application, there has been considerable growth in the designs, with about 35% of exoskeleton robots being used for logistics in factories, the majority of which augment power. Following the industrial exoskeleton, 15 papers focused on locomotion, and 30 papers discussed strength augmentation. The idea is to reduce worker injury and errors due to fatigue and increase muscle strength. In military application, threats to domestic law and order from the misuse of exoskeletons by rogue users and meeting soldiers' requirements have proved challenging. As a result, the military robots have not shown inclined growth, with about 15% corresponding to 15 reviewed papers in the last decade. The designs are still in the research institutes, pending approval, as they need to meet the standard compliance to regulations provided by the International Standard Organisation (ISO) and the International Electro-technical Commission (IEC) to prevent sanctions.

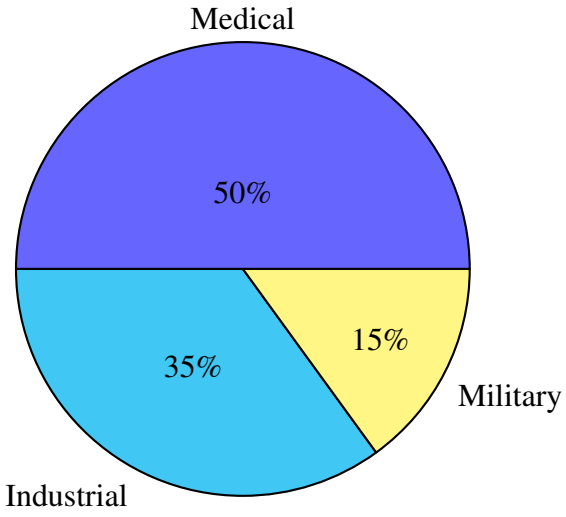

Figure 2.4: Classification of exoskeleton robots based on applications.

The bar chart shown in Figure 2.5 depicts the number of exoskeleton robots that will be considered for meta-analysis in the perspective of design and control of biped robots for human walking. It also corresponds to the percentage ratio that distinguishes the functionality of the three classifications of exoskeleton robots.

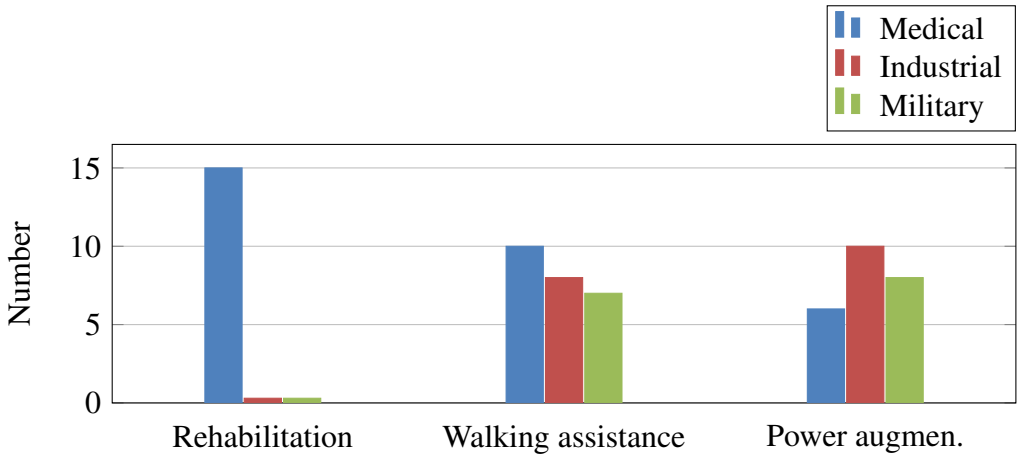

Figure 2.5: Number of exoskeleton robots according to domain area.

The histogram shown in Figure 2.6 depicts the distribution of the reviewed papers by publication year. It corresponds to the number of exoskeletons developed based on application over 60 years. Only some selected articles that are relevant to our work are included. We consider the development year of the exoskeleton designs for the three categories: In 1965, the first gait assistance exoskeleton was developed. In 1972 and 1978, respectively, a new design similar to the first design was developed. There was a dormancy period between the late 1970s and 1980s. A climax period that attracted the market began in the early 2000s, with progressive growth in the designs.

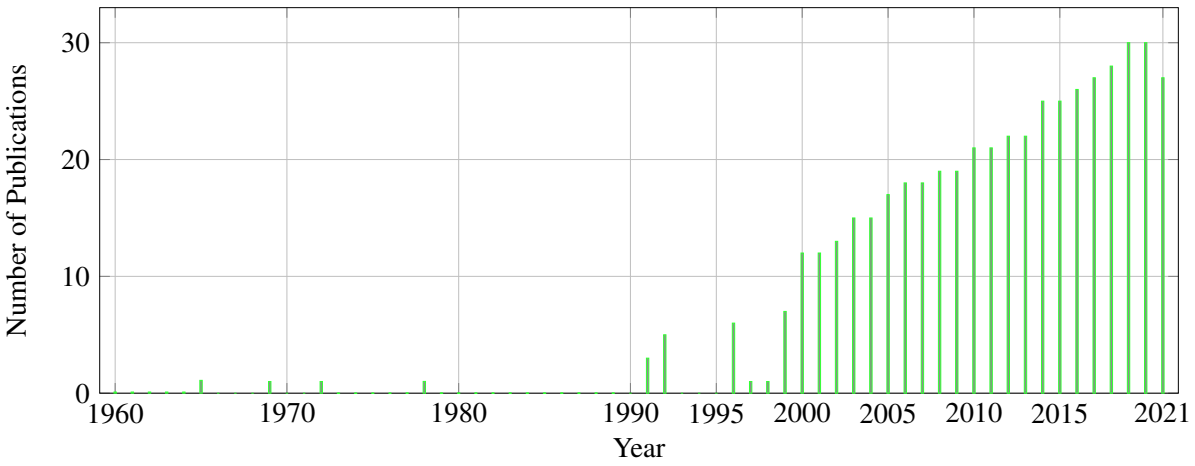

Figure 2.6: Histogram of the publication years of the considered works.

Finally, Table 2.5 shows the list of companies pursuing exoskeleton research based on our proposed classification. This demonstrates a decent interest from the private sector in investing into exoskeleton research.

Table 2.5: Overview of companies pursuing bipedal walking exoskeleton

Exoskeleton Name (Year)	**Company**	**Weight (kg)**
Military Applications		
Hardiman (1965) [143]	General Electric	680
BLEEX (2006) [224, 225]	Berkeley Bionics	41
Raytheon XOS 2 (2008) [168]	Raytheon Sarcos	95
HULC (2009) [67]	Lockheed Martin	24
Medical Applications		
HAL (2006) [177]	Cyberdyne	10
LOPES (2007) [205]	TWENTE University	N/A
Indego (2010) [204]	Parker Hannifin	12
ReWalk Personal 6.0 (2015), [198]	ReWalk Robotics GmbH	23.3
Walk Again (2014) [207]	Duke University	20
EksoGT (2015) [43]	Ekso Bionics	20
Phoenix Exo (2016) [155]	SuitX	12.25
REX (2016) [18]	REX Bionics	38
H-MEX (2017) [41]	Hyundai	18
Recupera Wheelchair [95, 101]	DFKI	29.7
Symbitron Exo (2018) [136]	TU Delft	37.2
BELK system (2019) [54]	Gogoa Mobility Robots	N/A
EksoNR (2019) [44]	Ekso Bionics	20
ATALANTE (2020) [69]	Wandercraft	75
Exo-H3 (2020) [195]	Technaid	17
Industrial Applications		
Power Assist Suit (2015) [142]	Mitsubishi	39
H-CEX (2017) [114]	Hyundai	1.6
ChairlessChair (2017) [59]	Noonee	2
Guardian XO (2019) [176]	Hyundai	68
LegX (2019) [192]	SuitX	11.7
PAEXO (2019) [153]	Ottobock Industrial	4
CrayX (2020) [17]	German Bionics	7.4

2.4 DESIGN CONCEPT FOR LOWER EXTREMITY EXOSKELETONS

In the past decade, LEEs were designed as series, parallel, or series-parallel hybrid mechanisms [110]. The former is built with kinematic chains arranged in a single series of links and joints while the latter is built by two or more kinematic chains mostly in closed loops [84]. Serial designs are known for their versatility, ample workspace, simple modeling, and control. Their drawbacks include their limited precision, low stiffness, poor dynamic characteristics, and limited speed and torque. In contrast, the parallel counterpart provides higher stiffness, speed, accuracy, and payload capacity. However, they have reduced workspace and complex geometry, which requires careful control analysis as a downside. Consequently, in an application point of view, the safety and comfort of the wearers of the exoskeleton is paramount in robot designs. Mimicking the human anatomic motions and augmenting muscle power comes next. For enhancing safety, the mimicking of the human gait pattern, a combination of both serial and parallel designs, has been employed recently, and is still ongoing, aiming for functionality that is closer to that of a human [101]. The Recupera-Reha full-body exoskeleton in Figure 2.7 with two system design configurations; the full-body (left) and wheelchair design mode (right), is a combination of serial and parallel designs, leading to series-parallel hybrid architecture. The blue highlighted labels represent the full-body system features while the green highlighted labels represent both system configurations, the full-body and the upper-body configuration. The modules for the upper-limb system have a link of serial chains at the forearm and elbow joint connected to the wrist. The joints are actuated with serial elastic actuators and are implemented as independent series kinematic chains. The shoulder joint is a parallel mechanism design that provides a large workspace and prevents collision with the human head due to the placement of the actuators behind the shoulder blade (details in [127]). The lower-limb has its hip and ankle joints treated as an ASPM modular design (more details in [104]). Each of the modules of the upper and lower-body are independently coupled, making the full-body a combination of a series-parallel hybrid design.

2.4.1 *Human and Exoskeleton Lower Extremity Joints*

Walking with an exoskeleton strapped to the human body without additional support poses significant challenges. However, tripedal locomotion is often more stable than bipedal walking. The anatomical study of the lower extremity skeletal system of a human as shown in Figure 2.8a is a crucial practice to clinical sciences and other health-related studies to mimic the biological design of the human limbs. The function of the human lower limb anatomy in [185] highlights the musculoskeletal function and how the structure is modified by gait or joint disorders. Therefore, it is essential to carefully study the human anatomical structure and function before designing an exoskeleton device that mimics the human gait. The human lower extremity is made up of three joints; hip, knee, and ankle. Each of these joints has an underlying bone that links up to form a single leg, with every joint having a role to play in order to enhance locomotion. The kinematic chain is insufficient to mimic the human joint kinematics and behavior when designing an exoskeleton. The exoskeleton surrounds the body and therefore needs more DOF

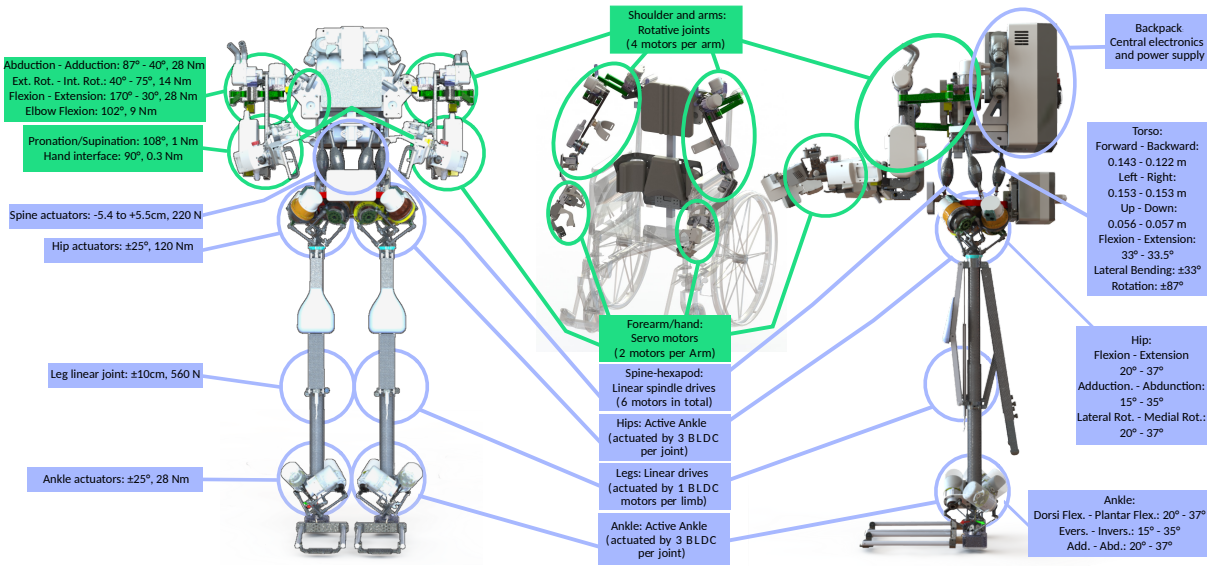

Figure 2.7: Series-parallel (hybrid) exoskeleton design [101].

to allow all human joint movements. The geometry or kinematic open chains of rotary and linear joints form the basis of robot motions from 2D cases like (RRR, RPR, RRP, PPP), representing planar walking in one direction, where the "R" and "P" stand for revolute and prismatic joints. The 3D cases (SRS, SRU, SPU, SPS) provide a realistic strategy as a bridge to the concept of design for the human leg structure. They serve as kinematic abstractions for a two joint structure (universal joint) or three joint structure (spherical joint), where the "S" and "U" in the 3D case stands for spherical joint and universal joint. The abstractions of the various joint structures as either a series of serial chains or closed-loop parallel chains is discussed in [102, 110].

HIP The hip is a ball and socket joint in the human anatomical system. It connects the pelvic girdle and the thigh, which permits movements in three DOF, also known as the principal motion trajectory, allowing flexion, extension, and rotational movements. They are the dorsiflexion/plantarflexion (DF-PF), eversion/inversion (EV-IN) and adduction/abduction (AD-AB) motions. The hip joint supports the body's weight in both static (standing) and dynamic (walking or running) posture and enhances stability. The skeletal muscle is a soft tissue composed of specialized cells called muscle fibers attached to the bones of the hip, thereby producing force and motion by contraction of the muscles.

KNEE The knee joint is a hinge-type synovial joint formed by articulations between the femur and tibia bones. It permits flexion, extension, and slight internal and external rotation while carrying the body's weight during movements in the horizontal and vertical directions.

ANKLE The ankle joint is a synovial joint located above the foot. It connects the bones of the leg (tibia and fibula) and the foot (talus). Functionally, it is a complex hinge type joint, permitting primarily (DF-PF) motion of the foot, and (EV-IN) movements are also produced at

the subtalar region of the foot. However, slight rotational movement of the foot also occurs as (AD-AB) motion.

EXAMPLE OF EXOSKELETON ABSTRACTING HUMAN LEG The Recupera-Reha lower extremity exoskeleton joints shown in Figure 2.8b is a prototype designed to mimic the anatomy of the human lower extremity. The Recupera-Reha lower extremity consists of modules representing hip (S), ankle (S), and a prismatic joint (P) connecting the hip and ankle joint with an extension from the hip, which supports sitting mode [101]. The three SPS modules correspond to SRS that represents the hip, knee, and ankle joints of the human leg as shown in Figure 2.8a. The Recupera-Reha ball and socket joint of the hip and the functional hinge joint of the ankle are both designed and treated as an almost spherical parallel mechanism (ASPM), which was introduced in [130] and later extensively analyzed in [104, 106]. Due to its complexity, the placement of the joints at an exact center of the pelvic and foot respectively defines the geometry of the human anatomy as a unique design [101, 104]. The motor actuators placed at the joints replace the muscle functionality in humans, while the number of actuators placed at each joint determines the directions of motion.

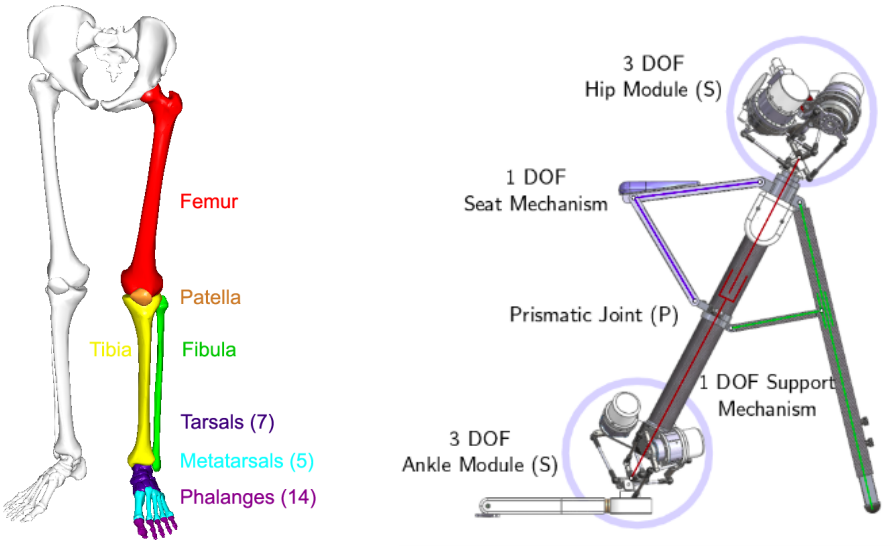

(a) Human leg [185] (b) Exoskeleton leg [101]

Figure 2.8: Structure of the Human and Exoskeleton Leg Joints

The design concept points out the mechatronic structure relative to the hardware usage, which leads to a single leg or a modular form of the hip, knee, and ankle joints for rehabilitation, assistance, and power augmentation towards effective locomotion. Table 2.6, Table 2.7, Table 2.8 review the mechanisms used for hip, knee and ankle designs, respectively. The composition of the modular joints as a single leg design for bipedal human walking has also been developed in some considerable research works [15, 69, 101, 209]. From the purview of bipedal walking exoskeletons, the tables give an overview of the significant design features, achievements, and limitations in the current designs. An acronym, not available (N/A), is used if no data is available.

Table 2.6: Review on hip joint

Institution/ Name	Actuation	DOF	Absolute ROM	Velocity Limit	Torque Limit	Application domain	Pros	Cons
HIT China [145]	BLDC Motor	3	N/A	N/A	22.3 Nm	Medical	The exoskeleton can stand, sit, and walk with stair ascending modes. A wearable device made from carbon fibre materials with a total mass less than 12 kg, it's designed by first simulating the biomechanics of the human body for joint alignment with LifeModeler tool. The actuators consist of encoders, planetary gear, and bevel gears to absorb shock.	Difficulty grounding it's own weight, with increased consumption power and stability control.
Recupera-Reha [101]	"	3	DF-PF=57°, EV-IN=57°, AD-AB=50°	132°/s	120 Nm	Medical	A 41 kg light weight modular exoskeleton is adaptable to different human sizes. Depending on the body part, the device is made from aluminum, steel, polyamide and carbon-fibre reinforced materials. The self-designed modular actuator units are capable of satisfying specific requirements.	The prototype only support sitting and standing modes but requires optimizing the design to incorporate a walking and running mode.
Necmettin University Turkey [150]	"	1	N/A	3190 rpm	N/A	Medical	An 18.5 kg light weight wearable orthotic device that supports ReWalk, CGA data from human joint motions is used to determine the orientation of the exoskeleton joints. The 24 V DC motors are powered by Li-Po battery pack used for actuation of the hip by 30 W power.	Limited workspace, underactuated and additionally supported with crutches.
Cuenca University Ecuador [140]	DC Servomotor	1	"	N/A	"	Medical	A wearable exoskeleton designed with real time fast data link between six sensor and actuator units with a main process unit.	Limited to few therapy motions due to less DOF.
BLEEX [224]	BLDC Motor	3	"	"	"	Military	A 41 kg wearable autonomous exoskeleton designed with extra payload capacity, using a bidirectional hip actuator for stance and swing mode compared to the previuos hydraulic actuated variant.	The exoskeleton hip joint axis only aligns with the biological joint from the CGA data.
Yonsei Uni. China [87]	"	3	DF-PF=20°, EV-IN=50°, AD-AB=40°	"	79.3 Nm	Medical	A wearable device embedded with sensor and inclinometer at the torso to measure COP and reaction forces. The CGA estimated a 200 W power required for the hip and knee joint actuators with harmonic drives.	To supplement the stability problem, forearm crutches that are controlled by the upper limbs supports the hip.

Table 2.7: Review on knee joint

Institution/ Name	Type	Actuation	DOF	Absolute ROM	Velocity Limit	Force/ Torque Limit	Application domain	Significant Feature
Recupera-Reha [101]	Wearable	Linear BLDC motors.	1	N/A	266 mm/s	560 N	Medical	A wearable device made from combinations of aluminum, steel, and carbon-fibre reinforced. The prismatic joint of the knee is designed with a seat plate and foldable support when required to make angular motions, the actuators and ball screw on the two prismatic joints of the legs can support a total force of 1120 N.
Vrije University Brussel [15]	Platform	Pleated pneumatic artificial muscles	Multiple	EV-IN=60°	N/A	80 Nm	Medical	A 5.8 kg light weight design made from thermoplastic materials, with artificial muscles that provides air-powered actuation in a design form of four-bar linkage, and generating linear motions with high force output that suits limb rehabilitation. A gravity supportive arm allows the platform device to mimic human posture and balance.
BLEEX [224]	Wearable	Electric Motors with harmonic drives	1	EV-IN=65°	"	34.7 W	Military	The CGA-data determined the knee flexion angles and torques required for alignment with the human knee joint. Such that the generated toe-off and stance torques have large enough power to back drive the harmonic drives and actuators in asymmetric manner.
Meltran V [78]	Platform	BLDC Servo motors	1	N/A	"	109 W	Industrial	The linear inverted pendulum mode design approach is used to determine the CoM, that aligns with the human hip joint on the 46 kg robot to maintain posture. It's designed with a synthetic rubber material from Neopren.
Yonsei University China [87]	Wearable	BLDC motors	1	EV-IN=100°	"	42.2 Nm	Medical	The sensor system design based on the COP and ZMP determines human intention to move the knee through force reactions measured between the wearer and the device. This enabled the proper mounting of the device onto the humans body complex. Duralumin material is used for the joint linkages while the actuators produces an estimated 200 W power.

Table 2.8: Review on ankle joint

Institution/ Name	Type	DOF	Absolute ROM	Velocity Limit	Force/Torque Limit	Application domain	Design Strategy
Beijing University of Tech. [226]	Wearable	3	DF-PF=75°, EV-IN=44°, AD-AB=72°	N/A	N/A	Medical	Workspace analysis
PARR [117]	Platform	3	DF-PF=68.16°, EV-IN=32.57°, AD-AB=64.20°	"	"	"	"
ASPM Active Ankle [104]	Wearable	3	DF-PF=57.06°, EV-IN=50°, AD-AB=66.16°	330°/s	28 Nm	"	Workspace and finding optimal placement of the mechanism in the leg.
Anklebot [53]	Platform	2	DF-PF=70°, EV-IN=45°	N/A	N/A	"	Workspace analysis
Purdue University Fort Wayne [16]	"	3	DF-PF=100.8°, EV-IN=56.0°, AD-AB=99.50°	"	"	"	"
Chongqing University China [208]	"	3	DF-PF=75.60°, EV-IN=39.0°, AD-AB=61.90°	"	"	"	"
Yonsei University China [87]	Wearable	3	DF-PF=10°, EV-IN=25°, AD-AB=50°	"	"	"	Stability criteria using COP to determine walking intention.
PKAnkle [128]	Wearable	3	DF-PF=75°, EV-IN=45°, AD-AB=30°	90°/s	52 Nm	"	Kinematic optimization (alignment with the human ankle joint complex).

2.4.2 *Actuator Design for Exoskeleton Robots*

The bio-mechanical exoskeleton devices strapped onto the human body are a vital tool that could fit into the biological structure of the body, since they are used in different application domains and try to mimic the natural human gait pattern. Considering the mechanical design perspective, material technology, alignment with the human joint complex, and meeting the requirements for actuation are key to human safety. Therefore, it is essential to evaluate the type of actuator to use before defining the basis for controlling the exoskeleton. Generally, exoskeletons are underactuated, and it is impossible to imitate all the motion trajectories in the human lower extremity, but it is possible to adapt the principal motion's trajectory suitable for the movement patterns in normal daily activities, such as climbing stairs, or in the rehabilitation of gait. The muscles of the human leg enhance movement strength when the muscular motor neurons are too weak to lift the legs of a paralyzed patient or aged person. The actuators on the wearable exoskeleton devices are designed to augment the muscular strength in humans to provide efficient power at the joints. Data evaluations from the CGA have been used in [87, 150, 224] to measure angular motions, forces, torques, and power to determine the type of actuator to use, while authors in [9] provided an optimal approach for selecting actuator design components for exoskeletons. As a motivation towards developing wearable exoskeleton devices, the devices are required to have a small size, be lightweight, generate torque effectively only when needed, affordable and available in the market, and be safety-minded. They should also have electromagnetic compatibility leading to high resistance to disturbance, backdrivability, high bandwidth, high power, and be easily controlled. Given these requirements, researchers have developed exoskeletons for human walking primarily from electrical [69, 95, 215], hydraulic [224], and pneumatic actuated [15] devices. Electric actuators are electrically driven by direct current (DC) motors, which create the necessary force for linear or rotary motions. They are available in small sizes and are reliable, cheap, have less noise output, and easy sourcing of power, with the risk of electric shock being a drawback. A broad overview of the actuation of the LEE for power augmentation is made in [4]; according to the authors, CGA data are essential factors for determining the power required to actuate an exoskeleton joint. Hence, they provide input data required for an actuator design. The authors in [60] stressed that the advantages electric actuators offer are preferential, in contrast to their hydraulic and pneumatic actuated counterparts, which are bulky in size. According to them, it is impractical to have each modular exoskeleton part designed with independent power units. Stiffness between the actuators and the material of which the exoskeleton frame is made is a common approach to exoskeleton design. Therefore, the authors in [160, 222] suggested that a serial elastic actuator (SEA) could be used to provide accurate torque delivery, disturbance rejection, transparency, repeatability, and compliance to force control. Although, SEAs are effective actuators that could enhance the backdrivability, they are still not good enough for high bandwidth control loops, which is an important factor for designing walking exoskeletons or legged locomotion in general. Quasi-direct drives (QDD) with low gear reduction meet many of the actuation requirements for legged locomotion due to their lightweight design, high backdrivability (allowing for good torque sensing), and high bandwidth (because they have low reflected inertia and stiffness). However, their effectiveness in

exoskeleton robots remains uncertain due to challenges such as high motor current and electrical power demands, reduced electromagnetic compatibility, and difficulties in controlling them with limited output torque. The application of QDD actuation was used in [57] as a low-cost compliant robot capable of force controlled manipulation, and in [219] to drive the hip of an exoskeleton. Results from the experiment produced a high control accuracy in the nominal torque, bandwidth, and backdrivability perspective. Recently, the experimental results from [164] suggests that QDD could provide enhanced torque bandwidth and backdrivability for robotic dynamic performance. Hydraulic actuators are often used for driving high-powered machines, mostly in industrial domains using hydraulic fluids. They deliver good work density, high power and forces, and are easily controlled, producing linear and rotary motions. The disadvantages are safety problems with regards to leakages and their flammability [13]. Pneumatic actuators work in principle similar to hydraulic actuators by converting compressed air to mechanical energy in the form of linear and angular motions. They have good work densities, but not as high as hydraulic actuators, they are easy to control, and have the ability to work at higher temperatures. However, they exhibit energy loss due to heat transfer, noise, and higher leakages. They are not often used in high force transmission or precise position control. Instead, they are used for "fixed motion systems" [19], where the motion required is repetitive, predictable, and does not need to be adjusted dynamically.

2.5 MODELING AND CONTROL OF EXOSKELETON ROBOTS

The motion of a multi-body exoskeleton robot and its interaction with the human musculoskeletal system necessitates a comprehensive grasp of the robot's geometry, kinematics, and dynamics with the various electronic sensing and measuring devices available. This subsection emphasizes the importance of utilizing available modeling tools and discusses applicable control methods within the exoskeleton robot domain.

2.5.1 *Modeling*

The interpretation of geometry, kinematics, and dynamics into a form of mathematical equation is termed modeling. The analytical computation of the kinematic and dynamic model of a serial chain robot is largely addressed in [84]. However, the closed chains or parallel structures involve solving complex non-linear equations, which could be too tedious to formulate both analytically and numerically using notable dynamic methods like Newton-Euler, and Lagrangian [110]. Hence, modeling tools are introduced to reduce the effort of solving complex equations generated from closed chain robots. Modeling tools are software frameworks used to deal with multi-body dynamic exoskeletons that have complex mechanical systems. Tools like RBDL [52], HyRoDyn [105], DART [32], and OpenSim [34] support closed-loop models that contain libraries for efficient computation of kinematics and dynamics (forward and inverse), Jacobian matrix and determinant, and constraints for contact and collision handling. The HyRoDyn solver was recently developed as a modular software workbench for solving robot kinematics and dynamics. Other open-source library tools like Drake [197], RBDyn [165], and Pinocchio [157]

support rigid and multi-body dynamic computations. The Robot Operating System (ROS) uses description format files such as Unified Robot Description Format (URDF) and Simulation Description Format (SDF) [172] as inputs to define a robot's physical characteristics. These files are essential for modeling the rigid robot system using various modeling tools. The modeling tools have been used in the design of humanoid robots [47, 147] and also in exoskeletons for human walking [101, 105]. A series-parallel hybrid design for, e.g., Recupera Exoskeleton (see Figure 2.7), has a large number of DOF in its spanning tree, and computing the complete kinematic and dynamic models can be computationally expensive. This poses a challenge for model-based control approaches. Model simplification approaches like the one described in [101] can be used for reducing the model complexity, which is crucial for the real time dynamic control of exoskeletons with closed loops.

2.5.2 *Control Methods*

In the realm of control systems, which are utilized in both humanoid and exoskeleton robots, two fundamental approaches stand out: model-based and model-free control schemes.

2.5.2.1 *Model-Based Control*

The model-based control scheme relies on algorithms derived from either the kinematic or dynamic model of the robot system. It encompasses methods like active impedance control, admittance control, optimal control, etc. These approaches have various control methods ranging from stability control [206], force feedback and torque control, master-slave control, and sensitivity amplification control, among others. Compliance control is inarguably the most crucial aspect of exoskeleton control. The active impedance control approach explicitly employs the dynamic model of the exoskeleton mechanism and attempts to regulate the position-to-force ratio, allowing for steady-state offsets in both position and force. For robots where torque sensing is not available, it is also possible to achieve compliance using the method proposed in [39]. The active impedance control approach was applied in [2] to improve the dynamic response of the human limbs as an alternative to the biosignal integration technique, which is complex and requires re-calibration of the model parameters. The biosignal integration is a part of neuroscience that creates communication between the exoskeleton and the wearer's brain or muscles by measuring electric potential signals on the surface of the living tissue with the help of biosensors like EMG, ECG, and EEG [91–93, 178]. The measured signals are collected as training data from different individuals, analyzed by selecting relevant states of the human brain, and classified according to patterns between training data sets, and healthy and unhealthy subjects. The exoskeleton model is used beneath the EMG-based control to capture the whole dynamics of the mechanism in [95]. Other sensors are the inertial measurement unit (IMU), torque encoders, force-sensing resistors (FSR), and many more as additional control elements. For example, a string encoder with IMUs [216], was used in teleoperation to measure the position and orientation of a teaching tool and then to apply the generated signals to a robot manipulator as a haptic device. FSR is applied in [149] to analyze muscle activity patterns during bicycling and in [98] to test the sensing limits in comparison with other sensing devices. Haptic control is a form of tactile feedback technology

that takes advantage of the user's sense of touch by applying forces, vibrations, and motions in the form of a master-slave operation in virtual environments or robotic systems. It was applied for teleoperation of the CAPIO upper-body exoskeleton in [127] and applied as a force feedback control in rehabilitation after stroke [21] as an additional control approach. Virtual model control is similar to force feedback technology. However, it uses virtual components to create virtual forces applied through real joint torques to create the illusion of connectivity with the robot. It was previously applied in [161] to control the walking of a bipedal robot on level terrain. Direct Collocation is a method for solving optimal control problems based on the direct transcription of the problem. This method approximates the state and control as piece-wise polynomial splines, and the constraints are enforced at the collocation points. Among the most common formulations is the Hermite-Simpson algorithm, which has been used, for example, in [69] as a high-level controller for the ATALANTE lower limb exoskeleton introduced above. In the meantime, in humanoid robots, there has been a progressive development in the use of optimal control to differentiate between continuous and discrete control problems [99]. To improve robustness and autonomous locomotion, one can use methods from control theory, like linear quadratic regulator (LQR), Time varying LQR (TVLQR), and other non-linear optimization-based controls combined with state estimation concepts. LQR is an optimal control design technique that provides feedback gains to enable stable and high system performance. It has, for example, been applied to find the optimal solution to swing up and balance the underactuated cart table model system that captures the human walking motion [196]. Hitherto, due to the inherent difficulty in modeling and controlling parallel and series-parallel hybrid-legged robots, most scientific researchers utilize the simplified serial or abstract model of the robot for control. However, Whole-Body Control (WBC) is a standard approach for controlling redundant robots. The idea is to formulate multiple task space objectives in the cost function of a numerical optimization problem, typically a quadratic program (QP). The solution of the QP provides joint velocities, accelerations or torques for the entire robot. Most existing WBC frameworks model the QP in independent joint space, which has several practical disadvantages [144]. Thus, we use a velocity-level WBC approach for series-parallel hybrid robots, which considers the full robot model including all parallel submechanisms by defining the QP in actuator space.

2.5.2.2 *Model-Free Control*

The model-free control scheme uses the trial-and-error method without having an explicit analytical or predefined model of the system to evaluate its control performance. Such schemes are classical control techniques like the proportional, integral, and derivative (PID). Machine learning (ML) encompasses various techniques and algorithms designed to learn patterns from data and make control predictions or decisions. The ML techniques includes both model-based and model-free approaches, for instance, reinforcement learning (RL) approaches are considered model-free because they learn to make decisions based on feedback from the environment rather than a predefined model of the system dynamics. In contrast to model-free ML techniques, model-based ML methods can employ supervised learning to predict future states of a robot or to enhance models of system dynamics. This is achieved through data-driven models used in conjunction with model predictive control (MPC). Other control approaches such

as neural networks, uses adaptive control to learn and approximate complex system's behavior. Fuzzy control is also a method that can be considered for the exoskeleton, especially when the dynamical model cannot be accurately formulated. This method is composed of modules that create the input membership functions, and defines the set of rules for processing by the inference engine [214]. Based on the extracted signal data, this method has been used as a Neuro-Fuzzy controller in [70] to control a lower limb exoskeleton for motion assistance of physically weak people. In addition to the two control schemes, other methods have been proposed, such as adaptive oscillator-based control, which has also been widely used in exoskeleton control. This method was originally proposed by [159] to synchronize the instantaneous frequency to any cyclic signal. Later it was used in robotics for pattern generation [169], then extended to the control of exoskeleton robots. In [134], this methodology was used to control a whole-body exoskeleton for gait assistance, which can adapt to motion pattern variations. Table 2.9 shows a review of the current state of the art for the control strategies and methods used in the domain of biped exoskeleton. It further highlights some mechatronic details and the choice of programming environment.

2.5.2.3 *Human-In-The-Loop Control*

Human-in-the-Loop (HITL) control also referred to as assist-as-needed control or user-adaptive control can be incorporated into both model-based and model-free control approaches. As a fundamental concept in RL, HITL improves both types of control schemes by introducing a layer of human adaptability. This allows humans to provide direct feedback to the model, participating actively in the decision-making process and guiding the model toward performance that aligns more closely with human behavior. This refinement is particularly crucial in applications such as exoskeletons, where human comfort and responsiveness are essential. For example, research conducted in [6] utilized human data such as gait cycle phases, joint kinematics related to flexion and extension, muscle coordination, and stability to control two bipedal walking robots. This was achieved by employing a human-inspired control approach framed as an optimization problem based on the parameters derived from the human data. Additionally, in [33], the authors present a HITL control strategy that utilizes estimated human motion trajectories and intended goal locations to create a safe reference trajectory for robots, which is subsequently tracked using an adaptive controller. Similarly, a bipedal walking chair robot described in [194] demonstrates the benefits of a HITL control method, showing that adjustments in human posture can enhance stability, particularly in unpredictable environments. However, it is important to note that this control strategy was tested in simulation rather than real-time systems. Furthermore, the authors of [132] introduce a HITL layered control architecture for a wearable ankle-foot robot, which allows for precise interaction and assistance during walking through chronological levels. This architecture was validated through both simulations and real-time experiments, demonstrating its effectiveness in ensuring safe and reliable performance in wearable robotics. Lastly, a survey that categorizes HITL into four key architectural models is presented in [174], although the classification is not strictly limited to these categories.

Table 2.9: Review on control methods and approaches for LEE.

Institution/ Name	**Programming language**	**Control Methods**	**Mechatronics Feature**
Recupera-Reha [95, 101]	Matlab, Python, Ruby, C++	Kinematic and Dynamic Model. Position, velocity, force and torque control. Low and mid level control hierarchy.	EMG and EEG sensors, FPGA electronics, Eye-tracker especially in Virtual Reality-based serious gaming.
University of Cuenca Ecuador [140]	Matlab	"	EMG and EEG sensors.
DRACO [3]	"	PID feedback controllers, observers & estimators.	Viscoelastic liquid cooled actuator (VLCA).
Vanderbilt University Nashville [10]	"	PD position control with a feedback sensing	Hydraulic actuators. IMU sensors and digital signal processor.
KIT-CO-1 [12]	Matlab, C++	PID controllers	Linear series elastic actuators. Force signals processed by Arduino.
ATALANTE [69]	"	Hybrid control combining dynamic model and state machine, gain tuning using virtual constraints via feedback control.	BLDC Motors, digital encoders with IMU's to measure joint velocity and displacements. Force sensors for detecting ground contacts.
MINDWALKER [209]	Matlab simulink	CoM transition with finite-state machine based controller.	Series elastic actuator. Motion steps are triggerered using arm muscle attached to IMU, EMG and EEG sensors.
HEE [120]	"	Fuzzy self-adaptive PI controller	No Information

2.6 DISCUSSION AND FUTURE RESEARCH DIRECTIONS

This section provides an overview of current methods utilized in the design and control of biped walking exoskeleton robots. It suggests a shift towards artificial intelligence in future research directions to enhance performance. These directions include human-robot interaction, control and safety, and cost considerations.

2.6.1 *Discussion*

The significance of improving the design and control of the bipedal walking exoskeleton is apparent due to its applicability to the daily life of humans to either assist or augment power. In medical application for rehabilitation purposes, careful design and control analysis must be met to imitate the natural human gait patterns. Therefore, misalignment of the exoskeleton joint articulation with the human biological limb will cause pain to the patient and increase the injury sustained. In industrial and military applications, precision is required to achieve specific tasks. Without effective control, there will be no dexterity in manipulation. These exoskeletons are still not readily available for personal use due to the size, cost, and safety measures. They are developed in healthcare and research facilities or upon special request. A question to ask is; how do we make the exoskeletons affordable to all without compromising the quality and performance of the sensors, drives, or actuators? Generally, exoskeletons are underactuated in their designs but then, how do we compensate for all human biological DOF? In addition, there is a need to exploit other materials such as carbon fiber, silicon, and aluminium alloys to minimize costs in designing lightweight robots. In the design of actuators, selecting components that best suit an exoskeleton requires torque, power, backdrivability, high bandwidth, efficiency, and most importantly safety. The advantages of electric actuators are their compact size, low cost, low noise, low weight, and easy sourcing of power. Unlike hydraulic and pneumatic actuators, which have the disadvantage of being heavy, space-consuming, expensive, and, most importantly, do not respect modularity. Geared electric motors have high friction, which makes force control difficult. SEA is a compromise, but still has bandwidth limitations for control loops. In contrast, direct drives and quasi-direct drives are perfect actuators for building next generation exoskeleton devices. The actuators are heavier than their geared counterparts, but are inexpensive, and meet the requirements for efficient and robust exoskeleton designs. Therefore, a paradigm shift into quasi-direct drives could be a better actuation option for developing biped walking exoskeletons. The MPC is a model-based control method that has found increasing utility in emerging complex engineering applications, including uncrewed vehicles, humanoid robots, and biomedical systems [173]. The MPC algorithm enables robots to be sufficiently responsive to perform dynamic tasks in real-time. It is achieved by updating the motion planning based on the current measured state of the robot at a sufficiently high-frequency [96]. MPC and LQR algorithms are based on optimal control methods. They are often used for trajectory tracking in robotics and for articulated vehicles [71, 138]. However, experiments have shown that MPC performs better than LQR [213], considering the modification of the robot's state according to its environment when updating the command. Moreover, it allows reacting quickly

enough to this modification by recomputing a new motion planning that allows, in the case of exoskeletons, to have a reactive and robust control to adjust a disturbing trajectory by a potential obstacle or instability of the patient. Furthermore, the combination of MPC and ML method was recently applied by the authors in [40] to develop autonomous vehicles for enhancing safety and comfort. MPC can provide robust, safety and oriented control, but in situations where the system is complex and challenging to model, MPC may have to utilize model learning techniques to control the system efficiently. ML includes both model-free and model-based approaches. These methods typically require substantial amounts of data, time, and training to recognize patterns in motion gestures, speech and images, as well as to determine positions and orientations. With the advent of deep learning (DL), which employs multi-layered neural networks (NN) that simulate the brain's data processing, the capacity to learn from unlabeled data without human supervision (unsupervised learning) and generate patterns for decision-making has greatly advanced. However, most NNs are still predominantly trained in a supervised way by humans (supervised learning) [48, 77]. As artificial intelligence (AI) continues to evolve rapidly, DL has become increasingly relevant in RL as a powerful function approximator. RL uses a form of trial and error training that teaches machines and robots the model of a system by reinforcing its ideas and establishing a result. They have recently been employed in the control of exoskeletons in [122, 126] which demonstrated efficient squatting assistance with human interaction. However, future work is needed to further extend the framework to a variety of human walking patterns. This work is still an open issue. Various control design methods are already successful in other domains (e.g., humanoid robots). The Atlas robot from Boston Dynamics which can dynamically walk like a human while traversing uncertain terrain [99] employs a model-based control method to successfully achieve balance and control in motion planning and locomotion by combining the full kinematic model with a reduced dynamic model (e. g., COM, COP) of the robot instead of the full dynamics, which could be computationally prohibitive in solving trajectory optimization. The analysis and control of the RH5 humanoid robot in [47] is based on differential dynamic programming (DDP). The full-body trajectory optimization of RH5 showcased contact stability with DDP while generating walking trajectories using the classical control technique (Proportional-Derivative) position control. The MIT Cheetah 3 Robot [24] showed good gait performances using the MPC model with a reduced model dynamics (using COM) of the robot to determine ground reaction forces. Without the kinematics of the leg, the approach helped reduce the optimization problem to a quadratic program formulation that captures the dynamics of the robot's locomotion. Technological advances have paved the way for combining ML methods and neuroscience to achieve efficient and reliable control of human-machine interaction. For example, the demonstration of an essential EEG signal based on human brain feedback in [88] is used to reinforce robot learning in human-robot interaction. Furthermore, the application of event-related potential (ERP) has created a communication gap between the human brain and the computer or machine interface. In [89], a single trial data analysis is used to classify the activities of the brain by the influence of an ERP, which could be used as a vital tool for the interpretation of brain processes. Bionics and cybernetics are both theories of biological systems regarding the design and control of human-to-machine or human-to-robot interaction. It has shown how technology is progressing. Human motion intent

is best reflected on the leg muscles. Using EMG sensors to measure the electrical activity of the lower limb muscles will give additional and effective control of a bipedal walking pattern. The measured signals, fed as inputs to the controller, will give a good estimation when combined in parallel with the model of the exoskeleton mechanism, thereby producing an effective control strategy.

2.6.2 *Future Research Directions*

To design and effectively control a robust, stable, and low-cost bipedal exoskeleton robot with wide motion ranges similar to the natural human gait pattern, the focal point for future research directions should be centered on the following features:

HUMAN-ROBOT INTERACTION The exoskeleton device that supports the human body externally enables humans with lower limb disabilities to walk again by enhancing locomotion. Patients with joint diseases caused by OA and paralysis have weaker muscles that are insufficient to allow for convenient self locomotion. There are already efficient exoskeleton designs present in research and clinical institutions. However, they are not available or sustainable to society. The sustainability reasons may vary from individual prototypes, but generally, trust, confidence, and the feeling of being in control of an exoskeleton when strapped to the human body is not felt, and that alone creates fear to the wearer. Therefore, there is a need to know the motion intent of the limbs to give input to the controller as a feedback control element. The application of biosignal integration should be incorporated with the model-based control for effective human-robot interaction. Designing robot devices without efficient communication with humans is not sufficient to be relied on entirely. For a reliable and effective human-robot interaction, the robot should interpret and send feedback of its current condition to the human interface. Therefore, control instructions must be integrated into the robot design as discussed in [91] which also forms a part of the safety standards. While ML solutions are known for producing predictions and results for multiple use-cases much faster than humans, they lack the ability to understand and adapt to emotions. Humans, on the other hand, can adjust their decisions based on emotional insight, particularly when recognizing and correcting mistakes. This emotional adaptability is something robots and ML methods struggle to replicate, making it challenging for them to adjust when errors occur. To this end, we are not confident of the predictions, decisions, and results obtained through tasks conducted by ML. Furthermore, we often lack a clear understanding of how ML methods make decisions, particularly when it comes to correcting errors, which adds to the hesitation in fully relying on ML-driven results. Therefore, a shift to the next generation of AI called Explainable Artificial Intelligence (XAI), is a new technological approach that enables human-robot interaction to adapt, learn, optimize functions, and return intuitive feedback that is reliable, accurate, informative, and with decisive results. Furthermore, XAI is capable of continuous model evaluation [181, 202] to improve model performances by combining human instincts, ML algorithms used as black-boxes in describing AI model, and the features that influence the output based upon the input decisions as a glass-box model [186]. Using XAI

combined with the noninvasive EEG and EMG signals, and model-based MPC, an efficient human-robot interaction for bipedal walking exoskeleton robot is feasible.

CONTROL AND SAFETY Safety in robotics is a challenging problem, especially when it involves human-robot interaction (HRI). The most effective way of ensuring safety in HRI is to implement safety criteria early during the design phase rather than the application phase. This criterion makes the robot permanently safe. In order to enhance reliability, safety can be achieved during the design phase by three-level approaches [91]. The first level of safety occurs at the preliminary stage of the mechatronic design, referred to as the "safety by design". This approach emphasizes using innovative technology such as 3D printing to intensify the usage of lightweight materials for the hardware. Methods using internal cabling, embedded power units, and electronic components already exist, aiming to create a compact hardware structure. It is also accompanied by the introduction of shock absorbers like dampers or springs to subdue the effect of forces exerted on the human body by the actuators or external obstacles that come in contact with the human body. To further enhance safety, sensors that simulate the sense of touch and motion can be combined with visual sensors, as seen in previous research [79, 125]. Moreover, the transmission of forces through soft tissues using elastic fibers, and viscoelastic elements can compensate for unnecessary force, providing an added layer of safety. The second level of safety, referred to as "low-level control," involves controlling the hardware components, specifically the joint actuators. Unlike positional control, which cannot adjust its trajectory in the presence of an obstacle, low-level control uses force and torque control to allow the robot to change its trajectory by adjusting the torque on its joints. This approach ensures that the robot can respond more dynamically to obstacles, reducing the risk of injury during operation [56]. The third level, termed "mid-level control," focuses on controlling the overall system. This level provides robust safety for humans by utilizing sensors both inside and outside the robot. These sensors monitor the robot's current state and intended trajectory, offering feedback control before the robot navigates its path. To guarantee safety at this level, it is important to consider the limitations of positions, velocities, and torque for both human joints and the exoskeleton system during trajectory design and feedback control. Advanced trajectory optimization methods can help manage the soft and hard constraints, ensuring safe operation [47, 107]. In all mechatronic designs, safety is paramount. Therefore, the exoskeleton's mechanical structure must align closely with the human limb's anatomical structure to prevent pain and injuries, providing users with a natural, comfortable experience. By incorporating nonlinear optimal control techniques, model-based control methods, and AI integrated with biosignal technology, future exoskeletons could offer a natural-feeling artificial device that disabled individuals can rely on for effective assistance. Additionally, the integration of HITL control will significantly improve the exoskeleton's adaptability, user interaction, and effectiveness, making it more suitable for diverse users (e.g., in rehabilitation)

COST Given the value of exoskeleton devices for military applications, the cost should not be a significant concern, especially since these devices are specifically commissioned by the government to enhance national security. In industrial application, start-up industries and already

established companies may wish to enhance the muscular strength of their workers, reduce fatigue, and provide fast workability with extra precision. In the case of medical applications, exoskeleton devices for personal usage are not affordable for low-income earners. The goal of developing medical exoskeleton devices is to assist the disabled and augment power for industrial purposes. Affordability should also be a vital key to consider while designing robots for these applications. The aim of the design could be defeated if the purchasing price is relatively high. Therefore, to make the device affordable and equally not compromising the quality and efficiency, the material technology used in building the hardware for the exoskeleton device should be lightweight and compact. The mechanical and electronic components such as actuators, sensors, power units, and configurable integrated circuits should be efficient, affordable, available, and conform to performance. There is a need to apply new technologies such as carbon nanotubes to produce artificial muscles to replace motor actuators, since carbon is abundant in nature. Silicon is readily available in nature with abundant quantity. It is cheap, synthetically purified into wafers, and serves as insulators and semiconductors for power transmission. Chips formed from the fabrication of the wafers can adapt to new information in transmitting signals for human-robot interaction. The silicon chips can be designed as integrated circuits embedded in the actuators, sensors, and other electronic devices for controlling the exoskeleton hardware framework. Robotics is not primarily about actuators, but by concentrating on actuator designs, sensors, software, control theory, mechatronics, and AI, using readily available elements from nature, we can achieve efficient exoskeleton control at a reduced cost.

2.7 CONCLUSION

This chapter presented the state-of-the-art (SOTA) design and control of exoskeleton robots for improving human locomotion. Through this survey, we gain insights into the substantial challenges faced in conceptualizing the design and implementing control strategies for these exoskeleton robots, as well as potential approaches to mitigate these challenges. Furthermore, the proposed future directions present innovative technological advancements that could enhance the commercial viability of exoskeleton robots while contributing to quality of life.

The subsequent Chapter 3 will present the insights gained from the design strategies discussed in Chapter 2, specifically focusing on the modular lower extremity joints of the Recupera-Reha exoskeleton. This could enable the implementation of optimized design approaches to address the drawbacks of the existing exoskeleton systems and improve its performance.

3

DESIGN ENHANCEMENT OF THE ASPM

"We have forty million reasons for failure, but not a single excuse."

— Rudyard Kipling

Tijjani, I. (2022). Finding Optimal Placement of the Almost Spherical Parallel Mechanism in the Recupera-Reha Lower Extremity Exoskeleton for Enhanced Workspace. In: Müller, A., Brandstötter, M. (eds) Advances in Service and Industrial Robotics. RAAD 2022. Mechanisms and Machine Science, vol 120. Springer, Cham.

3.1 INTRODUCTION

In the previous Chapter 2, we thoroughly discussed the various design and control strategies used to address the advantages and limitations of selected SOTA lower extremity joints.

This chapter delves into the basics of robot geometry in relation to the kinematic analysis of the Recupera-Reha exoskeleton's hip and ankle modules. The main goal is to improve the limitations of the system. The chapter is structured as follows:

- Section 3.2 delves into the significance of modular exoskeleton robots in aiding human locomotion, providing a concise overview of parallel mechanisms, particularly the ASPM, while discussing their strengths and weaknesses. Furthermore, the section addresses the main problems associated with the ASPM joint module, which represents the hip and ankle joints of the Recupera-Reha exoskeleton.
- Section 3.3 introduces the ASPM device's kinematic analysis to facilitate the formulation of its dynamic model.
- Section 3.4 outlines the procedure for determining the optimal placement configuration of the ASPM device within the leg.
- Section 3.5 presents preliminary simulation results and further discusses the method of improving the limitations of the ASPM device.
- Section 3.6 presents the kinematic analysis of the ASPM, as well highlights the design modification of the Recupera-Reha foot base to improve stability and enhance the performance of the exoskeleton robot.
- Section 3.7 offers a discussion.
- Finally, Section 3.8 concludes the chapter.

3.2 PROBLEM DESCRIPTION

The increased prevalence of conditions affecting mobility has resulted in a growing demand for innovative solutions to assist individuals with walking impairments. One such solution gaining prominence is the acquisition of modular lower extremity exoskeleton devices for walking assistance. These devices offer promising potential for enhancing mobility and independence for individuals with various mobility challenges, including those with neurological disorders, musculoskeletal injuries, or age-related mobility limitations [74]. Furthermore, with advancements in medical technology and rehabilitation practices, there is a greater emphasis on enabling individuals with mobility impairments to participate actively in physical exercise and social interactions [5]. Modular ankle exoskeleton devices offer a promising solution by providing customizable support tailored to users' specific needs, allowing for improved mobility and quality of life. The design of parallel mechanisms plays a crucial role in addressing the challenges associated with modular ankle exoskeleton devices. A parallel manipulator (PM) or parallel mechanism is a robotic system device that offers high stiffness, payload capacity, speed, and accuracy due to combination of two or more kinematic chains. In particular, spherical parallel manipulator (SPM) is a PM which allows only rotational motions of its end-effector platform. For instance, the prominent three (3) DOF Agile Eye [62] is a type of SPM and finds application in camera orienting devices. The PKAnkle [128] is a redesigned prototype of Agile Eye that fits in for ankle neuro-rehabilitation and is capable of providing wide ankle motion ranges but has problems associated to alignment with the human ankle joint complex. The majority of the researchers in the exoskeleton application domain for gait rehabilitation [16, 55, 95, 117, 130, 208, 226], exploits the advantages of an SPM design approach (see [111] for a recent survey), with emphasis on increasing the workspace limitation, and finding a suitable alignment configuration with the human ankle joint. Engineers can optimize ankle exoskeleton devices for improved performance, comfort, and user experience by integrating parallel mechanism designs. However, designing effective parallel mechanisms for ankle exoskeleton devices requires addressing several technical challenges. These include optimizing the kinematic and dynamic characteristics to ensure natural and efficient gait patterns, minimizing device weight and bulkiness to enhance user comfort and acceptance, and integrating intelligent control algorithms to adapt to user movements and environmental conditions seamlessly.

The novel Active Ankle (see Figure 3.1) first introduced in [130] is a wearable ankle exoskeleton device that exploits the advantages of a PM. It is an ASPM similar to the SPM in structural design, with 3 DOF and 3 actuators capable of three principal movements; DF-PF, EV-IN, and AD-AB motions. The design of the Active Ankle mechanism represents a module for the ankle and hip joints of the Recupera-Reha full-body exoskeleton [101] in Figure 3.2. An extensive kinematic analysis of the mechanism is available in [103, 104, 106]. The current configuration of the active ankle mechanism within the Recupera-Reha exoskeleton presents notable limitations. Specifically, the alignment of its joint axes on the exoskeleton leg does not correspond adequately with those of the human ankle joint complex, resulting in a restricted workspace. Therefore, identifying an optimal placement for the ankle mechanism within the exoskeleton leg design is crucial. Additionally, a challenge arises from the passive ball and

socket joint limit on the actuator, which further constrains the available workspace for the principal movements. To address these issues, modifying the actuator's physical limits and ensuring proper alignment with the human ankle joint complex could enhance the workspace for the principal movements and potentially serve as a tool for ankle joint rehabilitation.

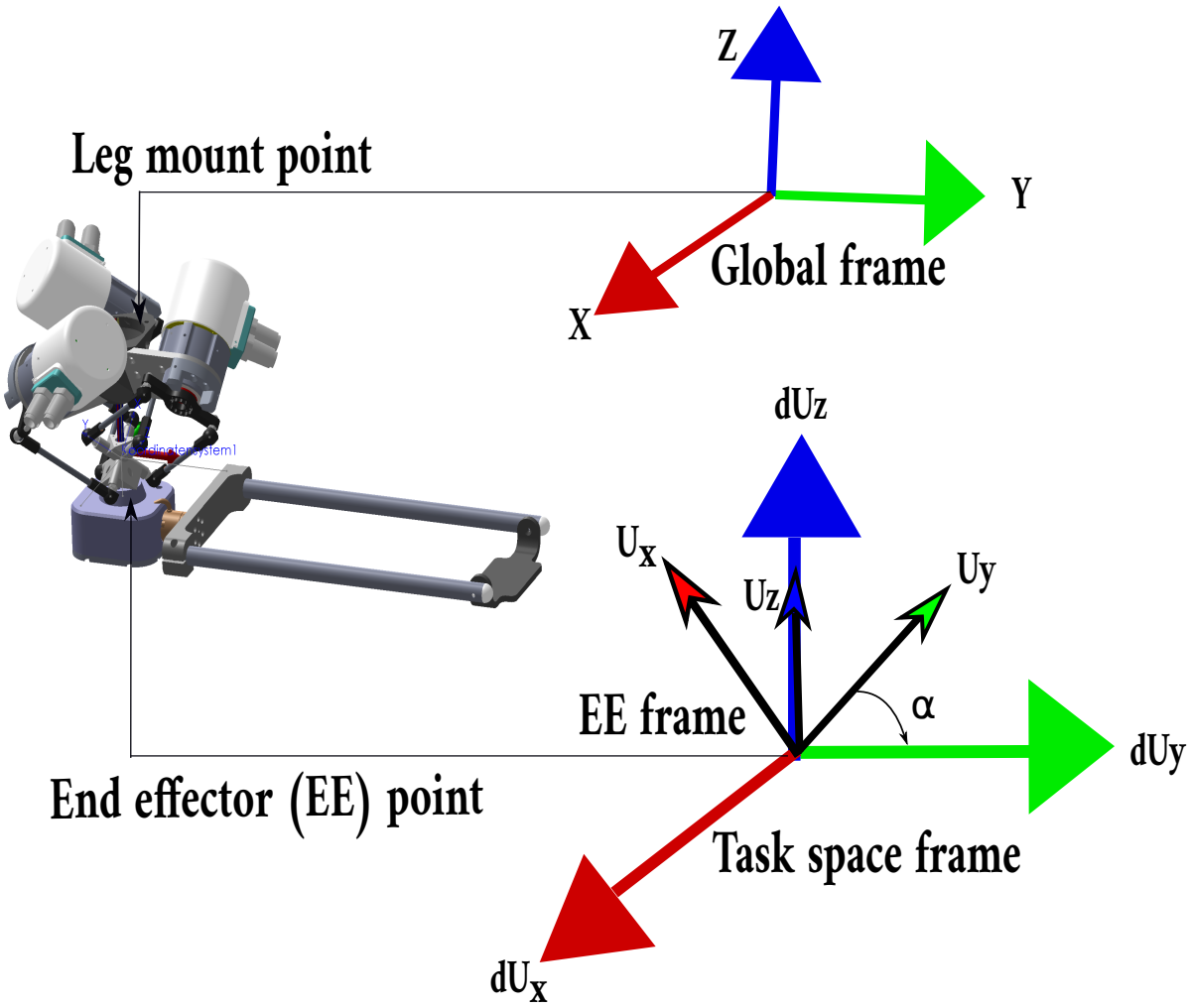

Figure 3.1: ASPM ankle device [104]

3.3 KINEMATIC ANALYSIS OF THE ANKLE AND HIP JOINT MODULES

This section highlights the analysis of the inverse kinematic problem of the active ankle mechanism adapted from [104]. As earlier stated, the hip and ankle joint modules are designed as ASPM, to drive a spatial quadrilateral that intersects its three rotative actuators perpendicularly at its end-effector (EE) point. The opening angle of the ball and socket joint for the mechanism is limited by $\pm 25^{\circ}$ actuator angle constraint (q_{min}, q_{max}), while the available ROM for the task space angles $(\theta_{min}, \theta_{max})$, is constrained by a $\pm 90^{\circ}$ physical limit (θ). The fascinating feature in the mechanism design structure is that the physical configuration of its joint axes is capable

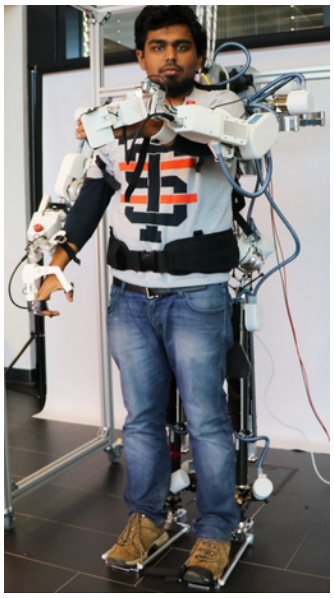

Figure 3.2: Recupera-Reha full-body exoskeleton [101]

of bearing any force applied without external torque from the actuators. In essence, a design structure of the joint axes different from the previous configuration will require additional torques from the actuators to drive the device, thus, increased cost. Due to the ASPM design nature, the existence of translation shifts in the EE point is neglected due to its small value when the mechanism is used in the application point of view. Hence, only the rotative universal joints with the spherical cut joints were utilized in the mechanical design structure, but in the analytical kinematic formulation, the translation shifts were included.

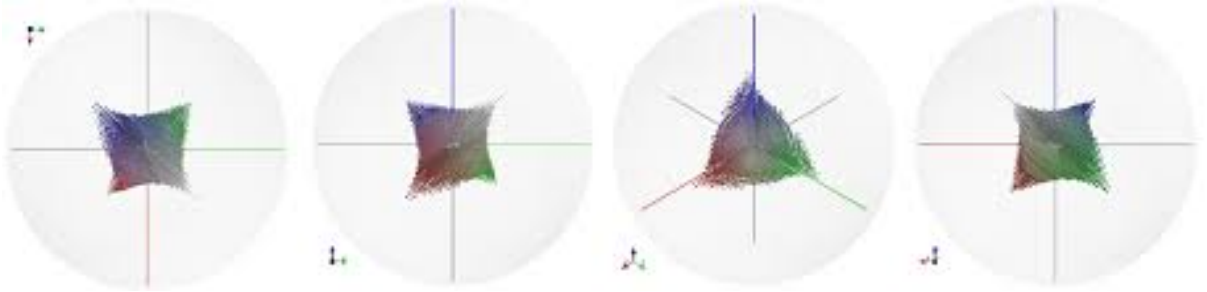

Figure 3.3: Feasible workspace configurations adapted in [104].

The forward kinematic problem that derives the position of the EE as a function of its joint variables is difficult to compute analytically for a complex PM like the ASPM since it has a limited usable workspace. Therefore, you can not ascertain the feasible workspace that fits into a specific joint configuration. For example, from the available workspace in the rotative domain shown in Figure 3.3 as reported in the previous variant of the active ankle mechanism, we can not discern the exact configuration for a given set of joint angles. Hence, the knowledge of the positional coordinates of the device alone is not sufficient to determine the placement of the mechanism in the leg. Therefore, we exploit the *RIGM* that computes the rotative joint space

angles and EE positional shifts from the desired orientation, similar to the human ankle joint. However, to achieve a desired orientation of the EE-frame, the *RIGM* uses the parameterized orientation of the principal movement joint axes vectors represented by $\mathbf{u_x}$ $\mathbf{u_y}$ and $\mathbf{u_z}$ instead of the position coordinates to find the input joint angles. The joint axes vectors are obtained from a computer-aided design (CAD) model of the active ankle device and adapted to the *RIGM*.

To find an optimal placement point of the ankle mechanism in the leg with an orientation aligned to the human ankle joint complex as shown in Figure 3.4a, three different coordinate systems were considered at the EE point as shown in Figure 3.4b. The first coordinate is the EE-frame (joint axes encoded in yellow color), with a different orientation not properly aligned to the ankle complex of the human leg. A second coordinate is the task-space frame located at the EE-point whose joint axes vectors ($\mathbf{u_x}$, $\mathbf{u_y}$, $\mathbf{u_z}$) are parallel to the global coordinate attached to the leg mount point. Our objective is to optimize the placement angle (α) so that the mounting frames at the leg mount point and the EE-point are aligned parallel to each other. The third coordinate frame (joint axes encoded in black color) is called the rotated frame. Considering the rotated frame with the joint axes ($\mathbf{du_x}$, $\mathbf{du_y}$, $\mathbf{du_z}$) at zero-configuration, only the $\mathbf{du_z}$ joint vector is fixed in the same direction with the z-axis (blue color) of the global frame, unlike $\mathbf{du_x}$ and $\mathbf{du_y}$ which are perpendicular to each other. The ASPM mechanism placement angle α is the angle between the joint vectors of the task-space frame and the rotated frame. We want to parameterize the rotated frame with respect to the task-space frame and map the generated joint angles which are within the actuator limit to the EE-frame.

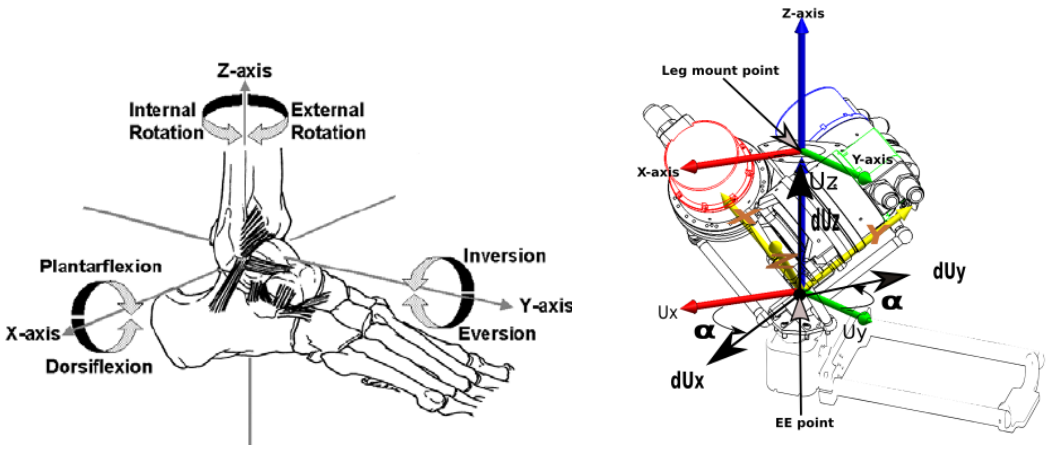

(a) Human ankle complex [220]

(b) ASPM coordinate frames

Figure 3.4: Human and ASPM ankle complex

Table 3.1 presents the ROM for the different motion types in comparison to the human ankle joint motions reported in [104]. At zero-configuration, discernible differences in the absolute sum of minimum (Min.) and maximum (Max.) angles indicate variances between the human ankle motion ranges and those of the three other mechanisms. The active ankle exhibits limited ROM in the DF-PF motion, as observed in the previous work [104], which is an essential motion trajectory for the ankle joint fucntionality. However, this may prove inadequate for dynamic walking, which is required in gait rehabilitation. Conversely, the SPKM

and PKAnkle devices showcase restricted ROM in their respective EV-IN and AD-AB motion types, potentially adequate for typical human daily walking activities. Nonetheless, according to the findings in [189], a minimum ROM of 37° for stair-ascending and 56° for descending is necessary for the DF-PF motion type movement, resulting in an absolute sum of 93°. For normal walking, however, a ROM of less than 93° is sufficient. Thus, an augmented ROM is essential to facilitate enhanced dynamic walking for common human daily activities and is also imperative for athletic pursuits.

Table 3.1: Comparison between the human and existing ankle joint ROM

Motion type	Human ankle			Active ankle [104]			SPKM [16]			PKAnkle [128]		
	Min.	Max.	Abs.	Min.	Max.	Abs.	Min.	Max.	Abs.	Min.	Max.	Abs.
DF-PF	-20°	50°	70°	-19.83°	37.23°	57.06°	29.8°	45.8°	75.6°	-40°	35°	75°
EV-IN	-15°	35°	50°	-15.00°	35.00°	50.00°	17 °	22°	39°	-25°	20°	45°
AD-AB	-30°	45°	75°	-29.20°	36.96°	66.16°	25.9°	36°	69.10°	-20°	10°	30°

3.4 OPTIMAL PLACEMENT FOR THE HIP AND ANKLE MECHANISMS IN THE LEG

It is of interest to know the criteria for modification of the current design even though the results obtained from the kinematic model analysis of the mechanism in [104] demonstrated the DOFs for the three rotative actuators with a workspace modality that shows three principal movements for application as an ankle joint. However, the use-case as an ankle joint rehabilitation device towards enhancing recovery from ankle sprain, the following two cases could be used to increase the usable workspace for the active ankle and obtain an optimal configuration point of placement in the exoskeleton leg:

1. **Case 1:** Increasing the opening angle for the ball and socket joint to have wider ROM.
2. **Case 2:** For the optimal placement point of the mechanism in the leg, we require the transformation of the task space frame with respect to the rotated frame.

3.4.1 *Parameterization Procedure*

The geometry of the ASPM device modules are analyzed using Matlab. The $\pm 25°$ actuator angle constraints are initially set for the simulation to compare the previous experimental results obtained in [104] and later increased to $\pm 27°$. The parameterization procedure is described in algorithm 1, for a range of α in line 1 which is limited by θ, the transformation matrix (T) in line 2 is built from a Matlab command *makehgtform*, that rotates the vector $\mathbf{u_z}$ by α in radians. Then, line 3 extracts the rotation matrix (R) part of T. The vectors $\mathbf{u_x}$ and $\mathbf{u_y}$ are now parameterized by R in line 4 and line 5 respectively as the orientation vectors, such that they are orthogonal to each other and lie on the same plane perpendicular to the $\mathbf{u_z}$ axis. The *RIGM*

function in line 7 takes into account the computed orientation vectors from the parameterized vectors, and the actuator constraints as input while line 8 produces the joint space angles which are within the actuator constraints as outputs.

In algorithm 2, the function routine *TaskSpaceAngles* in line 1 maps out the joint space angles to α in line 2, line 3, and line 4 respectively, to find the relationship between them. line 7 returns the boundary limits on the task space angle curves computed from line 5 and line 6. The function routine *IntersectCurves* in line 8 uses the Mathworks *InternX* function to compute the minimum and maximum intersection points on the three curves. The intersection points within the curves that are less than or greater than zero are computed in line 9 and line 10 respectively. These are the trade-off points within the actuator actuator limit and the physical limit.

Algorithm 1: Parameterization Procedure

Input: Joint axes vectors:
$\mathbf{u_x} = [-0.8165; 0.4082; 0.4082]$, $\mathbf{u_y} = [0; -0.7071; 0.7071]$, and $\mathbf{u_z} = [1; 1; 1]$
Output: Joint angles:
$q_x,\ q_y,\ and\ q_z$

1 **for** $\alpha = -\pi : 2\frac{\pi}{n} : \pi$; **do**

2 $\quad \mathbf{T} \leftarrow \begin{bmatrix} -0.3333 & 0.6667 & 0.6667 & 0 \\ 0.6667 & -0.3333 & 0.6667 & 0 \\ 0.6667 & 0.6667 & -0.3333 & 0 \\ 0 & 0 & 0 & 1 \end{bmatrix}$;

3 $\quad \mathbf{R} \leftarrow \mathbf{T}(1:3, 1:3)$;

4 $\quad \mathbf{du_x} \leftarrow (\mathbf{R} \cdot \mathbf{u_x})$;

5 $\quad \mathbf{du_y} \leftarrow (\mathbf{R} \cdot \mathbf{u_y})$;

6 $\quad \mathbf{du_z} \leftarrow (\mathbf{u_z})$;

7 $\quad$ **Function** `RIGM(`$\mathbf{du_x}$, $\mathbf{du_y}$, $\mathbf{du_z}$, q_{min}, q_{max}`)`**:**

8 $\quad\quad [q_x, q_y, q_z] \leftarrow (-25^\circ \geq q \leq 25^\circ)$;

9 $\quad\quad$ **return** q_x, q_y, q_z

10 **End**

Algorithm 2: Computation of task space angles

Input: $(\alpha, q_{min}, q_{max}, q_x, q_y, q_z)$
Output: (θ)
Function `TaskSpaceAngles(`α, q_x, q_y, q_z, q_{min}, q_{max}`)`**:**
  $L_x \leftarrow [\alpha; q'_x]$
  $L_y \leftarrow [\alpha; q'_y]$
  $L_z \leftarrow [\alpha; q'_z]$
  $L_{min} \leftarrow [\alpha; q_{min} \cdot length(\alpha)]$
  $L_{max} \leftarrow [\alpha; q_{max} \cdot length(\alpha)]$
  return L_{min}, L_{max}
  Function `IntersectCurves(`L_{min}, L_{max}, L_x, L_y, L_z`)`**:**
    $\theta_{min} \leftarrow max(\theta < 0)$
    $\theta_{max} \leftarrow min(\theta > 0)$
    return $\theta_{min}, \theta_{max}$
End Function

3.5 PRELIMINARY SIMULATION RESULT

The graphical representation for the variation of (θ_{min}, θ_{max}) and α, respecting the $\pm 25^\circ$ actuator constraint on the opening angle of the ball and socket joint is depicted in Figure 3.5, for different configuration points. For instance, at 0° configuration point, the sum of the intersection points on the lower and upper boundaries of each curve produced the absolute sum of 63.46° DF-PF, 74.35° EV-IN, and 71.29° AD-AB ROM for the three principal movements of the ASPM ankle joint module. Similarly, the process is repeated for the hip joint module shown in Figure 3.6. Additionally, Table 3.2 and Table 3.3 show the information extracted from the above figures. The green shaded rows in the tables are the chosen optimal placement configuration points of the ankle and hip mechanism in the leg because the configuration points provide a symmetric movement in both directions producing a wide ROM for the principal movements.

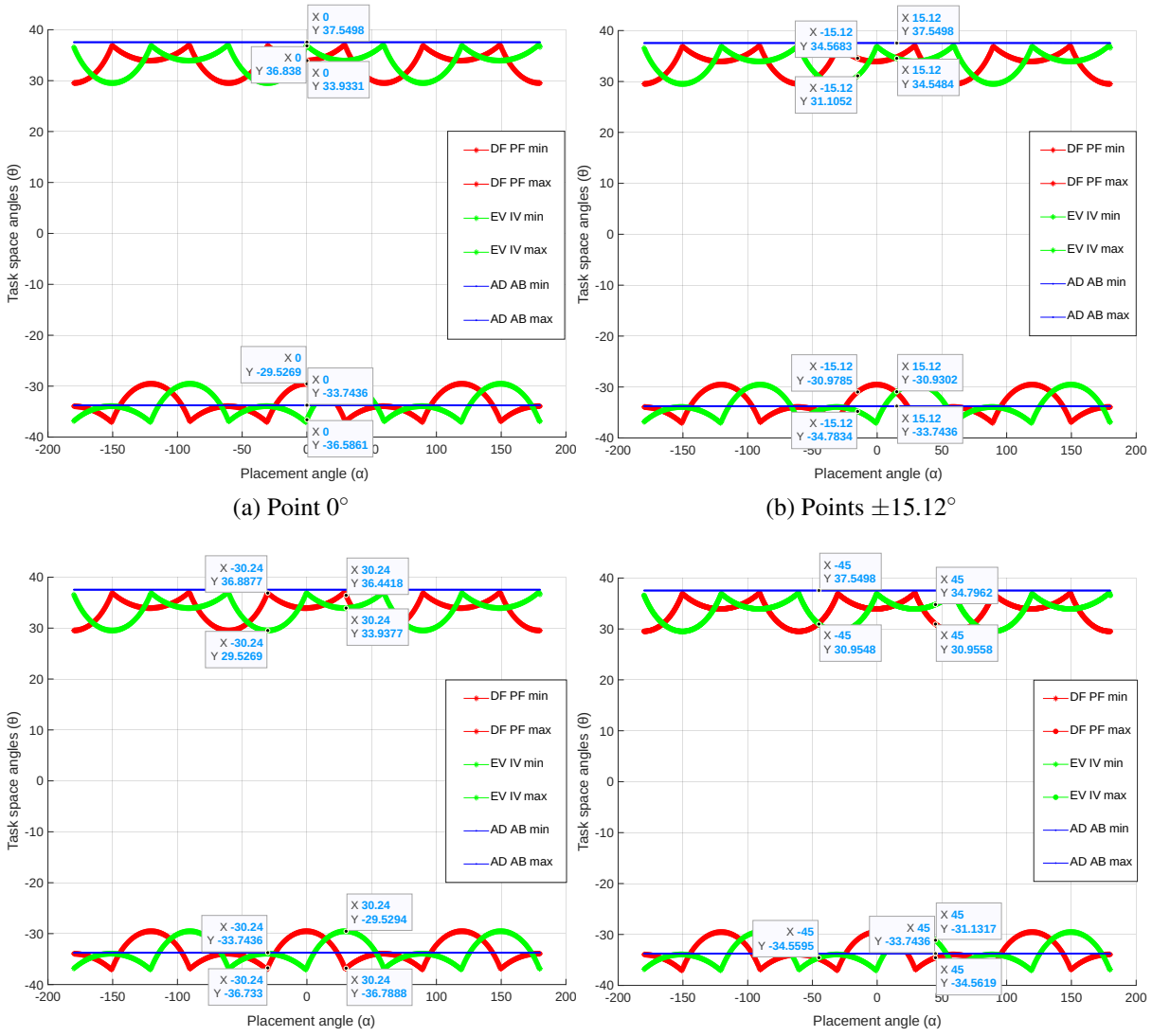

(a) Point 0° (b) Points ±15.12°

(c) Points ±30.24° (d) Points ±45°

Figure 3.5: Ankle configuration points with ±25° actuator constraint

Table 3.2: Ankle motion ranges with ±25° actuator constraint

Placement angle(α)	DF-PF			EV-IN			AD-AB		
	Min.	Max.	Absolute	Min.	Max.	Absolute	Min.	Max.	Absolute
0°	-29.53	39.93	69.46	-36.59	36.84	73.43	-33.74	37.55	71
−15.12°	-30.98	34.57	65.55	-34.78	31.11	65.89	-33.74	37.55	71
15.12°	-30.93	34.55	65.48	-30.93	34.55	65.48	-33.74	37.55	71
−30.24°	-36.73	36.89	73.62	-33.74	29.53	63.27	-33.74	37.55	71
30.24°	-36.79	36.44	73.23	-29.53	33.94	63.47	-33.74	37.55	71
−45°	-34.56	30.95	65.51	-34.56	30.95	65.51	-33.74	37.55	71
45°	-34.56	30.96	65.52	-31.13	34.80	65.93	-33.74	37.55	71

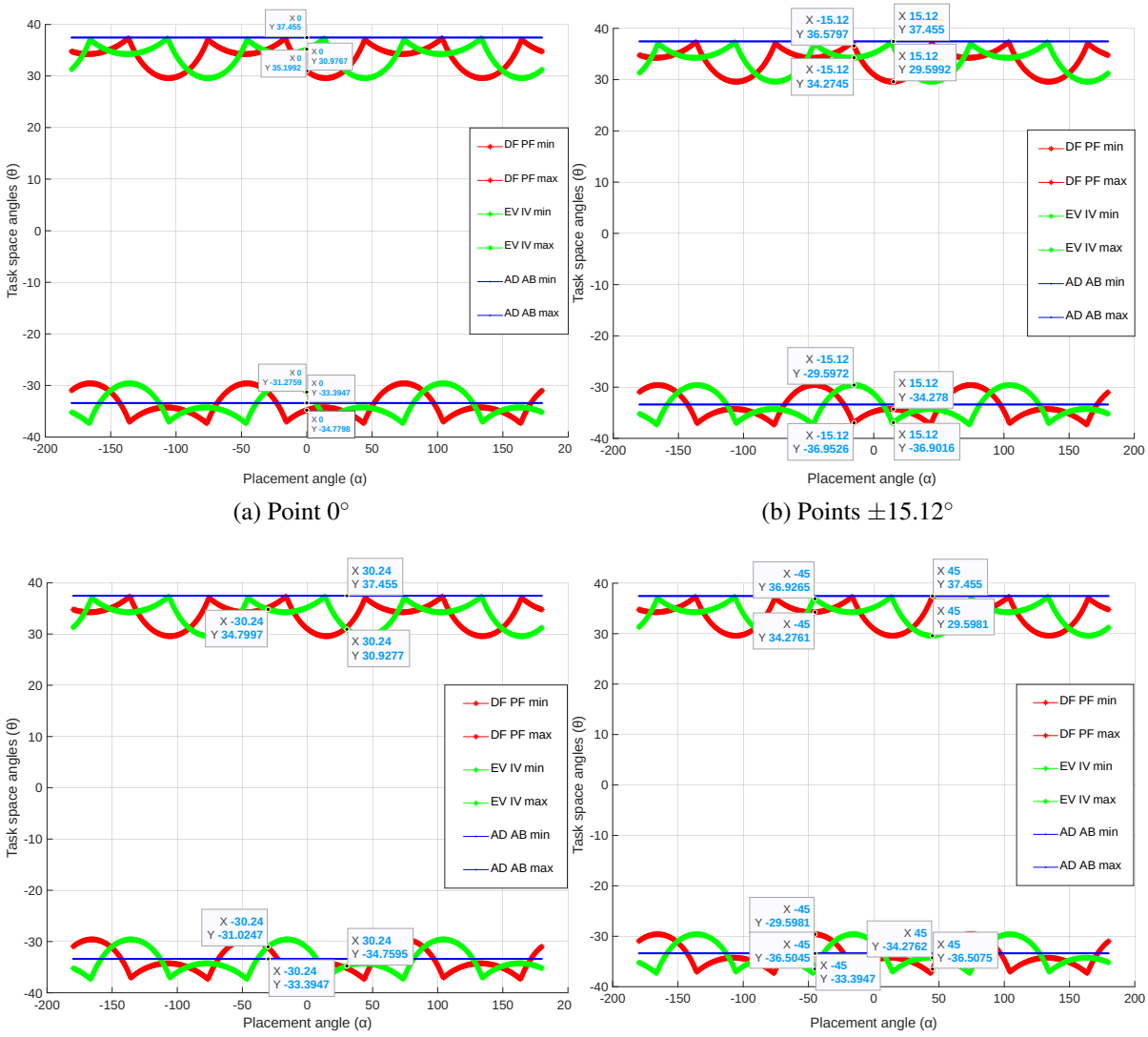

(a) Point 0° (b) Points ±15.12°

(c) Points ±30.24° (d) Points ±45°

Figure 3.6: Hip configuration points with ±25° actuator constraint

Table 3.3: Hip motion ranges with ±25° actuator constraint

Placement angle(α)	DF-PF			EV-IN			AD-AB		
	Min.	Max.	Absolute	Min.	Max.	Absolute	Min.	Max.	Absolute
0°	-34.78	30.98	65.76	-31.28	35.20	66.48	-33.39	37.45	71
−15.12°	-36.95	36.58	73.53	-29.60	34.27	63.87	-33.39	37.45	71
15.12°	-34.28	29.60	63.88	-36.90	37.45	74.35	-33.39	37.45	71
−30.24°	-31.02	34.80	65.82	-31.02	34.80	65.82	-33.39	37.45	71
30.24°	-34.76	30.93	65.89	-34.76	30.93	65.69	-33.39	37.45	71
−45°	-29.60	34.28	63.88	-36.50	36.93	73.93	-33.39	37.45	71
45°	-36.51	37.45	73.96	-34.28	29.60	63.88	-33.39	37.45	71

Furthermore, understanding the relationship between the active joint angles and the task space angles reveals a trade-off within the actuator constraint boundary points. However, the trade-off allows us to modify the opening angle of the ball and socket joint on the hardware mechanism to an actuator constraint of $\pm 27^{\circ}$. As a result, we have control over the possible task space angles. Our initial design optimization choice focuses on identifying an optimal configuration point that enhances the workspace for the principal movements of the ASPM joint modules. To achieve symmetric movement in both directions, it is necessary to establish a linear relationship between the physical limits on the actuator angles and the task space angles. The graphs in Figure 3.7 and Figure 3.8 are shown in more detail in Table 3.4 and Table 3.5, which are tables for certain configuration points (0°, $\pm 15.12^{\circ}$, $\pm 30.24^{\circ}$, $\pm 45^{\circ}$). The study shows that the ankle joint module has symmetrical movement with a wider ROM at the $\pm 30.24^{\circ}$ configuration point in Table 3.4. The hip joint module Table 3.5, on the other hand, has the most highest ROM at the -15.12° configuration point, but it doesn't have a symmetric counterpart. This asymmetry arises due to the interdependence between the mounting points of the right and left hip joints. Consequently, while a wider ROM is attainable, symmetry in the reachable workspace is not achieved at the hip joint, except for a lower ROM found at the $\pm 30.24^{\circ}$ configuration points.

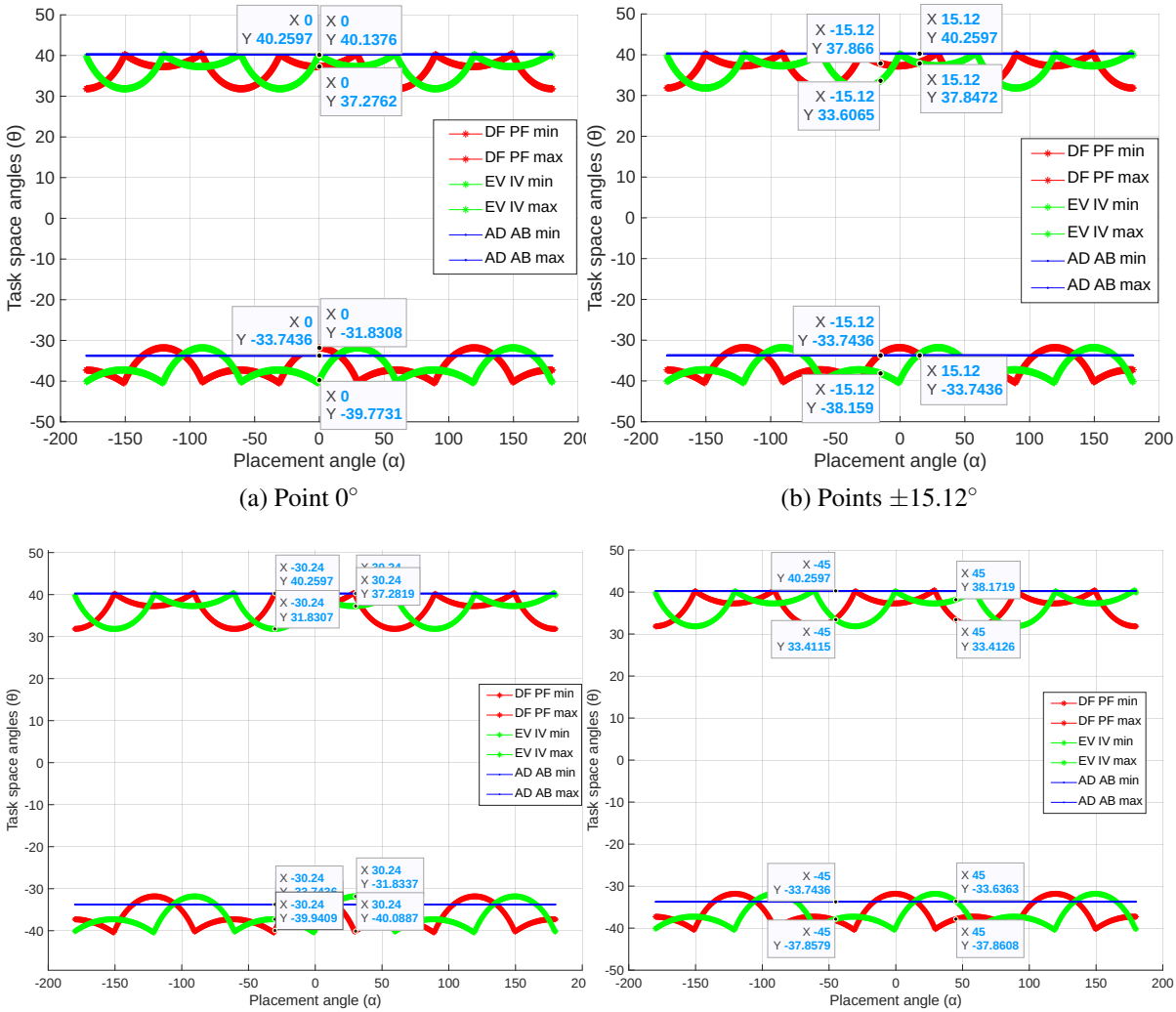

(a) Point 0°

(b) Points ±15.12°

(c) Points ±30.24°

(d) Points ±45°

Figure 3.7: Ankle configuration points with ±27° actuator constraint

Table 3.4: Ankle motion ranges with ±27° actuator constraint

Placement angle(α)	DF-PF			EV-IN			AD-AB		
	Min.	Max.	Absolute	Min.	Max.	Absolute	Min.	Max.	Absolute
0°	-31.83	37.28	69.11	-39.77	40.14	79.91	-33.74	40.26	74
−15.12°	-33.74	37.87	71.61	-38.16	33.61	71.77	-33.74	40.26	74
15.12°	-33.74	37.85	71.59	-33.74	37.85	71.59	-33.74	40.26	74
−30.24°	-39.94	40.26	80.20	-37.28	31.83	69.11	-33.74	40.26	74
30.24°	-40.09	40.26	80.35	-31.83	37.28	69.11	-33.74	40.26	74
−45°	-37.86	33.41	71.27	-37.86	33.41	71.27	-33.74	40.26	74
45°	-37.86	33.41	71.27	-33.64	38.17	71.81	-33.74	40.26	74

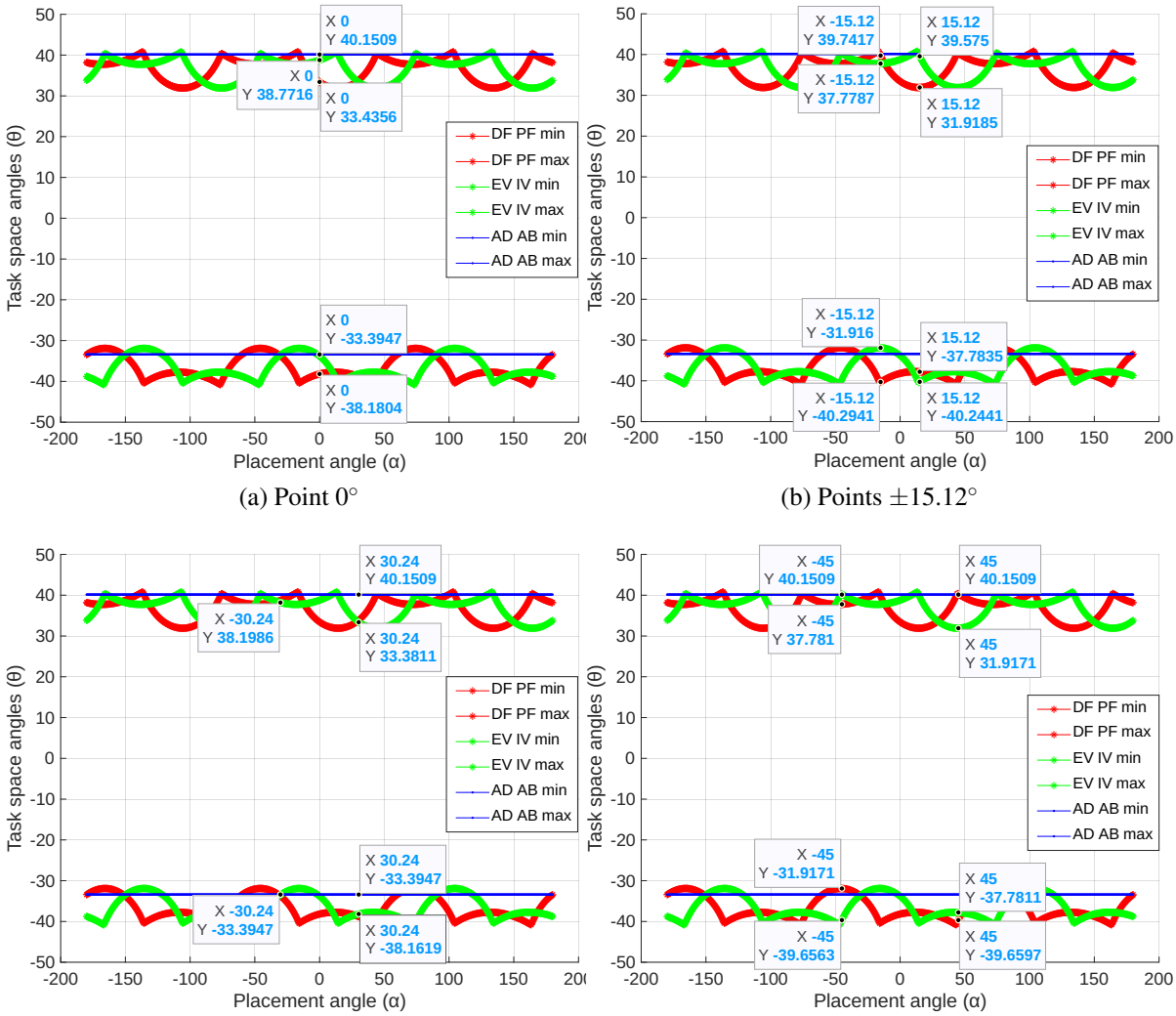

(a) Point 0°

(b) Points ±15.12°

(c) Points ±30.24°

(d) Points ±45°

Figure 3.8: Hip configuration points with ±27° actuator constraint

Table 3.5: Hip motion ranges with ±27° actuator constraint

Placement angle(α)	DF-PF			EV-IN			AD-AB		
	Min.	Max.	Absolute	Min.	Max.	Absolute	Min.	Max.	Absolute
0°	-38.18	33.44	71.62	-33.39	38.77	72.16	-33.39	40.15	74
−15.12°	-40.29	39.74	80.03	-31.92	37.78	69.70	-33.39	40.15	74
15.12°	-37.78	31.92	69.70	-40.24	39.57	79.81	-33.39	40.15	74
−30.24°	-33.39	38.20	71.59	-33.39	38.20	71.59	-33.39	40.15	74
30.24°	-38.16	33.38	71.54	-38.16	33.38	71.54	-33.39	40.15	74
−45°	-31.92	37.78	69.70	-39.66	40.15	79.81	-33.39	40.15	74
45°	-39.66	40.15	79.81	-37.78	31.92	69.70	-33.39	40.15	74

3.6 DESIGN MODIFICATION OF THE RECUPERA-REHA FOOT BASE

The design of the foot base plays a crucial role in enhancing stability and performance of the legged robotic systems. The feet are not just a base of support and point of contact with the ground; they are the cornerstone of balance. Studying the relation between foot design and stability is key to ensuring balance and posture of legged robots. The stability of the human body, as well as many bipeds, is intricately tied to the structure of the foot. A well-aligned foot base is crucial for maintaining balance and preventing instability, highlighting how foundational biomechanics contribute to overall stability. The foot base support is highly significant in assessing dynamic stability for an exoskeleton robot walking. A smaller foot base may suffice for certain applications but can lead to issues such as tipping or instability when the system is subjected to lateral forces or operates on uneven terrain. To achieve balance and posture, the robot's COM and COP should be within the foot base support [73], i.e., the support polygon is dependent on the frame in contact with the ground surface.

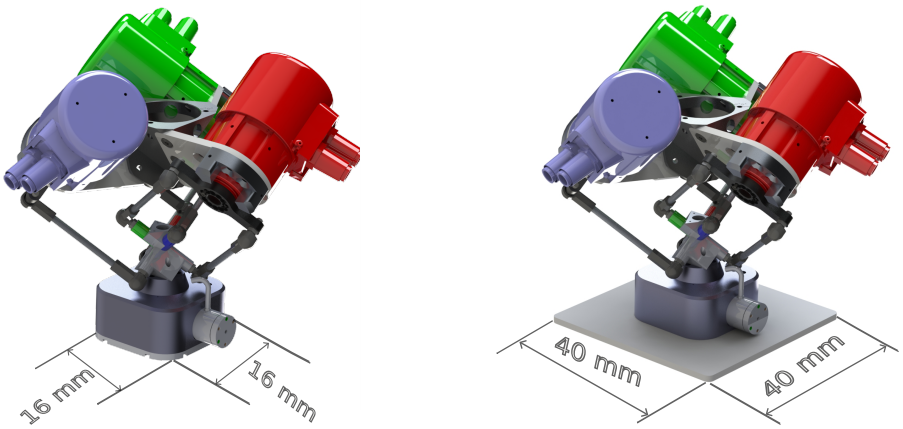

(a) Existing ASPM ankle foot base (b) Modified foot base

Figure 3.9: CAD prototype of the Recupera-Reha foot base

The geometry of the foot base have been modified to increase ground contact area while maintaining compatibility with the existing robotic system. The design modification includes features such as:

- Increased surface area for better stability and center of pressure distribution.
- Reinforced edges to prevent deformation under load.
- Mounting points compatible with existing system components.

The two-foot bases shown in Figure 3.9 provide varying levels of stability depending on their dimensions. The 40 mm x 40 mm foot base shown in Figure 3.9b is the modified foot base, which has a wide support base area that comes into contact with the ground. It offers

enhanced stability due to its broader surface area. The increased dimensions help distribute weight more evenly, significantly reducing the risk of tipping or wobbling. This makes it particularly advantageous for applications requiring a stable and secure foundation, such as supporting human body weight or maintaining balance on even surfaces. In contrast, the 16 mm x 16 mm foot base shown in Figure 3.9a with a smaller foot base has a more compact footprint. Although it suits applications with limited space or lighter loads, its smaller surface area results in less stability than the larger base during standing and walking. This could increase the risk of instability or tipping under heavier or uneven loads. Therefore, the 40 mm x 40 mm foot base is ideal for scenarios where maximum stability is crucial, while the 16 mm x 16 mm foot base is better suited for situations with lighter requirements and spatial constraints.

3.7 DISCUSSION

The goal of this study is to determine the optimal position and orientation of the ankle and hip joint mechanisms within the leg structure of the Recupera-Reha exoskeleton. The existing ASPM prototype imposes a constraint on the actuator movement, limiting it to $\pm 25^{\circ}$, which in turn restricts the workspace available for the mechanism's primary movement. Given the intricate design complexity of the ASPM, identifying an optimal placement point within the leg structure poses a significant challenge. But by using the RIGM method on the mechanism and changing the actuator constraint to $\pm 27^{\circ}$, it was possible to identify an optimal placement point that allows for an expanded workspace encompassing a wider ROM. The underlying rationale behind these three principal movements is to facilitate extensive motion capability, adaptation to uneven terrain, balance maintenance, and provision of stability and propulsion during various activities such as standing, walking, running, and rehabilitation from ankle sprain.

3.8 CONCLUSION

This chapter presents a comprehensive kinematic analysis of the hip and ankle joint modules for their optimal placement in the Recupera-Reha leg. Since finding the optimal placement of the ASPM modules in the leg is an inverse kinematic problem, the analysis exploits the RIGM to compute the rotation joint angles and end-effector positional shifts from a desired orientation, in order to find the task space angles with wide motion ranges suitable for the principal movements of the ASPM joint modules. The kinematic analysis of the ASPM joint modules, detailed in this chapter, will serve as the foundation for extending its dynamic modeling solution in Section 4.2 of Chapter 4. This extension will be integrated into the intricate model of the Recupera-Reha exoskeleton lower extremity joints. Subsequently, in Chapter 5, which focuses on application scenarios, the experimental outcomes derived from actuator joint tracking for the three primary movements of the ASPM joint modules will be presented. Additionally, the control strategies implemented to enhance the exoskeleton robot's capabilities in facilitating walking motion will be outlined. On a related note, the information regarding the modification of the foot base pertains solely to the preceding chapter's research efforts for achieving enhanced stability and performance during walking motion.

4

MODELING AND CONTROL STRATEGY

"Will robots inherit the earth? Yes, but they will be our children"

— Marvin Minsky

Tijjani, I., Kumar, R. and Boukheddimi, M. and Trampler, M. and Kumar, S. and Kirchner, F. (2024). "Sitting, Standing and Walking Control of the Series-Parallel Hybrid Recupera-Reha Exoskeleton". The 2024 IEEE-RAS International Conference on Humanoid Robots, Nancy, France, November 22-24

4.1 INTRODUCTION

This chapter lays the groundwork for this thesis's modeling and control aspects, drawing attention to related works and highlighting the ability of a kinematic and dynamic software framework to manage model complexity and apply control strategies using a high-fidelity model. Consequently, allowing the formulation of the optimal control problem used to produce desired motions like sitting, standing, and walking. The chapter is organized as follows: Section 4.2 provides illustrations of the Recupera-Reha exoskeleton robot and its model formulation. Section 4.3 outlines the OC method for sitting, standing, and static walking. Section 4.4 offers a discussion and lastly, Section 4.5 presents a conclusion.

4.1.1 *Background of the Study*

Exoskeleton robot research focuses on developing wearable devices that enhance human capabilities, particularly in mobility and strength. These devices, often inspired by the structure and function of the human body, are designed to augment, assist, support, or rehabilitate individuals with various needs, including those with mobility impairments, injuries, or conditions affecting muscle strength. In recent years, exoskeleton research has gained significant traction due to its potential to address a wide range of needs across various domains of which researchers explore areas such as control algorithms, biomechanics, and human-robot interaction to optimize exoskeleton performance, comfort, and usability. Key goals include improving mobility, enhancing rehabilitation outcomes, and promoting independence and quality of life for users. Overall, exoskeleton research represents a dynamic and multidisciplinary field with significant potential to revolutionize healthcare, industry, and everyday life by enhancing human capabilities, promoting rehabilitation, and improving overall well-being [61],[148]. Ongoing research efforts

aim to address challenges, optimize performance, and unlock the full potential of exoskeleton technology for a wide range of applications.

4.1.2 *Related Works*

Over the years, researchers have actively designed wearable exoskeleton robots to improve ambulatory abilities. Upper-body designs have seen increasing implementation, while lower-body designs deployed commercially remain comparatively fewer. A survey on design and control of lower extremity exoskeletons has been presented in [201]. Exoskeleton robots with a series-parallel hybrid structure face challenges in kinematics and dynamic modeling due to their closed-loop formation and kinematic constraints. Modeling tools and software frameworks [25, 35, 51, 115] typically use numerical methods to solve loop closure constraints in lower-body exoskeletons reported in [68, 85, 137] but their solvers may suffer from insufficient accuracy and slow convergence rates. Recent progress in robot and mechanism modeling has focused on the modular resolution of closed-loop constraints [100, 105, 111, 146]. The use of both numerical and analytical methods, offers a balanced strategy by leveraging existing analytical solutions and employing numerical resolution where analytical solutions are not available. Figure 4.1 illustrates the Recupera-Reha exoskeleton with a human wearer in three modes: (1) sitting, (2) standing, and (3) static walking. The exoskeleton incorporates a parallel configuration of linear actuators at the spine and knee joints, alongside reported variants of the ASPM [104, 106, 130, 200] representing the hip and ankle submechanisms. This complex design yields a series-parallel hybrid structure with numerous kinematic loops, posing challenges in both modeling and control (see [111] for a survey on such systems). Nonetheless, this exoskeleton has a unique feature of transferring the upper-body weight to the ground while standing during upper-limb assistive rehabilitation. It holds the potential to combine the advantages of a walking exoskeleton for assistive support and that of a user-scalable chair to offer relief to disabled patients from prolonged periods of standing.

When it comes to controlling the gait motion of an exoskeleton, whether through position, force, or torque control, it's crucial to carefully define the control algorithm to ensure adaptability to the system. Many exoskeleton designs [26, 199, 218] rely on classical PID controllers, trajectory tracking, gait pattern generation, motion capture, and EMG signals from healthy human muscles to assess assistive performance. Unlike these methods, the outcome of an exoskeleton robot walking in [182] relies on MPC based on a quadratic program. This approach specifies kinematic tasks to determine desired joint positions and velocities. In [68], OC based on direct collocation is used on the full exoskeleton model to produce walking motions. This method formulates OC in a discrete-time domain rather than continuous, simplifying the numerical solution using a non-linear program. However, this method has the tendency to get stuck in local minima and has poorer convergence property in comparison to OC methods based on DDP.

Figure 4.1: The Recupera-Reha exoskeleton robot in (1) sitting, (2) standing and (3) static walking mode

4.2 MODELING OF RECUPERA-REHA EXOSKELETON ROBOT

The mechanical structure of the Recupera-Reha exoskeleton contains various parallel submechanisms that pose a major challenge in terms of modeling and control. This section describes the modeling approach for the Recupera-Reha system that takes into account the loop closure constraints and enables computationally efficient solutions for the kinematics and dynamics of the robot.

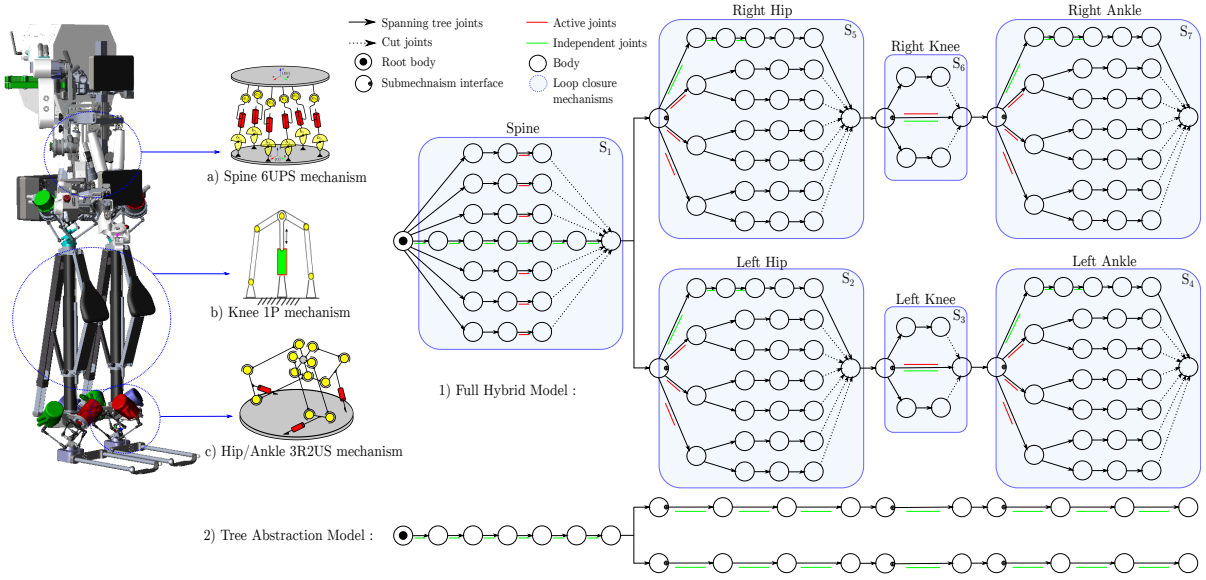

Figure 4.2: Recupera-Reha system and its topological graph

4.2.1 *Modeling of Closed Loops as Explicit Constraints*

Loop closure constraints in rigid body systems are the non-linear constraints on the motion variables. They can be expressed in implicit and explicit form [49]. Any rigid body system can be seen as a tree-type system with combination of links and joints. Let $\mathbf{q}$ be the vector of spanning tree joints and $\mathbf{y}$ a vector of independent joint variables that define $\mathbf{q}$ uniquely.

Table 4.1: Loop closure constraints [49]

Type	Position	Velocity	Acceleration
Implicit:	$\phi(\mathbf{q}) = \mathbf{0}$	$\mathbf{K}\dot{\mathbf{q}} = \mathbf{0}$	$\mathbf{K}\ddot{\mathbf{q}} = \mathbf{k}$
Explicit:	$\mathbf{q} = \gamma(\mathbf{y})$	$\dot{\mathbf{q}} = \mathbf{G}\dot{\mathbf{y}}$	$\ddot{\mathbf{q}} = \mathbf{G}\ddot{\mathbf{y}} + \mathbf{g}$

In Table 4.1, $\mathbf{K} = \frac{\partial \phi}{\partial \mathbf{q}}$, $\mathbf{k} = -\dot{\mathbf{K}}\dot{\mathbf{q}}$, $\mathbf{G} = \frac{\partial \gamma}{\partial \mathbf{y}}$, and $\mathbf{g} = \dot{\mathbf{G}}\dot{\mathbf{y}}$. If both implicit and explicit constraints define the same constraint in the system, then it can be deduced that $\phi \circ \gamma = \mathbf{0}$, $\mathbf{KG} = \mathbf{0}$, and $\mathbf{Kg} = \mathbf{k}$. The main focus is on the explicit constraints as it eliminates the possibility of constraint violation. In [100], a modular approach is described where explicit constraints are derived numerically from implicit constraints in a computationally efficient way.

4.2.2 *System Description*

This section describes the loop closure mechanisms present in the 34.68 kg Recupera-Reha exoskeleton robot. It has 20 active DOFs and consists of an electronic backpack, spine, and the lower-limb joints. In Figure 4.2, the system is represented as a serial composition of 7 submechanisms, all of them are closed-loop mechanisms. It consists of 148 spanning tree joints ($n = 148$) of which 20 are independent joints ($m = 20$) and 20 are actuated joints ($p = 20$). All the independent joints are shown as green edges and the actuated joints are shown as red edges. The remaining spanning tree joints are passive in nature. The cut joints for loop closure are denoted by dotted lines. The three major loop closure mechanisms are present in the spine, hip and ankle, and in the prismatic knee of the system.

4.2.2.1 *Spine Mechanism*

The first loop closure submechanism (denoted as S_1 in Figure 4.2) is a stewart platform [190] of type 6UPS, actuated by 6 linear actuators. Here, the spherical joint is considered as the cut joint and each cut joint imposes 3D translation constraint. This submechanism imposes a total of 18 constraints.

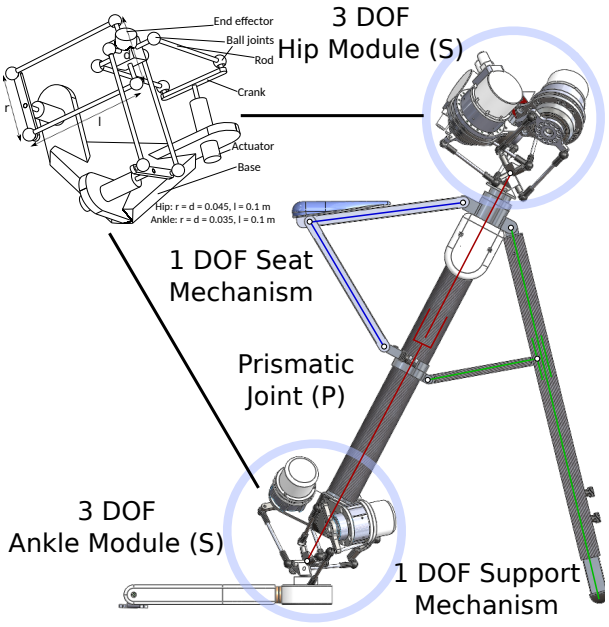

Figure 4.3: Leg in the Recupera-Reha exoskeleton [112]

4.2.2.2 *Knee Mechanism*

The second loop closure submechanism is an active-passive knee mechanism actuated by a single prismatic actuator. The knee is designed in such a way that it can be used as a chair to support a person through its passive 1 DOF support and seat mechanism in Figure 4.3. The support and seat mechanisms considers revolute joints as a cut joint and imposes a total of 6 constraints (3 per planar translation constraints). The submechanism is denoted as S_3 and S_6 in Figure 4.2.

4.2.2.3 *Hip and Ankle Mechanism*

The third submechanism in the system is a multi loop closure mechanism of type 3R2US with 3 DOF, present in the hip and ankle of the system. The independent joints are roll, pitch and yaw movements that are used to provide control commands to the three actuators present in the submechanisms. The loop closures are defined using spherical cut joints that impose 3D translation constraint. Six cut joints in the submechanism contribute to 18 constraints. The submechanisms are denoted as S_2, S_4, S_5, and S_7 in Figure 4.2.

4.2.2.4 *Numerical-Analytical Resolution of Loop Closures as Explicit Constraints*

The numerical-analytical hybrid approach is used to model the loop closures as explicit constraint for the system [100]. In this scenario, an analytical approach was exclusively applied to resolve the spine mechanism due to the availability of symbolic expressions. However, tackling the hip and ankle mechanisms required a significant investment of expert knowledge and time to derive the necessary analytical expressions, as they lacked existing symbolic representations. Adopting

a numerical-analytical approach proved highly advantageous, enabling the explicit resolution of loop closures and ultimately saving a lot of effort. The explicit constraints can be written as

$$\gamma = \begin{bmatrix} \gamma_{1,a}^T & \gamma_{2,n}^T & \gamma_{3,n}^T & \gamma_{4,n}^T & \gamma_{5,n}^T & \gamma_{6,n}^T & \gamma_{7,n}^T \end{bmatrix}^T \tag{4.1}$$

$$\mathbf{G} = \text{diag}\left(\mathbf{G}_{1,a}, \mathbf{G}_{2,n}, \mathbf{G}_{3,n}, \mathbf{G}_{4,n}, \mathbf{G}_{5,n}, \mathbf{G}_{6,n}, \mathbf{G}_{7,n}\right) \tag{4.2}$$

$$\mathbf{g} = \begin{bmatrix} \mathbf{g}_{1,a}^T & \mathbf{g}_{2,n}^T & \mathbf{g}_{3,n}^T & \mathbf{g}_{4,n}^T & \mathbf{g}_{5,n}^T & \mathbf{g}_{6,n}^T & \mathbf{g}_{7,n}^T \end{bmatrix}^T \tag{4.3}$$

where a denotes analytical resolution and, n denotes numerical resolution of loop closures in the above equations. The submechanisms are denoted by S_i where $i = 1 \ldots 7$ as shown in Figure 4.2. It is tested on the real system where the resolution of loop closures happens at 1kHz in real time including the calculation of inverse dynamics in actuation space.

4.2.2.5 *Overall Range of Motion*

The studies discussed in [104], [200] explores the ROM capabilities of the Recupera-Reha lower extremity joints for improved workspace. The spine joint consists of 6 DOF active joints and six independent joints: three prismatic joints translating along the X, Y, and Z axes and three revolute roll, pitch, and yaw joints. Similarly, the prismatic knee joint functions as the active and independent joint. Furthermore, three actuators each exists within the hip and ankle mechanisms, incorporating three distinct revolute joints operating as the independent joints. The ROM, maximum force and torque, and maximum velocity available at each actuator joint of the exoskeleton full hybrid model is listed in Table 4.2. Table 4.3 provides details of the independent joints, outlining the ROM used in the tree-abstraction model of the exoskeleton.

Table 4.2: ROM for the Actuator Joints

Actuators	Force / Torque	Max. Vel.	ROM
6 Spine Actuators	570 N	0.34 m/s	[0 , 0.11] m
Knee Actuator	662 N	0.34 m/s	[-0.064 , 0.09] m
3 Hip Motors	176 Nm	2.39 rad/s	[-0.436 , 0.436] rad
3 Ankle Motors	28 Nm	7.17 rad/s	[-0.436 , 0.436] rad

4.2.3 *Tree Abstraction Model*

The full hybrid model in Figure 4.2 is complex in nature due to multiple loop closures . All the submechanisms in the system impose a total of 102 constraints ($n_c = 102$) to be resolved. Although HyRoDyn can promptly resolve these constraints in real-time, integrating them into an

Table 4.3: ROM for the Independent Joints

Independent joints	ROM
Spine X	[-0.143 , 0.122] m
Spine Y	[-0.153 , 0.153] m
Spine Z	[-0.056 , 0.057] m
Spine Roll	[-0.576 , 0.585] rad
Spine Pitch	[-0.576 , 0.576] rad
Spine Yaw	[-1.518 , 1.518] rad
Knee joint	[-0.064 , 0.09] m
Hip Roll	[-0.349 , 0.646] rad
Hip Pitch	[-0.262 , 0.611] rad
Hip Yaw	[-0.349 , 0.646] rad
Ankle Roll	[-0.349 , 0.646] rad
Ankle Pitch	[-0.262 , 0.611] rad
Ankle Yaw	[-0.349 , 0.646] rad

optimization process poses a considerable challenge. Incorporating the intricate hybrid system into an OC framework necessitates derivatives for the loop closures, which are presently unavailable. Consequently, integrating these constraints into motion generation becomes inherently complex. As a result, a tree-abstraction model of the entire system is typically preferred. A tree abstraction of the Recupera-Reha exoskeleton is shown in Figure 4.2. The tree abstraction model of the robot consist of 20 DOF ($m = 20$) that can be used for motion generation.

4.3 MOTION GENERATION DEFINED AS AN OPTIMIZATION PROBLEM

In this section, we describe the motion generation for the Recupera-Reha exoskeleton using OC. This includes the constrained multibody dynamics up to the detailed formulation of the OCP for each movement. From this section onward, the tree abstraction model will be considered, where $\mathbf{q}$ is the vector of independent joint coordinates $\in \mathbf{R}^m$ including the virtual floating-base joints.

4.3.1 *Whole-body dynamics under constraints*

The exoskeleton is a rigid, articulated multi-body system whose dynamics include K contact constraints. The equation of motion for this type of system is based on the Euler-Lagrange equations of motion (Equation 4.4):

$$\mathbf{M}(\mathbf{q})\ddot{\mathbf{q}} + \mathbf{b}(\mathbf{q},\dot{\mathbf{q}}) = \mathbf{S}^\intercal\tau + \sum_{k=1}^{K}\mathbf{J}_k(\mathbf{q})^\intercal\lambda_k \tag{4.4}$$

where,

- $\mathbf{q}$ is the vector of joints' rotations including the virtual floating-base joints.
- $\dot{\mathbf{q}}, \ddot{\mathbf{q}}$ are the vectors of generalized velocities and accelerations.
- $\mathbf{M}(\mathbf{q})$ is the inertia matrix.
- $\mathbf{b}(\mathbf{q},\dot{\mathbf{q}})$ is the vector of gravity and non-linear forces.
- $\mathbf{S}$ is the selection matrix for the actuated elements.
- τ is the vector of internal joints torques.
- $\mathbf{J}_k(\mathbf{q})$ is the contact constraints' Jacobian matrix.
- λ_k is the vector of contact forces.

Given that the system dynamics are defined in the acceleration dimension, the k^{th} contact is expressed as a second-order static constraint (Equation 4.5):

$$\mathbf{J}_k\ddot{\mathbf{q}} + \dot{\mathbf{J}}_k\dot{\mathbf{q}} = \mathbf{0} \quad \forall k \in 1\cdots K \tag{4.5}$$

The constrained dynamics is expressed as the combination of (Equation 4.4) and (Equation 4.5) in (Equation 4.6) :

$$\begin{bmatrix}\mathbf{M} & \mathbf{J}_c{}^\intercal \\ \mathbf{J}_c & \mathbf{0}\end{bmatrix}\begin{bmatrix}\ddot{\mathbf{q}} \\ -\lambda_c\end{bmatrix} = \begin{bmatrix}\mathbf{S}^\intercal\tau - \mathbf{b} \\ -\dot{\mathbf{J}}_c\dot{\mathbf{q}}\end{bmatrix} \tag{4.6}$$
$$\mathbf{J}_c = \begin{bmatrix}\mathbf{J_1}^\intercal\cdots\mathbf{J_k}^\intercal\cdots\mathbf{J_K}^\intercal\end{bmatrix}^\intercal, \lambda_c = \begin{bmatrix}\lambda_1{}^\intercal\cdots\lambda_k{}^\intercal\cdots\lambda_K{}^\intercal\end{bmatrix}^\intercal$$

4.3.2 *Optimal Control Problem Definition*

The trajectory optimization problem is descretized and formulated as follow:

$$\min_{\mathbf{x},\mathbf{u}} l_N(\mathbf{x}_N) + \sum_{t=0}^{N-1} l(\mathbf{x}_t,\mathbf{u}_t)dt \tag{4.7a}$$
$$s.t. \quad \mathbf{x}_0 = \mathbf{f}_0, \tag{4.7b}$$
$$\forall i \in \{0...N-1\}, \quad \mathbf{x}_{i+1} = \mathbf{f}_t(\mathbf{x}_i,\mathbf{u}_i) \tag{4.7c}$$

where:

- $\mathbf{x} = (\mathbf{q},\dot{\mathbf{q}})$ is the state of the system,

- $\mathbf{u}$ is the torque control variable,
- l_N is the Terminal cost model,
- l is the Running cost model,
- $\mathbf{f}_t$ is a discrete function describing the system dynamics
- $\mathbf{x_0}$ is the initial state of the system,
- N is the number of nodes over a trajectory.

In this study, the OCP was resolved using a shooting method [37], namely the Box-FDDP algorithm [23]. The DDP algorithm is well suited to this type of optimization problem, as it exploits the system's sparsity in a highly-iterative way. FDDP (Feasibility DDP) [129] enables us to find a solution even from an infeasible guess, and overcomes the numerical restrictions of single-shot algorithms like the original DDP. The box allows the resolution within the robot's permissible torque limits. The open-source software *Crocoddyl* [133] with its Box-FDDP solver was employed for this resolution. The dynamics and their derivatives have been computed in a fast and efficient manner using the open-source software *Pinocchio* [25] .

4.3.3 *Desired Motions Formulated As Cost Models*

In order to evaluate the robot's capabilities, two movements have been designed as OCPs. In the following, the OCPs will be described as cost models.

4.3.3.1 *Sitting and standing movements*

It's well known that sitting in a wheelchair for long periods of time leads to numerous health problems [119, 121]. The Recupera-Reha exoskeleton was originally designed for upper-body rehabilitation, making the ability to stand up and sit down an essential task for the system. This prevents the user from sitting for long periods. This movement consists of a single phase for the sitting movement and a single phase for the standing movement. The movement is designed such that the COM is lowered for sitting and raised for standing, while maintaining the system's balance.

4.3.3.2 *Static walk movement*

The trajectory optimization allows to generate a wide variety of movements that add flexibility and versatility to the rehabilitation training. With this in mind, a static walk has been designed while respecting the joints limits of the system. This movement was selected to assess the robot's ability to move through its environment, in order to be able to provide lower limb rehabilitation exercises as well in the future. The static walk movement represents only an example of the movements that could be designed or scaled to suit different walk models and rehabilitation needs.

The static walk movement is composed of a right and a left stride. Each stride is divided into two phases: the support phase and the swing phase.

- *Support Phase*: In this phase, the COM (x,y) is shifted over the supporting foot before moving the opposite foot forward. Both feet are in contact in this phase.
- *Swing Phase*: In this phase, the swing foot breaks contact with the ground to move forward.

4.3.3.3 *Cost Models Definition*

To achieve these movements, the following Running and Terminal Cost Models have been implemented.

$$l = \sum_{c=1}^{C} \alpha_c \Phi_c(\mathbf{q}, \dot{\mathbf{q}}, \tau), \quad l_N = \sum_{c_F=1}^{C_F} \alpha_{c_F} \Phi_{c_F}(\mathbf{q}, \dot{\mathbf{q}}), \tag{4.8}$$

Where, Φ_c, Φ_{c_F} represent the cost of the running and terminal models respectively, $\alpha_c, \alpha_{c_F} \in \mathbb{R}$ represent their respective weights, which have been empirically determined. In both movements, the cost functions composing the cost models are the following:

- *COM target*: COM placement $\mathbf{c}_w$ tracks the COM reference placement at the end of each phase of movement. $\Phi_1 = \| \mathbf{c}_w(t) - \mathbf{c}_w^{\text{ref}}(t_N) \|_2^2$
- *Torque regularization*: Joint torques minimization to ensure the dynamic feasibility. $\Phi_2 = \| \tau(t) \|_2^2$
- *Posture regularization*: This cost manages the redundancy of the multi-body dynamics. $\Phi_3 = \| \mathbf{q}(t) - \mathbf{q}^{ref}(t_N) \|_2^2$

t_N represents the final time of each phase of the motion.

The static walk movement requires an additional cost, the foot-tracking cost, in order to move the swing foot forward.

- *Foot Tracking*: The foot placement $\mathbf{r}_w$ tracks the final foot position of each phase (right or left, depending on the movement phase). $\Phi_4 = \| \mathbf{r}_w(t) - \mathbf{r}_w^{\text{ref}}(t_N) \|_2^2$

The terminal cost model excludes the Torque regularization cost function.

4.4 DISCUSSION

This research work is committed to advance the capabilities of the Recupera-Reha LEE, specifically tailored to support upper-body weight during upper-limb assistive rehabilitation. First, we extend the kinematic and dynamic analysis to encompass the complete model of the exoskeleton robot, addressing its inherent closed-loop mechanisms through a hybrid approach facilitated by the HyRoDyn [109] software framework. To the best knowledge of the author, this is one of the most kinematically complex robots shown to be solved with a model-based approach in

the literature. This study demonstrates the successful OCP formulation and execution of sitting, standing and static walking movements on a series-parallel hybrid Recupera-Reha exoskeleton. Exploiting a DDP-based OC algorithm to generate feasible movements highlights the potential for enhancing the exoskeleton capabilities. Additionally, the HyRoDyn software framework efficiently handles loop closure constraints in the exoskeleton model and enables a smooth mapping between the independent joint and actuator spaces. In this work, the formalization of OCPs was achieved using the tree abstraction model, due to the high complexity of our system involving a total of 102 constraints. Including closed-loop constraints in the optimization process is an effective way to explore the full capabilities of a series-parallel hybrid robot as recently reported in [20]. However, the inclusion of such a large number of holonomic constraints makes the resolution of OCP very challenging. In our future work, we will develop new techniques to include the large number of closed-loop constraints in the optimization problem in a computationally efficient manner such that the extreme capabilities of the system can be exploited. The system was originally designed for upper-body rehabilitation and has not been optimized for lower-limb rehabilitation, making this work more challenging. Furthermore, analysis of the range of motion in the exoskeleton leg joints demonstrates its potential for integrating functional rehabilitation exercises for patients.

4.5 CONCLUSION

This chapter presents the resolution of loop closure constraints in a hybrid and explicit manner for the complex Recupera-Reha LEE. It achieves this by leveraging the features of HyRoDyn to resolve all the loop closure constraints. Next, we examine the OCP formulation, which generates the desired motions, using a tree abstraction model that incorporates constraints on the exoskeleton independent joints. In this study, the OC approach employs a shooting method that incorporates a discrete-time OC formulation. This method enables us to find feasible solutions even from an initially unfeasible guess, overcoming numerical limitations while adhering to the robot's torque constraints. Therefore, by utilizing the DDP-based OC method, we have improved the functionality of the exoskeleton, facilitating motions such as sitting, standing, and static walking. The subsequent Chapter 5 will illustrate the experimental pipeline, showcasing the low-level control architecture and present results from simulations as well as experiments conducted on the exoskeleton robot.

5 RESULTS AND APPLICATION SCENARIO

"Productivity is never an accident. It is always the result of a commitment to excellence, intelligent planning, and focused effort"

— Paul J. Meyer

5.1 INTRODUCTION

This chapter presents the results of the overall thesis research work to illustrate the enhanced capabilities of a series-parallel hybrid Recupera-Reha exoskeleton. It focuses on implementing the novel low-level control architecture and integrating it with a high-level software framework to improve control performance. Furthermore, this research's practical application has the potential of integrating the human-exoskeleton interaction in optimal control loops and in real-world situations. The contents presented in this chapter are drawn from the research conducted in Chapter 4. The chapter's structure unfolds as follows:

- In Section 5.2, the focus lies on elucidating the low-level control architecture, and establishing the integration of a high-level software framework to enhance control performance.
- Section 5.3 delves into the simulation and experimental pipeline, highlighting the environments, software components, communication protocols and control method employed.
- Section 5.4 presents the simulation and experimental results, beginning with the ROM tracking for the exoskeleton's lower leg joints. To validate the efficacy of the OC approach used to generate trajectories, the simulation results for desired motions (sitting, standing, and static walking) are verified experimentally on the exoskeleton robot.
- The practical application of this research in a specific human-robot-interaction scenario is demonstrated in Section 5.5.
- Finally, Section 5.6 provides a conclusion for the chapter, summarizing the key findings and implications of the research.

5.2 LOW-LEVEL CONTROL ARCHITECTURE

The foundational control layer serves as the initial architectural framework for managing the joints driven by actuators in the exoskeleton. As depicted in Figure 5.1, decentralized Actuator Control Units (ACUs) housed within a compartment of the exoskeleton backpack control these actuators. Every ACU comprises a printed circuit board (PCB) divided into three

distinct sub-units responsible for power distribution, logic processing, communication and data acquisition. There are two different voltages that power each ACU. A voltage of 48 V is allocated for the actuator phases, while 12 V is designated for logic and communication purposes. Communication between the exoskeleton joint actuators and the ACU is facilitated through a Node Data Link Communication (NDLCom) network, enabling the implementation of cascaded position-velocity-current control. This control is achieved using dedicated field programmable gate array (FPGA) electronic boards integrated within each Brushless Direct Current (BLDC) actuator located on the joints of the exoskeleton. As a precautionary measure to ensure safety, the FPGA incorporates a customizable firmware-based fuse on the hardware. This fuse is designed to deactivate the system in the event of voltage fluctuations or when the actuators fail to supply the necessary current to drive the joint. Sensing devices on the exoskeleton are placed at the joint actuator side to enable position, speed, force and torque control; for instance, the linear actuators available at the (spine and prismatic knee) joints are equipped with draw-wire and stiff-type linear sensors respectively for sensing the linear speed and absolute position via current measurement. Force sensors are also available on the linear actuators to enable force control, but due to high friction, they are not enabled in the FPGA electronics of the low-level control architecture. The BLDC actuators of the (hip and ankle) joints are coupled with harmonic gear drives, inertia measurement unit (IMU), and equipped with sensors that allows absolute postion and torque control via current measurement. These actuators offer high power density and minimal backlash, though they also exhibit significant friction, resulting in some energy loss.

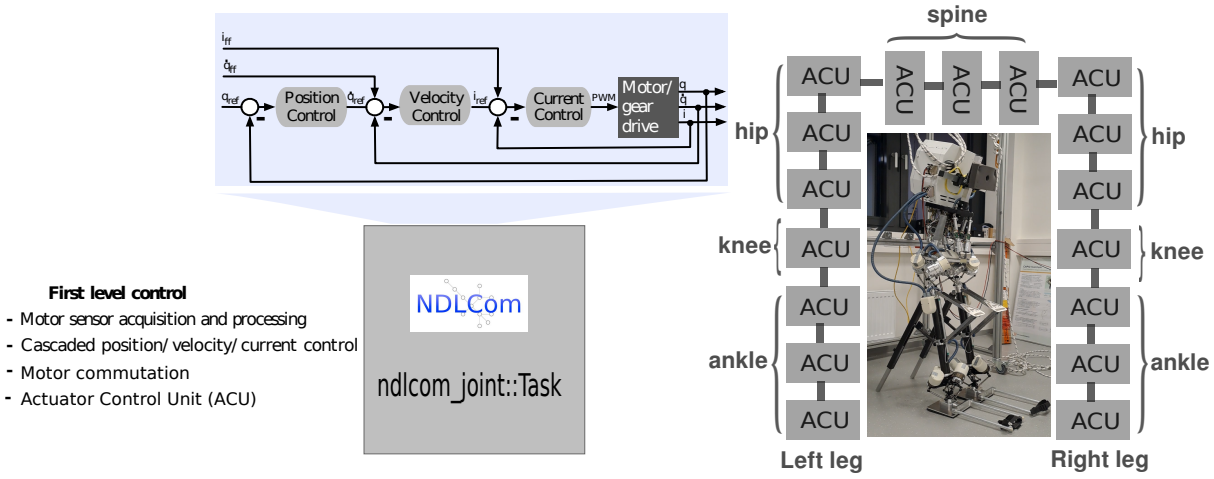

Figure 5.1: Low-level Control Architecture for the Recupera-Reha exoskeleton

5.2.1 *Integrating the Low-level Architecture with a Software Framework*

Integrating the low-level control architecture with a software framework is crucial for enabling higher-level functionalities and applications. The Robot Construction Kit (RoCK) [76] is a software framework tailored for developing robotic systems, facilitating integration of readily available drivers and modules into systems and incorporating new components. It utilizes a

component model based on the Orocos Real-Time Toolkit (RTT). HyRoDyn's control capabilities address the kinematics and dynamics of series-parallel hybrid robots, and its orogen component is integrated with RoCK. HyRoDyn can perform tasks such as forward and inverse kinematics and control operations, ensuring smooth mapping between independent joint space and actuator space. As depicted in Figure 5.2, at the lower left hand corner is HyRoDyn's orogen module interface, independent joint state parameters (position, velocity, or acceleration) from NDLCom's first output port are channeled to HyRoDyn's input port. HyRoDyn then sends joint commands to RoCK-QT-Widget visualization component for showcasing robot motion and inspecting task data after solving either of the forward or inverse dynamic task. The second output from NDLCom relays status data to the FPGA, which implements position, velocity, or current control on the exoskeleton joint actuators via the ACU. Furthermore, the low-level control architecture features a graphical user interface (GUI) named CommonGUI. This interface allows the configuration of PID gains, scaling factors for position-velocity-current control, and movement of each exoskeleton joint through the BLDC joint control widget embedded as a CommonGUI-RoCK component. Alternatively, you can directly write these values to an external Extensible Markup Language (XML) file, which will then serve as commands to the FPGA electronic registers of the exoskeleton robot.

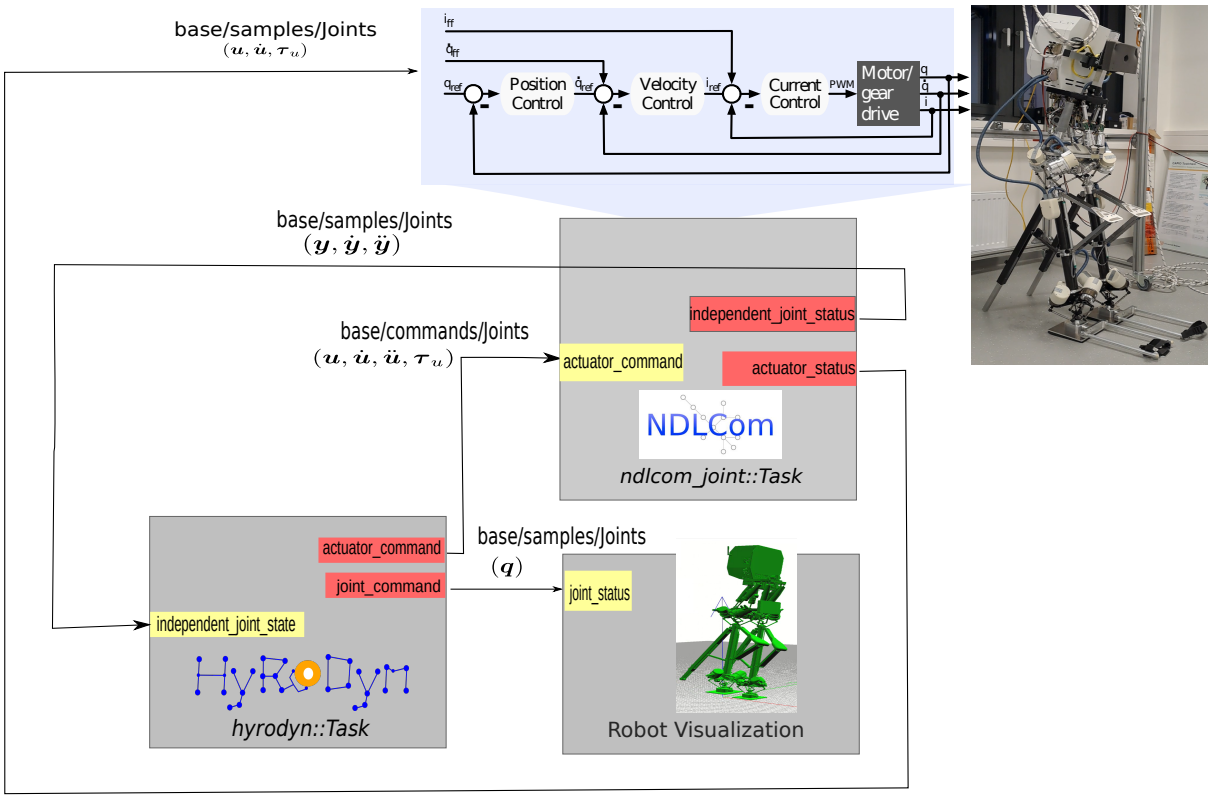

Figure 5.2: Integrating low-level control with HyRoDyn software([101])

5.3 SIMULATION AND EXPERIMENTAL PIPELINE

To validate the effectiveness of our control architecture and its integration with the software framework, we conducted extensive simulations and experiments. This section provides a detailed account of the simulation environment, the experimental design, and the data collection processes. As shown in Figure 5.3, given the exoskeleton robot joint limits (position, velocity, and torque) representing the state and control, dynamics and contact constraints from the feet as inputs, the DDP-based CROCODDYL software framework is used to generate feasible motion trajectories in the independent joint space. The resulting output of the CROCODDYL software framework is a trajectory file containing the joint state and the optimal control measure which is tested in a PyBullet [31] dynamic simulation environment.

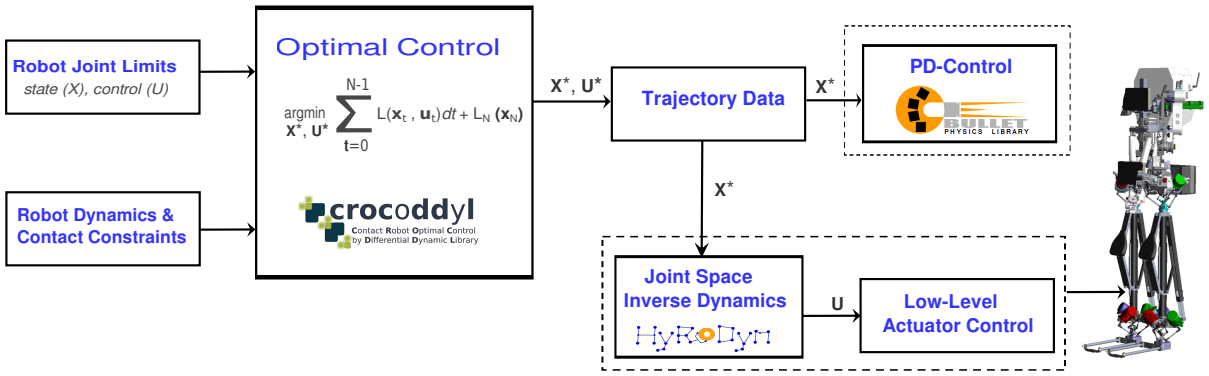

Figure 5.3: Overall Simulation and Experimental Pipeline

SIMULATION SETUP PyBullet is an open-source physics engine primarily used for simulating robotics and physics-based simulations. It provides a platform that enables efficient computation of rigid-body dynamics, collision detection, and motion control in a virtual environment. Its motion tracking functionality is engineered to replicate real-world robotic testing procedures, involving trajectory interpolation and closed-loop control at the joint position level. The OC approach generated the optimal state trajectories, X^*, as shown in the trajectory file in Figure 5.3. We then tracked these trajectories using a PD controller in the PyBullet simulator. We used the cubic interpolation method to estimate the trajectories up to 1 kHz so that there would be a smooth transition between the parts of the proportional and derivative trajectories in the joint space. The desired motions obtained from the OCP are validated through joint tracking in simulation. Figure 5.4 shows the physics engine simulator's outcome for the exoskeleton's four-step static walk motion. Solid lines represent the reference trajectory from OC, while dotted lines represent the physics engine simulator's generated trajectory. By tracking the joints of the left and right leg, we can analyze the performance of the exoskeleton as it follows the trajectory defined by the OC algorithm during a specific period.

The floating base's motion shown in Figure 5.5 is a result of joint space control during static walking. In the graphical legend, "des" indicates the desired trajectory from OC, while "act" denotes the actuator's response. The deviations observed in the X, Y, and Z axes of the floating

base are not a result of inadequate controller tracking, but rather stem from the performance of the joint space control. A noticeable spike in the z-axis oscillation at the beginning of the motion indicates the robot's effort to stabilize itself before the first leg stride. We attribute the discrepancies in the physics simulator's graphical result to model inaccuracy. Using the complete exoskeleton model in the physics simulator leads to a prolonged processing time, which may result in the simulator shutting down due to the intricate nature of the full model. The simulator attempts to mimic and reproduce the given reference trajectory, however it is unsuccessful. Therefore, a simplified tree-type abstraction model of the exoskeleton, which comprises only the independent joints is utilized but it does not accurately capture the physical system's dynamics. Hence, result in slight deviations. Addressing these discrepancies could be achieved by directly controlling the position and orientation of the exoskeleton directly in the Cartesian space rather than specifying each joint's desired angles, velocities, and torques. Nevertheless, the robot effectively adhered to the trajectory set by the OC and reached the desired position. Overall, the plots suggest that while the system is capable of following the desired trajectories, there are areas where the actual movements deviate from the intended path, potentially indicating areas for improvement in control algorithms or mechanical design.

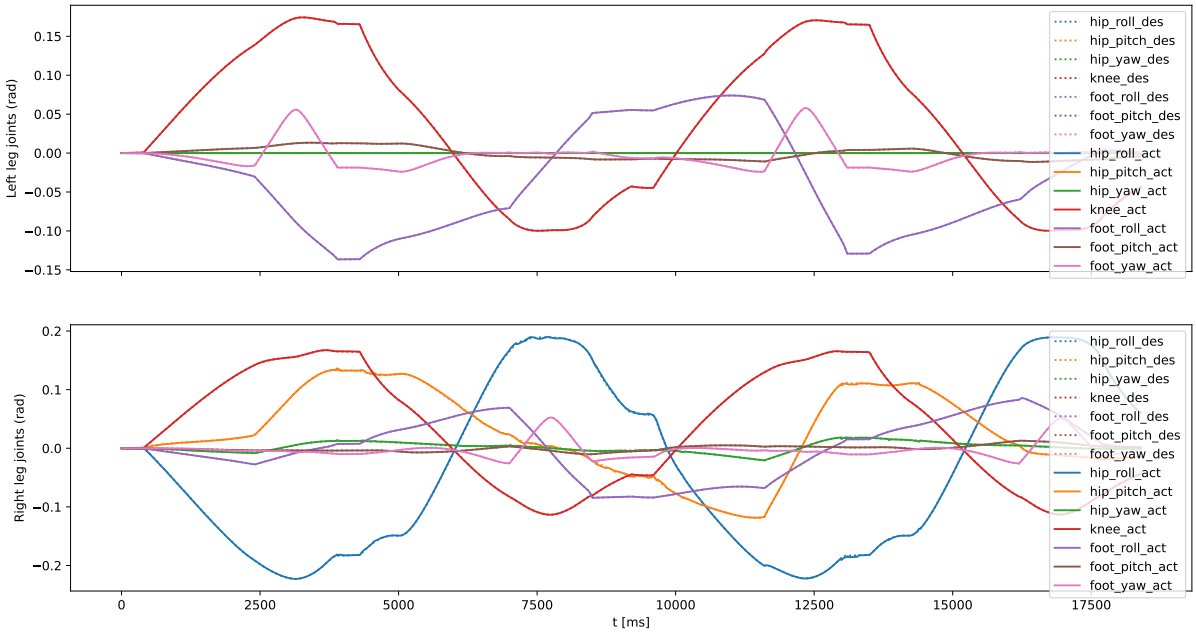

Figure 5.4: Joint space tracking in PyBullet simulator during four-steps static walk

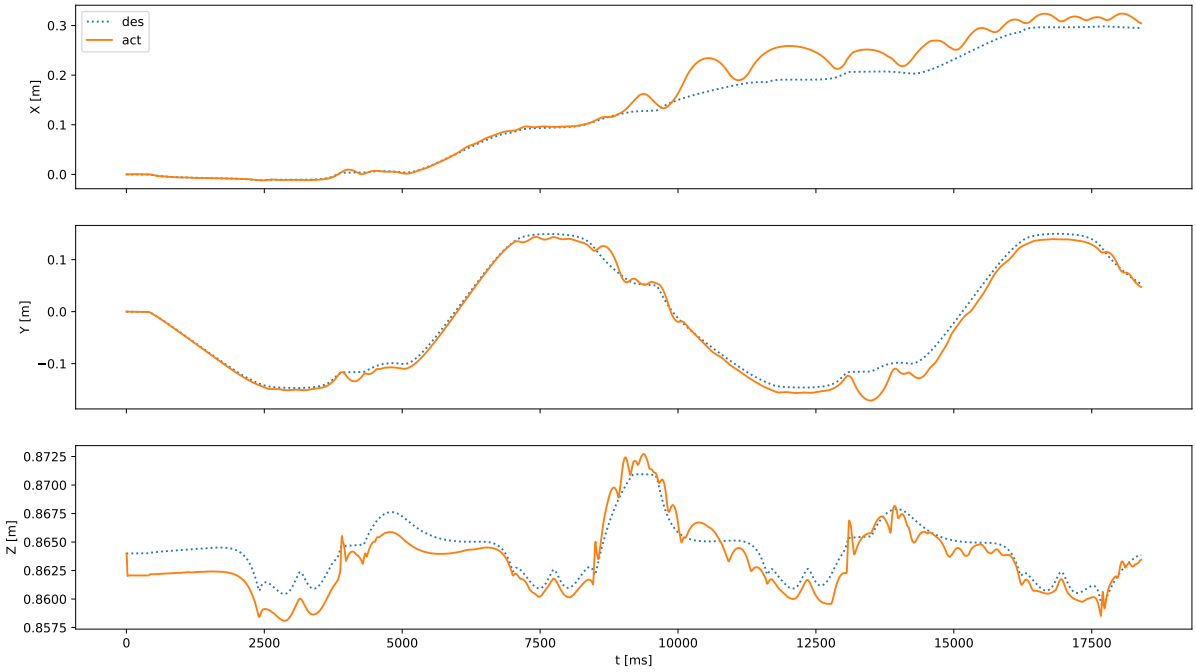

Figure 5.5: Floating base motion in PyBullet simulator during four-steps static walk

EXPERIMENTAL SETUP In the experimental setup, the following experiments were conducted. Firstly, the exoskeleton joints ROM's tracking was evaluated, using the full series-parallel hybrid exoskeleton model. To test the ROM of the robot in the independent joint space, reference joint positions are provided to HyRoDyn software framework as waypoints to compute the actuation space positions. These joint positions were then sent to the low-level actuator controller for communication with the exoskeleton joint actuators, results were assessed through the tracking of the joints.

Secondly, a trajectory file containing both the optimized state and control input stores specific movements generated by the OC method within the independent joint space. HyRoDyn receives the optimized state trajectory to compute the actuation space trajectory, which it then sends to the exoskeleton's low-level actuator control unit for joint communication. We then evaluate the performed movements by controlling the joints' tracking and using graphical plots to assess their dynamic feasibility.

5.4 RESULTS

This section presents the outcomes obtained from both simulations and experiments, providing a comprehensive analysis of the exoskeleton robot's capabilities and performance. Additionally, a comparative analysis between the simulation and experimental results was conducted, shedding light on the exoskeleton robot's joint tracking capabilities and validating the reliability of HyRoDyn in accurately mapping joint spaces.

5.4.1 *Leg joints ROM verification*

The screenshot of the symmetric movements of the leg joints tracking is as shown in Figure 5.6

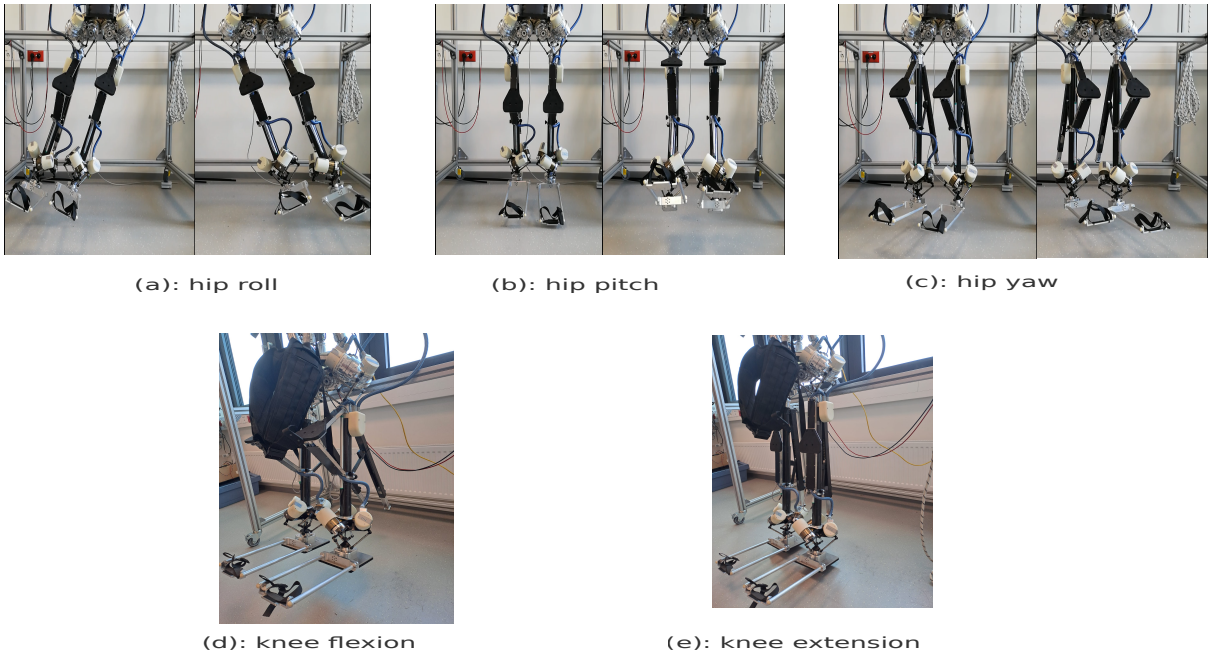

(a)

Figure 5.6: The screenshot of the exoskeleton leg joints symmetric movements

The goal is to demonstrate that HyRoDyn accurately maps the independent joint space to the actuator space. Therefore, the reference positions given to HyRoDyn as waypoints in the independent joint space are translated to the actuator joint space of the Recupera-Reha exoskeleton. Consequently, the measured positions should align with the reference positions. The Table 4.3 from the Chapter 4 presents the ROM of the independent joint space of the system. The Figure 5.7 shows a smooth tracking between the measured and reference position of the joint actuators for the exoskeleton robot's right and left hips. Similar accuracy is observed in Figure 5.8 and Figure 5.9 for the prismatic knee and ankle joints, respectively. Based on these figures and the consistency in the tracking results of the three lower-body joints of the exoskeleton, it indicates that the actuation space tracking that HyRoDyn software framework provides works correctly with the independent joint space references, thereby ensuring optimal

performance of the exoskeleton and making it a reliable tool for other applications. Furthermore, despite the control loop is position-based, maximizing the actuator joints speed limit on the low-level control side is necessary to achieve optimal joint tracking saturation. Therefore, it is crucial to correctly set up the low-level configuration to ensure the robot adheres to these limits.

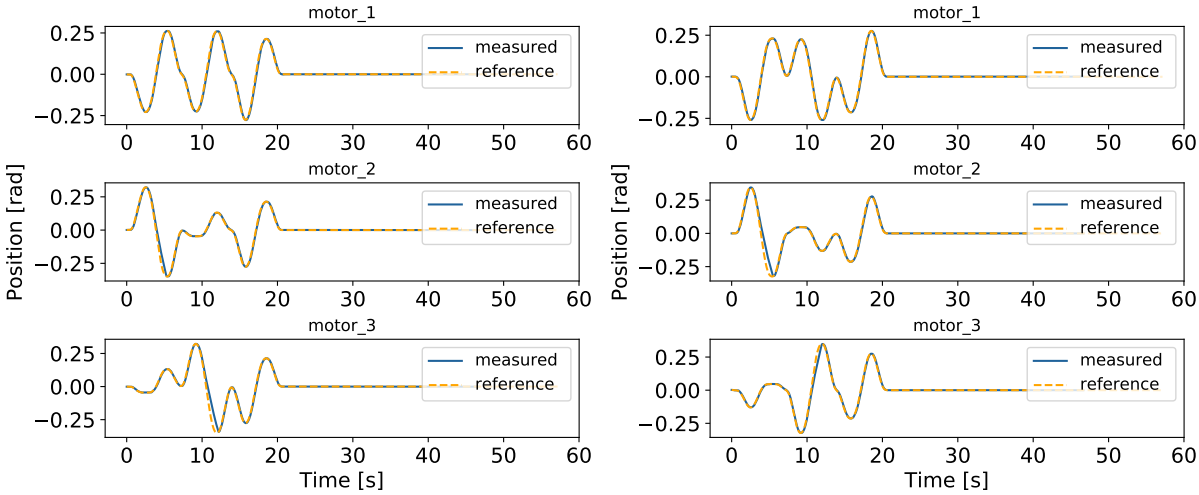

(a) Right hip joint motors

(b) Left hip joint motors

Figure 5.7: Hip joint's ROM tracking

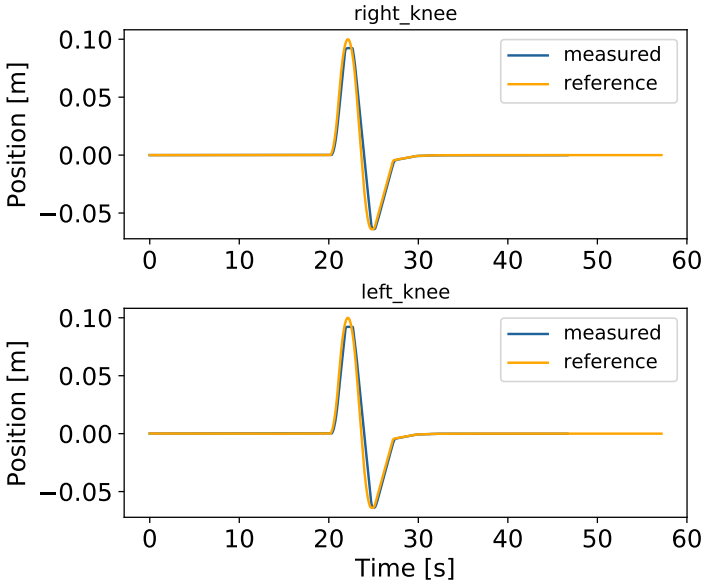

Figure 5.8: Prismatic Knee joint's ROM tracking

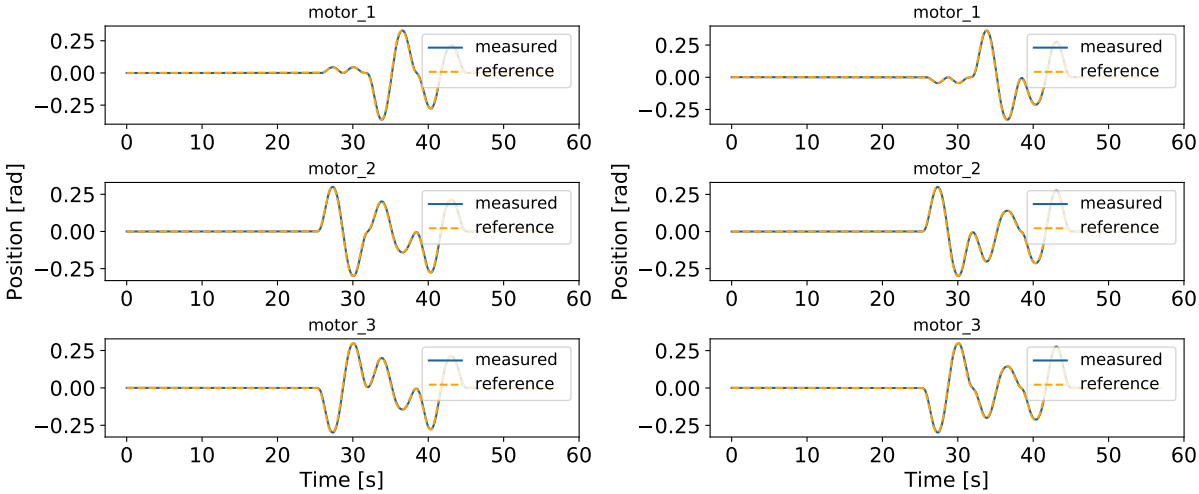

(a) Right ankle joint motors

(b) Left ankle joint motors

Figure 5.9: Ankle joint's ROM tracking

5.4.2 *Sitting and standing motion*

Figure 5.10a shows the sitting and standing motion obtained in simulation. Figure 5.10b presents the experimental results of this motion.

For the sitting and standing motions, the results from the hip and prismatic knee joints were chosen for analysis because they are the most actively engaged joints. The curves in Figure 5.11 depict the motion of the knee joints throughout the transition phases. During the sitting phase, the measured position of the actuator closely matches the reference position obtained from the OC method, as shown in Figure 5.11a. However, towards the end of the standing phase, as depicted in Figure 5.11b, the measured position of the actuator deviates from the reference position. This deviation occurs because standing requires more energy (i.e, more force and torques), particularly for lifting the upper body's weight against gravity. Despite this, the exoskeleton reached the target position as intended. Notably, the measured position of the hip joint actuators aligns closely with the reference position in both transition phases, as shown in Figure 5.12 and Figure 5.13 respectively. Based on these figures and the results shown in the video, we can conclude that the robot has successfully executed the motions.

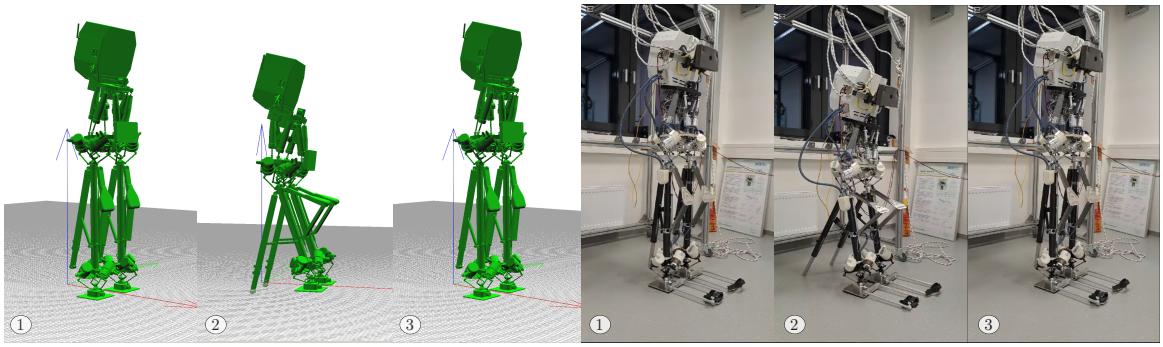

(a) Simulation (b) Real system

Figure 5.10: The screenshot of the exoskeleton at initial standing, sitting, and final standing position, both in simulation and on the real system

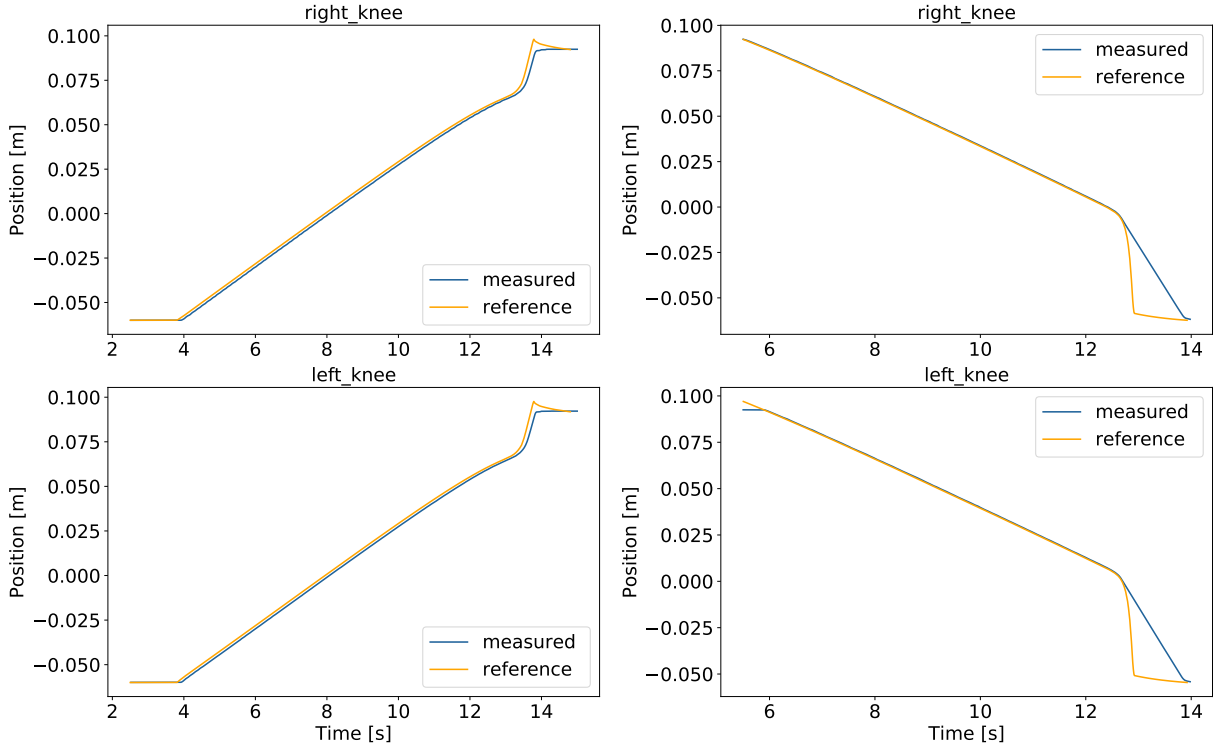

(a) Sitting (b) Standing

Figure 5.11: Sitting and standing motion of the prismatic knee joints

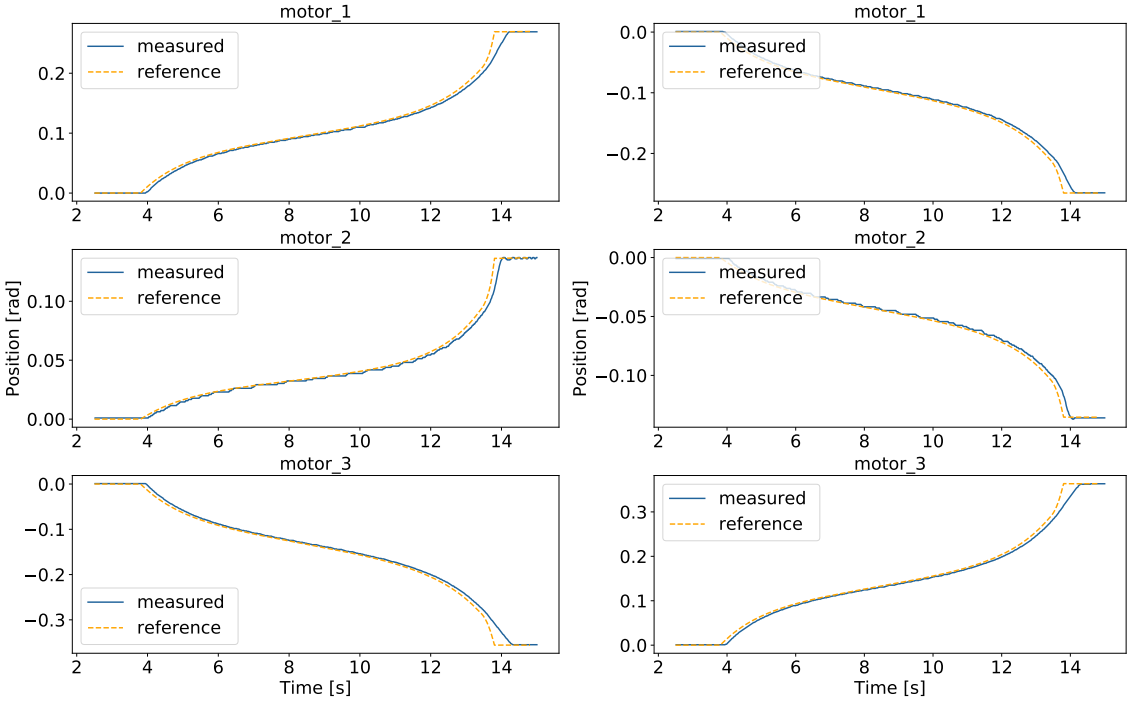

(a) Right hip motors (b) Left hip motors

Figure 5.12: Position of the hip joint motors during the sitting motion

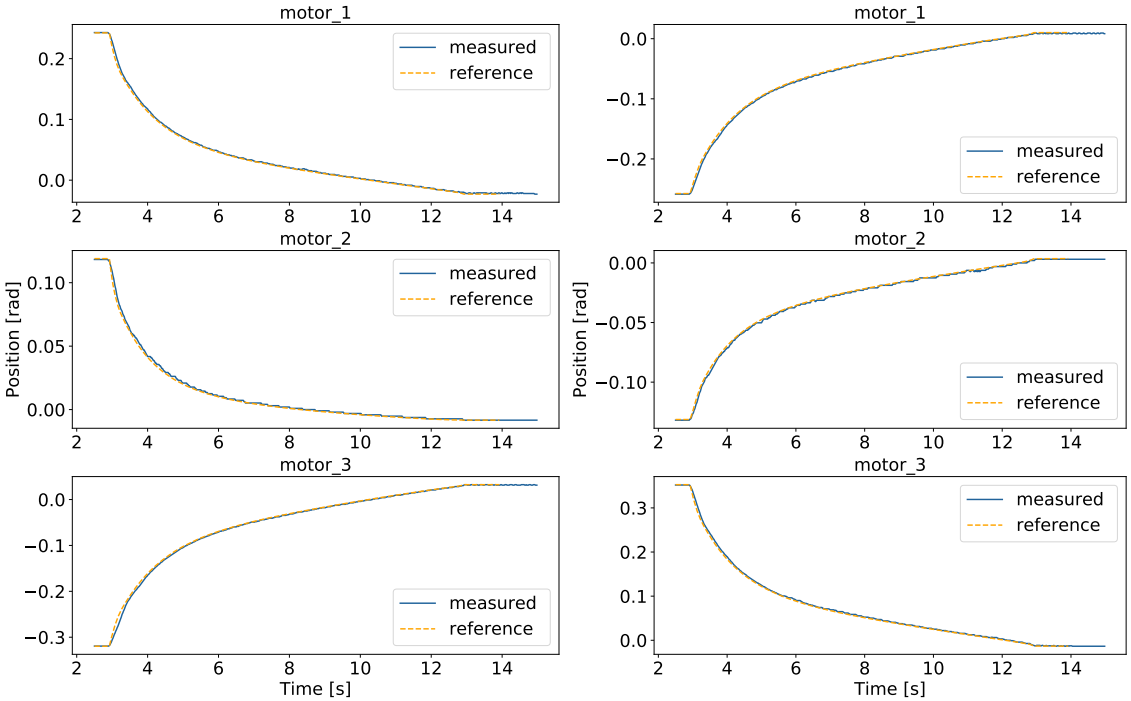

(a) Right hip motors (b) Left hip motors

Figure 5.13: Position of the hip joint motors during the standing motion

5.4.3 *Static walk motion*

The four-step static walking motion in simulation and on the real system are illustrated in Figure 5.14a and Figure 5.14b respectively. The sequence begins with the initial standing position with both feet at stance phase, followed by the left leg stride, right leg stride, and ends with the final standing position.

During exoskeleton static walking, various joints actively contribute to movement, balance, and propulsion. The OCP formulation employs a simplified model of the exoskeleton where spine joints are fixed, providing a stable posture. All three lower body joints, however, actively participate in motion. Therefore, this section includes simulation and experimental results focusing on the hip, prismatic knee, and ankle joints. In Figure 5.15, Figure 5.16, and Figure 5.17, the reference curve depicts the motion generated from OC, while the measured curve illustrates the actuator positions for the joint actuators. All the joint actuator positions during the experiment closely matches the reference position from OC. The smooth alignment between measured and reference position curves suggests a successful execution of the static walk motion on the real robot.

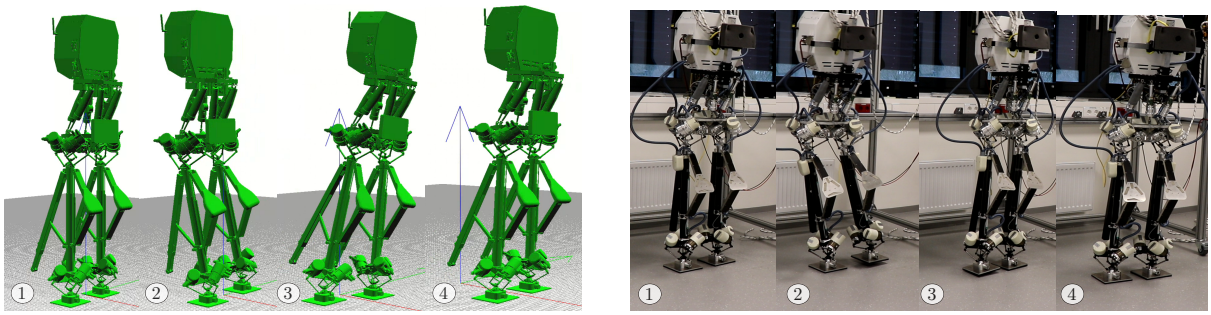

(a) Walking in simulation

(b) Walking on real system

Figure 5.14: The Recupera exoskeleton four-steps static walking motion in simulation and on the real system

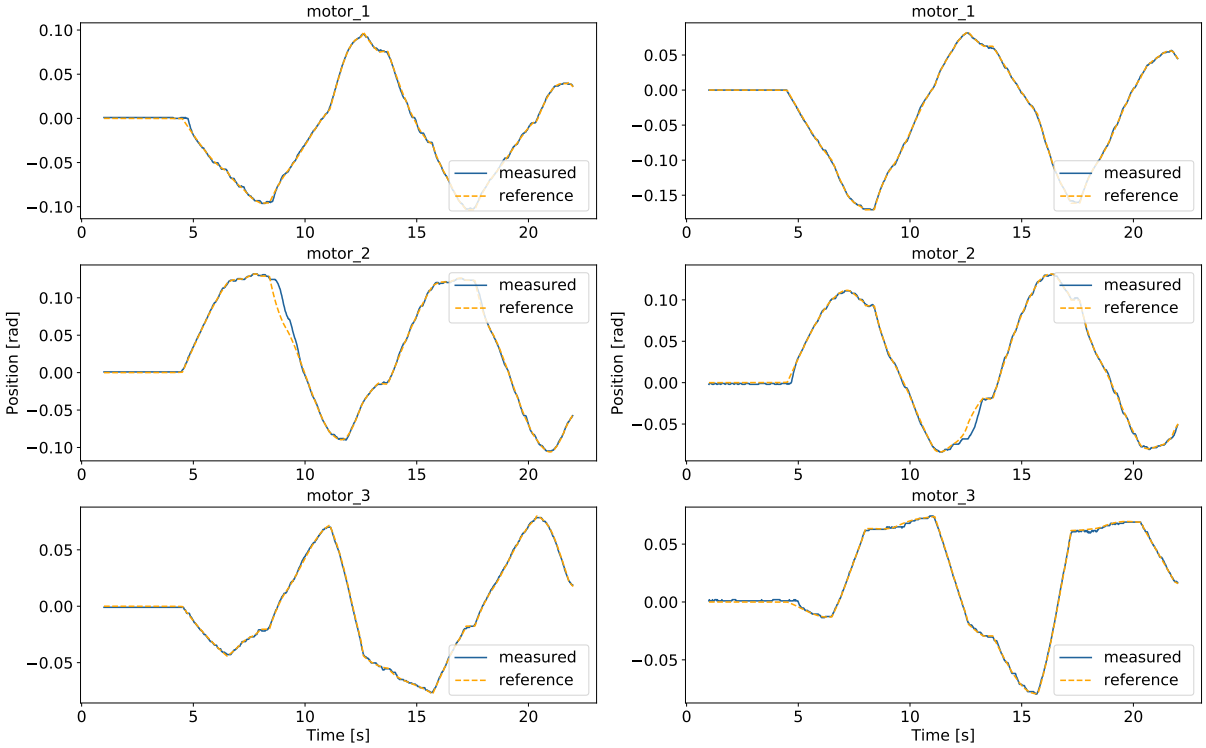

(a) Right hip joint position tracking

(b) Left hip joint position tracking

Figure 5.15: Hip joint's position during four steps static walk motion

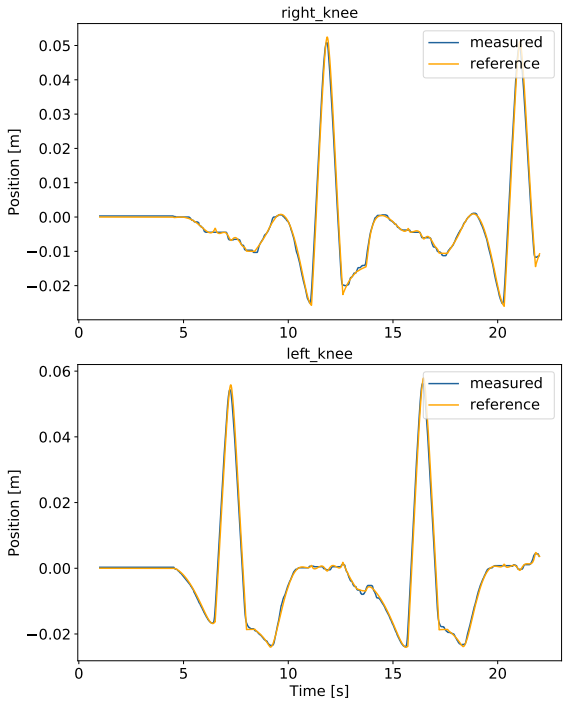

Figure 5.16: Prismatic Knee joint's position tracking during four steps static walk motion

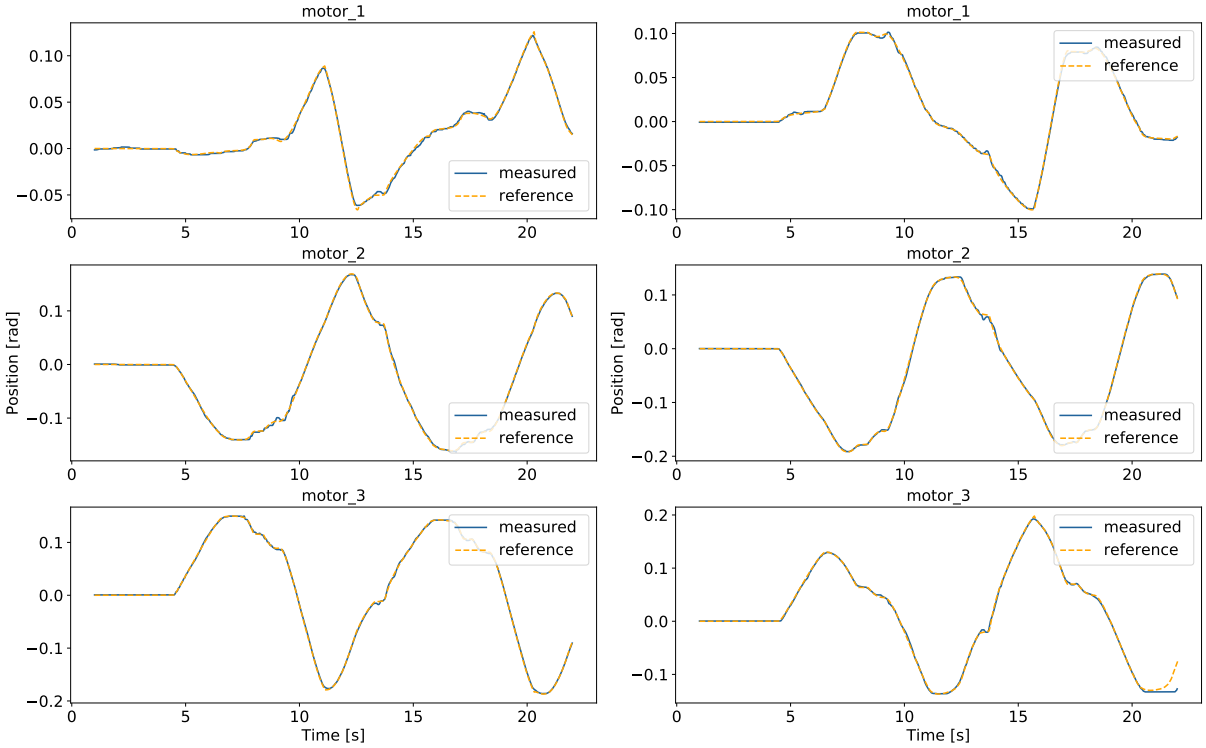

(a) Right ankle joint position tracking

(b) Left ankle joint position tracking

Figure 5.17: Ankle joint's position tracking during four steps static walk motion

5.5 APPLICATION IN HUMAN-ROBOT INTERACTION

To demonstrate the practical utility of our system and it's extreme capability, this section explores its application in a real-world human-robot interaction scenario. Looking ahead, the goal is to optimize the exoskeleton's design for lower-body locomotion, thereby expanding its range of applications. Future work will focus on modeling human-robot interactions with closed-loop constraints and integrating them into the trajectory optimization process, involving humans in decision-making. This approach could advance exoskeleton control, enabling the safe and efficient execution of highly dynamic movements with a human in the loop.

5.5.1 *Experiments with a human wearing the robot for sitting motion*

In Figure 5.18, Figure 5.19, and Figure 5.20, you can see the graphical results of the hip, prismatic knee, and ankle joint actuator trackings while a person wearing an exoskeleton sits down. We observed smooth joint tracking between the generated sitting motion trajectory from OC and the measured motion trajectory for all the exoskeleton leg joints. The HyRoDyn software framework successfully replicates OC's reference trajectory.

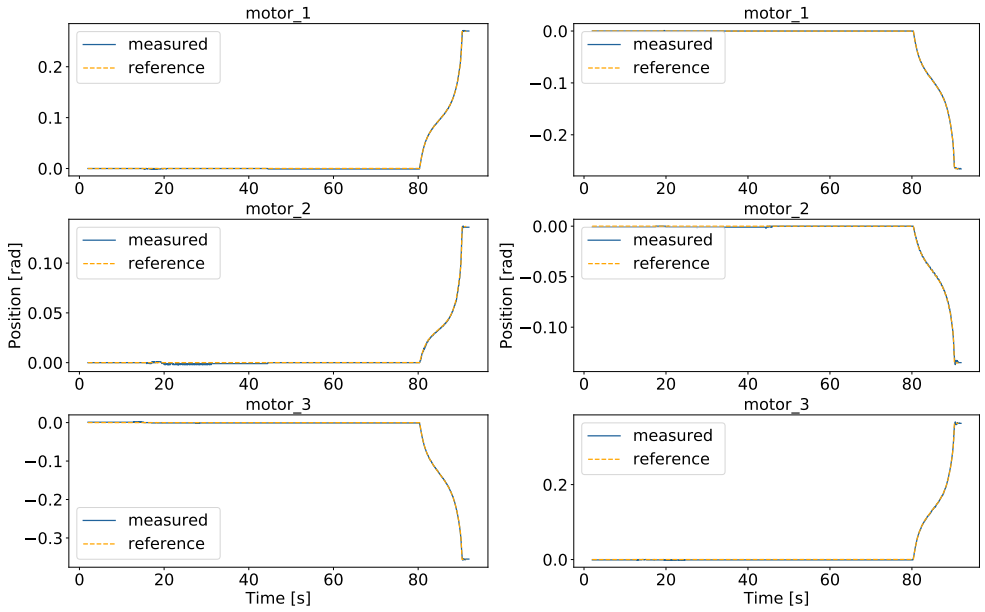

(a) Right hip joint position tracking (b) Left hip joint position tracking

Figure 5.18: Hip joint's position during sitting motion

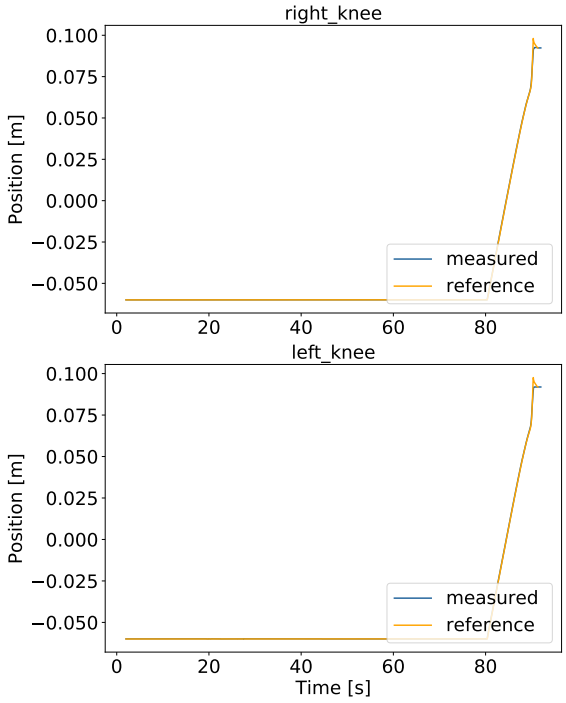

Figure 5.19: Prismatic Knee joint's position during sitting motion

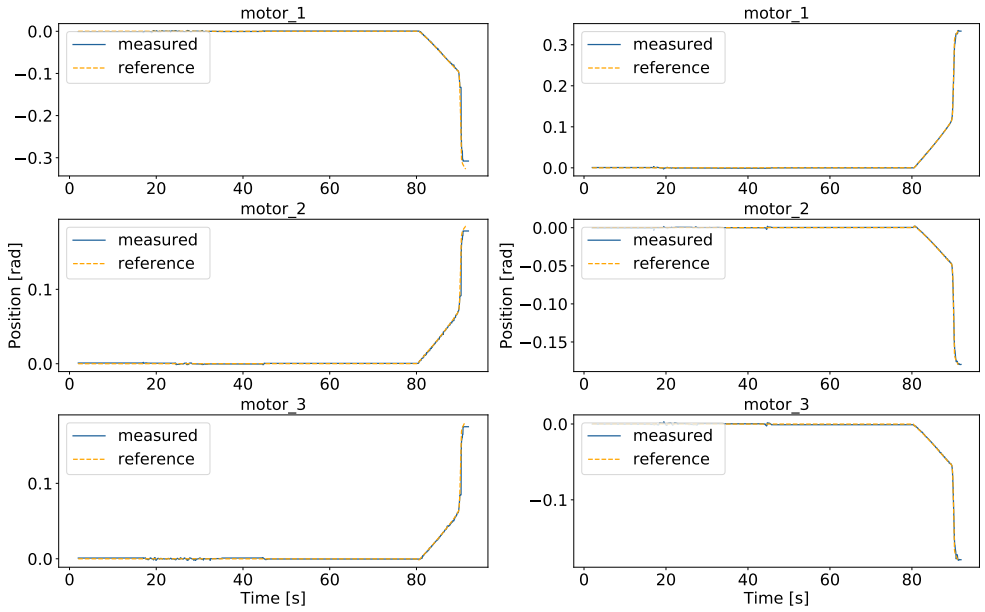

(a) Right ankle joint position tracking (b) Left ankle joint position tracking

Figure 5.20: Ankle joint's position during sitting motion

5.5.2 *Experiments with a human wearing the exoskeleton robot for static walking*

The screenshot of the human wearing the exoskeleton during standing, sitting and static walking mode is shown in Figure 4.1. Figure 5.21 shows a human wearing the exoskeleton during the four-step static walking. The figure depicts the following walking phases: 1) both legs at stance position, 2) left leg stride, 3) right leg stride, and 4) both leg stance position for the fourth step. The graphical result representations of the hip, prismatic knee and ankle joint actuator trackings during the four-step static walk with a human wearing the exoskeleton are shown in Figure 5.22, Figure 5.23, and Figure 5.24 respectively, also seen in the accompanying video[1]. Despite the added weight of the human, the joint actuators effectively compensated for the additional torque and accommodated the external force from the human wearer. We can observe a smooth tracking of joint movements, maintaining close alignment between the reference and measured trajectories.

1 https://youtu.be/1FrfVyCFANM

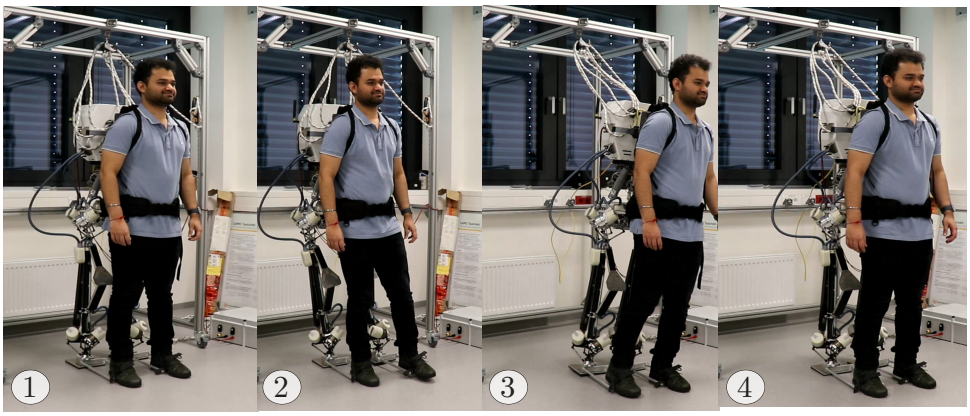

Figure 5.21: The screenshots of the Recupera exoskeleton in sitting, standing, and static walk during the experiment with a human

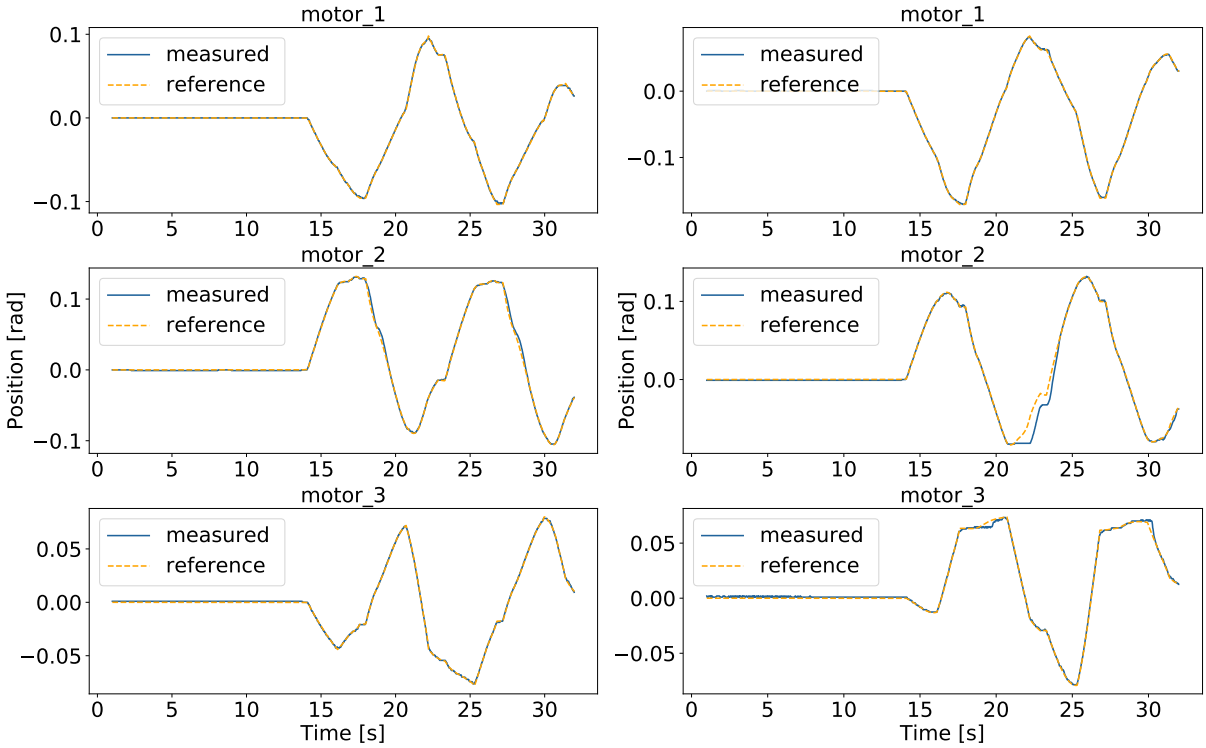

(a) Right hip joint position tracking

(b) Left hip joint position tracking

Figure 5.22: Hip joint's position during four steps static walk motion with human wearer

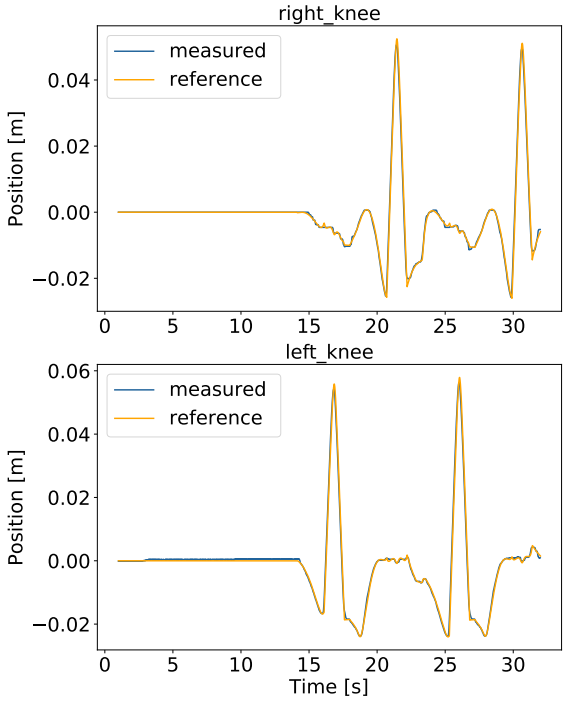

Figure 5.23: Prismatic Knee joint's position tracking during four steps static walk motion with human wearer

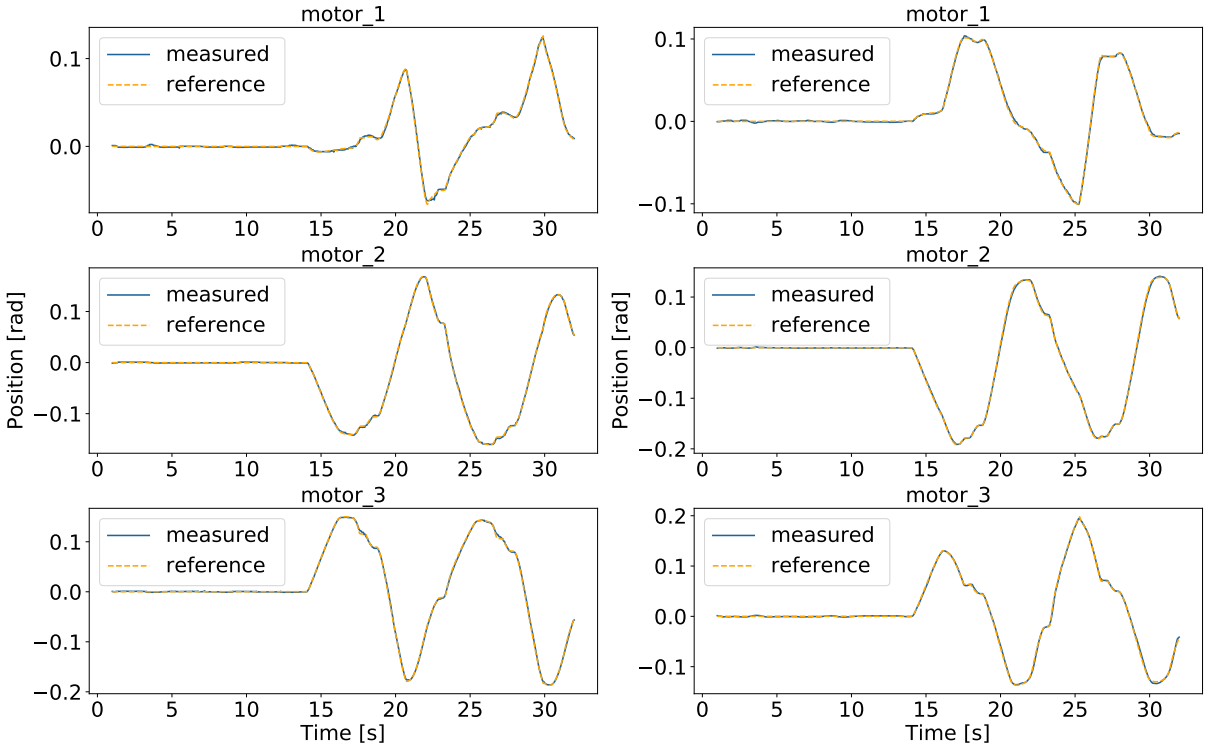

(a) Right ankle joint position tracking

(b) Left ankle joint position tracking

Figure 5.24: Ankle joint's position tracking during four steps static walk motion with human wearer

5.5.3 *Explicit feedback assessments from human interaction with the Recupera-Reha exoskeleton*

Explicit feedback assessment and ratings from human interaction with an exoskeleton play a crucial role in improving user-adaptive control strategies. This approach enhances user comfort and adaptability, positively impacting the design and performance of the system. By considering human factors, such as ergonomics and cognitive load, the control system can be made more intuitive, accessible, and efficient, leading to a more seamless interaction. Incorporating user feedback fosters a user-centered approach, ensuring that the system adapts to real-world needs and promotes more effective and engaging experiences for the user. The sitting and standing movement experiments with the exoskeleton were performed at varying trajectory speeds, but were discontinued due to concerns about biased assessments from different users. The mechanical design of the exoskeleton, particularly the scalable passive leg joint intended to facilitate sitting mode without affecting movement, may have influenced users' perceptions. Additionally, the system's ergonomic design caused the spine joint module to impact the downward sitting movement, further complicating the accuracy of user feedback and hindering intuitive insights for improvement.

5.6 DISCUSSION

This study demonstrates the successful execution of sitting, standing and static walking movements on a series-parallel hybrid Recupera-Reha LEE. Exploiting the DDP-based OC algorithm to generate feasible movements highlights the potential for enhancing the exoskeletons' capabilities using OC methods. Additionally, the HyRoDyn solver efficiently handles loop closure constraints in the exoskeleton model and enables a smooth mapping between the independent joint and actuator spaces. In this work, the formalization of OCPs was achieved using the tree abstraction model, due to the high complexity of our system involving a total of 102 constraints. Including closed-loop constraints in the optimization process is an effective way to explore the full capabilities of a series-parallel hybrid robot as recently reported in [20]. However, the inclusion of such a large number of holonomic constraints makes the resolution of OCP very challenging. In our future work, we will develop new techniques to include the large number of closed-loop constraints in the optimization problem in a computationally efficient manner such that the extreme capabilities of the system can be exploited. In the future, we would like to optimize the exoskeleton's design for whole-body rehabilitation, which could increase the system's range of application. Additionally, motors used in the system have a high gear ratio and hence the drives are not mechanically transparent. We would like to investigate the design of a lightweight exoskeleton robot with high-power quasi-direct drives for precise torque control in the future. The experiment with the human wearing the exoskeleton was carried out without modeling of the human-robot connections, as the formulation of these connections is not yet mature enough in the literature. Extending this work, we plan to model these human-robot connections with closed-loop constraints and include them in the trajectory optimization process involving the presence of the human in the decision process. This methodology could open up a

new avenue for the control of exoskeletons, giving them the ability to perform highly dynamic movements with a human in the loop, in a safe and efficient manner.

5.7 CONCLUSION

This chapter details the application and experimental outcomes of the DDP-based OC method for generating feasible trajectories in simulation. It also explores the application of the HyRoDyn software framework to seamlessly map these trajectories from independent joint spaces to actuator space commands for the series-parallel Recupera-Reha exoskeleton. Joint tracking within motion ranges demonstrates the effectiveness of the HyRoDyn framework, while the successful execution of sitting, standing, and static walking movements underscores an effective approach to fully utilize the robot's capabilities. Additionally, experiments involving a human wearing the exoskeleton further assess the robot's capabilities and potential for future applications.

6 CONCLUSION AND OUTLOOK

The motivation for this thesis stems from the growing need to address the mobility challenges faced by individuals with lower-limb disabilities, which are increasingly prevalent due to aging populations and various neurological and musculoskeletal conditions. According to the World Health Organization, a significant portion of the global population experiences disabilities that impact their mobility, with conditions such as stroke, spinal cord injury, and osteoarthritis being prominent contributors. Traditional mobility aids like crutches, canes, and wheelchairs, while helpful, often fall short of addressing the long-term physical and psychological needs of their users. These aids can lead to discomfort, additional health complications, and a diminished sense of independence. This has led to an increasing interest in advanced assistive technologies, particularly wearable exoskeleton robots, which offer a promising solution to enhance mobility and quality of life for individuals with lower-limb disabilities. Initially designed to support upper body weight during upper-limb rehabilitation, the Recupera-Reha exoskeleton offers a unique opportunity to expand its application to dynamic walking motions. However, the exoskeleton's current design and control mechanisms do not fully optimize for walking, posing several critical challenges. These include ergonomic design limitations, suboptimal joint module placement, and inadequate motion control methods. Addressing these challenges is crucial for improving the exoskeleton's effectiveness and user acceptance. The need to optimize the design of the Recupera-Reha exoskeleton, integrate a comprehensive kinematic model, and develop an effective control method for dynamic motions motivates this thesis. By overcoming the existing limitations, the research aims to enhance the exoskeleton's performance and contribute to the broader field of exoskeleton technology. The ultimate goal is to create a more effective and user-friendly device that can independently support itself while walking.

6.1 SUMMARY OF CONTRIBUTIONS

This thesis addresses the pressing need to enhance the functionality and effectiveness of lower-extremity exoskeletons, focusing specifically on the Recupera-Reha system. The research explores the integration of advanced kinematic and dynamic analysis techniques to overcome significant limitations in existing exoskeleton designs and control methodologies. The study begins by highlighting the increasing prevalence of musculoskeletal disabilities and the potential of exoskeleton robots to improve mobility and quality of life for affected individuals. It identifies key challenges with the current design and application of the Recupera-Reha exoskeleton, particularly its limitations in ergonomic design, optimal placement of joint modules, and motion control. To address these issues, the thesis sets forth two primary goals: optimizing the modular joint module placement in the exoskeleton's leg and developing a robust control method to enable

effective sitting, standing, and walking motions. This work has made scientific contributions, including the following:

In Chapter 2, a comprehensive review of the latest advancements in the design and control of exoskeleton robots aimed at enhancing human locomotion. It emphasizes the significant challenges encountered in designing and implementing control strategies for these robots and explores potential solutions to overcome them. Additionally, the chapter outlines future directions for technological innovations that could improve the commercial feasibility of exoskeleton robots and contribute to an enhanced quality of life for their wearers. Chapter 3 presents a detailed kinematic analysis of the almost spherical parallel mechanism device used in the hip and ankle joints of the Recupera-Reha legs. We addressed the limitations of the ASPM devices by improving the workspace and alignment of these components to better match human joint dynamics. Solving the limitations of the device lays the foundation for more advanced dynamic modeling and enhances the potential for functional rehabilitation exercises. The design modification of the exoskeleton's foot base has significantly improved the exoskeleton's stability while walking. The previous prototype featured a small surface area foot base, which introduced instability while the exoskeleton independently walked. In contrast, the new foot base design with a larger surface area ensures that the exoskeleton's center of mass remains within its supporting polygon, enhancing both static and dynamic stability. Chapter 4 demonstrates the implementation of an OC approach using a DDP-based algorithm to generate feasible trajectory motions for sitting, standing, and static walking. It also effectively utilizes the HyRoDyn software framework to explore hybrid solutions for resolving closed loops and providing smooth mapping of independent joint space trajectories into actuation space trajectories. Chapter 5 presents simulation and experimental results, highlighting the enhanced capabilities of the Recupera-Reha exoskeleton. From an application perspective, we experimented with static walking motion with a human wearer. Although no modeling of human-robot connections is formulated in the trajectory optimization process because the formulation of these connections is not yet mature enough in the literature, the results of the motion tracking show better performances compared to the trackings without a human wearer. This is because the system utilizes a capable human body's natural biomechanics to enhance stability and balance. While the exoskeleton effectively manages and distributes the load across the user's body, conversely, only a specific system adaptation can achieve similar benefits for a disabled individual.

6.2 OUTLOOK

Adding a model of the connection between the human and exoskeleton to the process of optimizing trajectories with closed-loop constraints will be a significant advancement in the development of exoskeleton robots. By integrating this model, trajectory optimization will more accurately reflect the dynamic interactions between the human user and the exoskeleton, thereby enhancing the realism and effectiveness of the generated motions. This approach will enable a more nuanced understanding of how the exoskeleton and user influence each other during movement, leading to better alignment of the exoskeleton's actions with the user's intentions and natural motion patterns. Implementing closed-loop constraints ensures that the system can

adapt in real-time to discrepancies or deviations from the intended trajectory, enhancing stability and performance. In practice, this means that the exoskeleton will not only follow pre-defined paths more accurately but will also respond dynamically to variations in user input and external conditions. This could significantly enhance the user experience by providing more intuitive and responsive control, leading to improved mobility, comfort, and overall effectiveness of the exoskeleton in real-world applications.

Furthermore, implementing a machine learning algorithm such as deep reinforcement learning that learns from human input feedback or assessments represents a transformative step in exoskeleton technology. Such an algorithm would enable the exoskeleton to adapt and refine its performance based on user experiences and evaluations. By leveraging human feedback data, the system will continuously improve its control strategies and motion optimization. This adaptability means the exoskeleton could better accommodate individual user needs, preferences, and physical conditions over time. For example, the algorithm could learn to adjust gait patterns or response behaviors based on user comfort levels, mobility improvements, or specific feedback. In practice, this could lead to a more personalized and effective exoskeleton, enhancing user satisfaction and performance. The integration of machine learning would not only enable real-time adjustments but also facilitate long-term improvements, making the exoskeleton increasingly responsive and efficient in supporting human locomotion and rehabilitation.

Although this thesis primarily focused on the technical aspects of design and control strategies, user feedback is a critical component for optimizing exoskeletons for real-world applications. During the human-robot interaction experiments, limited user feedback was collected, which nonetheless provided valuable insights into the design's impact on comfort, usability, and adaptability. The incorporation of human factors, such as the ease of use and the physical and cognitive load on the user, has the potential to further enhance the exoskeleton's performance and overall user experience. Future studies should place greater emphasis on gathering comprehensive user feedback to assess factors like ergonomics, fatigue, and emotional response during exoskeleton use. This data will inform iterative improvements in the design, ensuring that the exoskeleton meets both functional and human-centered needs. Addressing these human factors will also contribute to the device's success in practical deployment across medical, industrial, and assistive contexts.

Part I

APPENDIX

A

KINEMATIC AND DYNAMIC ANALYSIS OF A 2R1P ROBOTIC LEG

A.1 SPHERICAL MANIPULATOR AND ITS TOPOLOGICAL SCHEME

Spherical manipulators (SM) are robotic systems designed with a topology that allows movement within a spherical workspace, typically featuring multiple revolute joints that enable motion in all three spatial dimensions. Applications such as robotic arms in manufacturing, medical robotics, and space exploration utilize them for their versatile motion capabilities. The topology of a spherical manipulator permits the end-effector, or tool attached to the manipulator, to reach any point within a spherical volume around the base of the robot, making them valuable tools for tasks that demand a high degree of flexibility and precision. It also provides a structural framework for understanding the relationships and properties of the system, which is crucial for analysis, design, and control purposes. Spherical manipulators offer similar advantages to their parallel manipulator (PM) counterparts. However, they are prone to reduced manipulability and versatillity with a complex design structure [104]. The PMs offer large workspace and high payload capacity, having rigid and stiff structures contributes to their high accuracy suitable for heavy-duty applications. The camera orienting devices, agile eye [62, 187] in Figure A.1a is a type of SM used in solar tracking. The serial chain of this device have limited degrees of freedom, designed in two dimensions combining either a rotational (R) or translational (P) joint like (RRR, PPP, RRP, PPR, RPR, PRP). Each of this combinations are designed from the devices in Figure A.1b

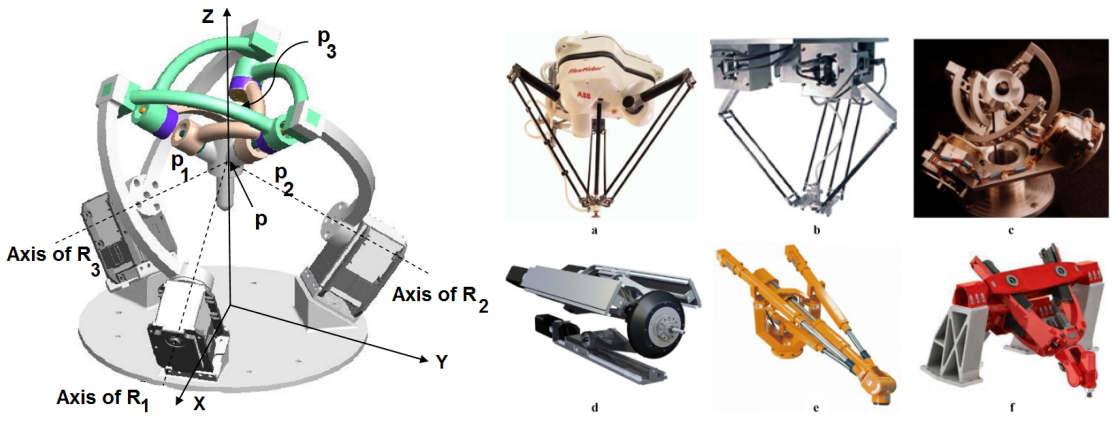

(a) Agile eye manipulator [187]

(b) Typical spherical manipulator robots [217]

Figure A.1: Topology of spherical manipulators

A.1.1 *The 2R1P Robotic Leg*

The 2R1P robotic leg is a type of spherical manipulator used as an abstraction for spherical joints like the human elbow, wrist, hip and ankle etc., the aim of this module is to establish kinematic and dynamic model formulation for a 2R1P robotic leg that could be used as a spherical joint for different application mechanisms. The 2R1P robotic leg is considered as a spherical manipulator. The robotic leg in Figure Figure B.1(a) is composed of three joints: first two joints u_1 and u_2 are revolute, with their axes oriented orthogonally to each other and the third joint q_3 is prismatic, carrying the end-effector point E. From Figure Figure A.2a, the generalised joint coordinates (u_1, u_2, q_3) are represented by ($q1$, $q2$, $q3$) in Figure Figure B.1(b). The direction of the joint coordinates in Figure Figure A.2b includes two rotations and a translation about and along the joint axes respectively.

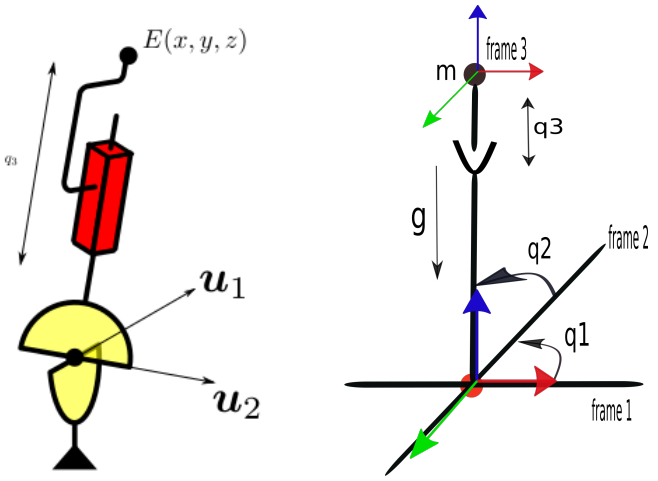

(a) 2R1P robotic leg (b) Joint frame configurations

Figure A.2: kinematic architecture

Considering an initial configuration as shown in Figure Figure A.2b, the prismatic joint carrying the end-effector slides along the (z-axis) direction of the global coordinate frame. Hence, $q = [q_1, q_2, q_3]^T = [0, 0, mg]^T$. The robotic leg is related with a point mass m and its center of mass is located at the end-effector point. Therefore, masses of the first and second links are zeros respectively while the third link has a mass value of one. The gravity g of course projects along the z-axis direction of the sliding prismatic joint q_3.

A.2 GEOMETRIC MODEL FORMULATION FOR A 2R1P ROBOTIC LEG

A robot geometric model formulation denotes the mathematical representation of a robot's geometry and kinematics. This formulation allows engineers and researchers to describe the robot's physical structure and how it moves in space. Several components make up a robot's geometric model. These include setting up coordinate frames, forward and inverse kinematics (which show how joint positions and angles relate to each other), the physical dimensions of each

Table A.1: DH-parameters for 2R1P robotic leg

Link	$\alpha_j(degree)$	d_j (m)	θ_j (degree)	r_j (m)
1	0	0	θ_1	0
2	$\pi/2$	0	$-\pi/+\theta_2$	0
3	$\pi/2$	0	$\pi/2$	q_3

link parameter, and how it connects to other joint parameters. The analysis also encompasses aspects of singularity and workspace. These component elements assemble to form the geometric model, which is vital for applications like trajectory planning, motion control, and simulation. An accurate representation of the robot's geometry and kinematics is essential for the effective design and analysis of robotic systems. For a 2R1P robotic leg, the geometric model formulation is associated with the ASPM active ankle device's spherical joint mentioned in Chapter 3, which elucidates the transformation between joint space and task space. In the realm of robot control, kinematics and dynamics are fundamental concepts, with geometric model formulation serving as a cornerstone in robotic design and control. The Denavit-Hartenberg (DH) parameter approach is used in the method described in [82] to figure out the robot's homogeneous transformation model between its joint and task space. Given by;
$({}^{j-1}T_j) = Rot(x,\alpha_j)Trans(x,d_j)Rot(z,\theta_j)Trans(z,r_j)$
where

${}^{j-1}T_j$	Transformation matrix
Rot	Rotation matrix
α_j	link twist
d_j	link offset
θ	joint angle
r_j	link length
$j=$	$0,1,2,...,n$

DIRECT GEOMETRIC MODEL (DGM) The direct geometric model of a robot, also known as forward kinematics (FK), describes the relationship between the robot's joint angles and its end-effector position and orientation in the workspace. This is mathematically represented as;
$X = f(\theta) = {}^{j-1}T_j$

$$x = -cos\theta_1 cos\theta_2 d_3 \tag{A.1}$$
$$y = -sin\theta_1 cos\theta_2 d_3 \tag{A.2}$$
$$z = sin\theta_2 d_3 \tag{A.3}$$

where

$X = [x,y,z]$	end-effector position coordinates
$\theta = [\theta_1,\theta_2,d_3]$	joint variables

INVERSE GEOMETRIC MODEL (IGM) The inverse geometric model of a robot, also known as inverse kinematics (IK), defines the relationship between the desired position and orientation of the robot's end-effector in the workspace and the corresponding joint angles required to achieve that position and orientation. This can be mathematically represented as follows;
$(\theta_1, \theta_2, d_3) = f'(x, y, z)$

$$\theta_1 = \frac{-y}{z} tan\theta_2 \tag{A.4}$$

$$\theta_2 = \frac{z}{d_3} \tag{A.5}$$

$$d_3 = \sqrt{x^2 + y^2 + z^2} \tag{A.6}$$

A.2.1 *Velocity Analysis*

The time derivative of the end-effector positional coordinates gives the velocity $\dot{\mathbf{X}}$ in terms of its joint velocities $\dot{\theta}$, also known as the kinematic velocity or jacobian $\mathbf{J}$. To control a robot manipulator from one point to another, the joint angles and position parameters are not sufficiently enough to effectively enhance control. Since the control actions occur at the joints, information about the joint velocities are also important. The analysis of the inverse kinematic solution is computed analytically and compared with the numerical computation. Thus, the FK is evaluated in order that the applications of jacobian are explored. The graphical result between the task space velocity over a period of time for the spherical manipulator in Figure A.3, depicts the comparison between the analytical and numerical computation of jacobian. The curves shows a smooth matching plots that verifies the correctness of the jacobian computation.

$$\dot{x} = d_3\dot{\theta}_1 sin\theta_1 cos\theta_2 + d_3\dot{\theta}_2 cos\theta_1 sin\theta_2 - \dot{d}_3 cos\theta_1 cos\theta_2 \tag{A.7}$$

$$\dot{y} = -d_3\dot{\theta}_1 cos\theta_1 cos\theta_2 + d_3\dot{\theta}_2 sin\theta_1 sin\theta_2 - \dot{d}_3 sin\theta_1 cos\theta_2 \tag{A.8}$$

$$\dot{z} = d_3\dot{\theta}_2 cos\theta_2 + \dot{d}_3 sin\theta_2 \tag{A.9}$$

where

$\mathbf{J}(\theta)$	denotes the (mxn) Jacobian matrix
$[\dot{x}, \dot{y}, \dot{z}]$	end-effector coordinate velocities
$[\dot{\theta}_1, \dot{\theta}_2, \dot{d}_3]$	joint angular velocities
$\dot{X}$	denotes the forward kinematic
$\dot{\theta}$	denotes the inverse kinematic

$$\mathbf{J} = \begin{bmatrix} \frac{\partial x}{\partial \theta_1} & \frac{\partial x}{\partial \theta_2} & \frac{\partial x}{\partial d_3} \\ \frac{\partial y}{\partial \theta_1} & \frac{\partial y}{\partial \theta_2} & \frac{\partial y}{\partial d_3} \\ \frac{\partial z}{\partial \theta_1} & \frac{\partial z}{\partial \theta_2} & \frac{\partial z}{\partial d_3} \end{bmatrix} \tag{A.10}$$

$$\dot{X} = \mathbf{J}(\theta)\dot{\theta} \tag{A.11}$$

$$\dot{\theta} = \mathbf{J}^{-1}(\theta)\dot{X} \tag{A.12}$$

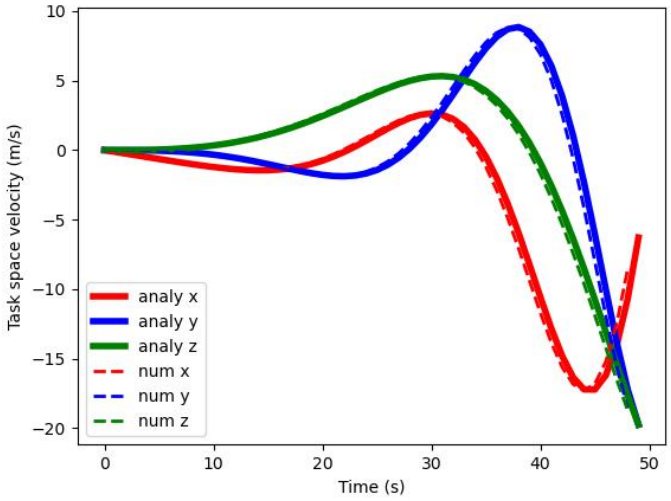

(a)

Figure A.3: Velocity analysis of 2R1P robotic leg

A.2.2 *Acceleration Analysis*

The acceleration analysis plays a fundamental role in the design, analysis, and control of robotic systems. It provides valuable insights into the dynamic behavior of the systems and enables roboticists to develop efficient and reliable solutions for a wide range of applications. The purpose is to optimize the FK equations for the 2R1P robotic leg and return a set of angular joint accelerations in task space. This is represented in a matrix form. Figure A.4 depicts the comparison between the numerical and analytical computation of the acceleration over a period of time. The smooth tracking between the two curves shows the correctness of formulated equations.

$$\ddot{X} = J\ddot{\theta} + \dot{J}\dot{\theta} \tag{A.13}$$

$$\begin{bmatrix} \ddot{x} \\ \ddot{y} \\ \ddot{z} \end{bmatrix} = \begin{bmatrix} d_3 \sin\theta_1 \cos\theta_2 & d_3 \cos\theta_1 \sin\theta_2 & -\cos\theta_1 \cos\theta_2 \\ -d_3 \cos\theta_1 \cos\theta_2 & d_3 \sin\theta_1 \sin\theta_2 & -\sin\theta_1 \cos\theta_2 \\ 0 & d_3 \cos\theta_2 & \sin\theta_2 \end{bmatrix} \begin{bmatrix} \ddot{\theta}_1 \\ \ddot{\theta}_2 \\ \ddot{d}_3 \end{bmatrix} +$$

$$\begin{bmatrix} d_3\dot{\theta}_1C1C2 - d_3\dot{\theta}_2S1S2 + \dot{d}_3S1C2 & -d_3\dot{\theta}_1S1S2 + d_3\dot{\theta}_2C1C2 + \dot{d}_3C1S2 & \dot{\theta}_1S1C2 + \dot{\theta}_2C1S2 \\ d_3\dot{\theta}_1S1C2 + d_3\dot{\theta}_2C1S2 - \dot{d}_3C1C2 & d_3\dot{\theta}_1C1S2 + d_3\dot{\theta}_2S1C2 + \dot{d}_3S1S2 & -\dot{\theta}_1C1C2 + \dot{\theta}_2S1S2 \\ 0 & -d_3\dot{\theta}_2S2 + \dot{d}_3C2 & \dot{\theta}_2C2 \end{bmatrix} \begin{bmatrix} \dot{\theta}_1 \\ \dot{\theta}_2 \\ \dot{d}_3 \end{bmatrix}$$

$\ddot{X}$ acceleration component in task space

$J, \dot{J}$ Jacobian and time derivative of the Jacobian respectively

$\dot{\theta}, \ddot{\theta}$ joint angular velocity and acceleration respectively

$S = \sin\theta$ and $C = \cos\theta$

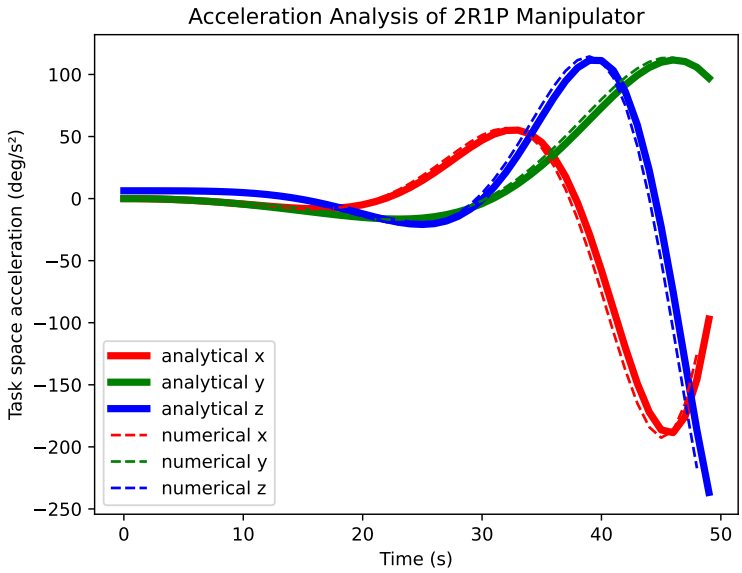

(a)

Figure A.4: Acceleration analysis of 2R1P robotic leg

A.3 DYNAMIC MODEL FOR A 2R1P ROBOTIC LEG

The dynamic model for a robot manipulator describes the relationship between the forces applied to the manipulator and the resulting motion. This model takes into account the mass distribution, inertia, and dynamics of the robot's links and joints. Developing the dynamic model for a 2R1P robot manipulator involves determining the mass distribution, inertial properties, and other physical characteristics of its links and joints. With these components, the dynamic model can be expressed using equations of motion, such as Euler-Lagrange equations or Newton-Euler equations [83]. These equations relate the forces and torques applied to the robot to its acceleration and motion. Once the dynamic model is established, it can be used for various purposes, including motion planning, control design, and simulation of the robot's behavior in different application scenarios. We evaluated the formulated equations of motion for a spherical joint, making them applicable to any type of spherical manipulator. Comparing Figure A.5a and

Figure A.5b reveals that the relationship between the numerical computation using Lagrangian methods and the analytical performance from the HyRoDyn software is approximately linear.

$$L(\theta\dot{\theta}) = K(\theta\dot{\theta}) - P(\theta) \tag{A.14}$$

$$\tau = \frac{d}{dt}\frac{\partial L}{\partial \dot{\theta}} - \frac{\partial L}{\partial \theta} \tag{A.15}$$

$$\tau_1 = md_3^2\ddot{\theta}_1 cos\theta_2^2 - 2md_3^2\dot{\theta}_1\dot{\theta}_2 sin\theta_2 cos\theta_2 \tag{A.16}$$

$$\tau_2 = md_3^2\ddot{\theta}_2 + md_3^2\dot{\theta}_1^2 sin\theta_2 cos\theta_2 + mgd_3 cos\theta_2 \tag{A.17}$$

$$\tau_3 = m\ddot{d_3} - d_3\dot{\theta}_1^2 cos\theta_2^2 - md_3\dot{\theta}_2^2 + mgsin\theta_2 \tag{A.18}$$

where

L	denotes the lagrangian
$K = \frac{1}{2}mv^2$	kinetic energy
m	mass
v	velocity
$P = mgh$	potential energy
g	acceleration due to gravity
h	height of the center of mass
$\tau = [\tau_1, \tau_2, \tau_3]$	vector of joint torques or forces
$[\theta, \dot{\theta}, \ddot{\theta}]$	vectors of joint position, velocity, and acceleration resp.

$$\tau_{ID} = M(\theta)\ddot{\theta} + C(\theta, \ddot{\theta})\dot{\theta} + g(\theta) + f\dot{\theta} \tag{A.19}$$

$$\ddot{\theta}_{FD} = M^{-1}(\theta)\ddot{\theta}(\tau_{ID}) - (C(\theta, \ddot{\theta})\dot{\theta} + g(\theta) + f\dot{\theta}) \tag{A.20}$$

τ_{ID}	denotes the *Inverse Dynamics*
$\ddot{\theta}_{FD}$	denotes the *Forward Dynamics*
M	is the (nxn) generalized mass-inertia matrix
C	is an (nx1) vector for centripetal and coriolis force
g	gravity terms
f	frictional force

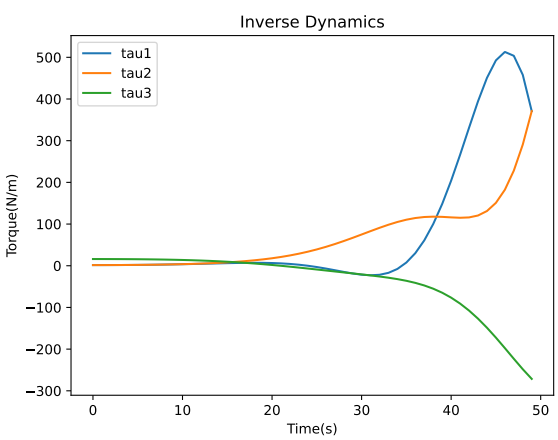

(a) Numerical computation using Lagrangian formulation

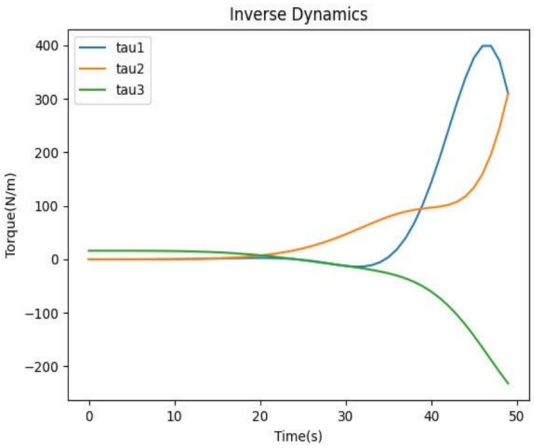

(b) Analytical computation using HyRoDyn software

Figure A.5: Inverse Dynamic analysis of 2R1P robotic leg

B

SYMBOLIC COMPUTATION OF 2R1P ROBOTIC LEG USING MATLAB SNIPET

The goal of this module is to symbolically derive the motion equations for a 2R1P robotic leg, commonly known as a spherical manipulator. Initially, we obtained these equations using a Matlab snippet. However, the demand for greater computational efficiency requires transitioning to advanced Python and C++ tools. The equations of motion derived in Matlab snippet are symbolically expressed as follows;

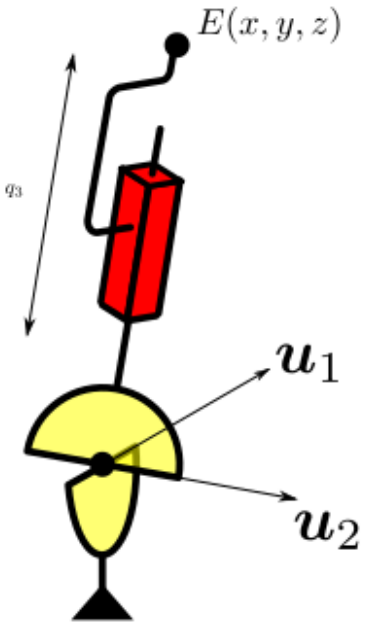

Figure B.1: 2R1P robotic leg

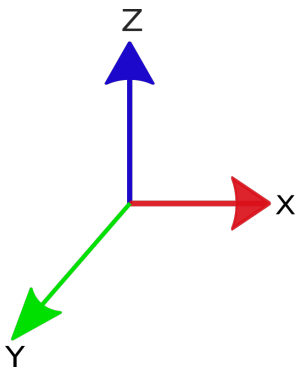

Figure B.2: Global coordinate

The 2R1P spherical manipulator is considered as a robotic leg. The robotic leg shown in Figure B.1 is composed of three joints: first two joints u_1 and u_2 are revolute with their axes oriented orthogonally to each other and the third joint q_3 is prismatic, carrying the end effector point E.

From Figure B.1, the generalised joint coordinates (u_1, u_2, q_3) are represented by ($q1$, $q2$, $q3$). Now, comparing the direction of the joint cordinates shown in Figure B.1 with the global coordinate frame shown in Figure B.2 depicts the rotations and translation about and along the joint axes respectively.

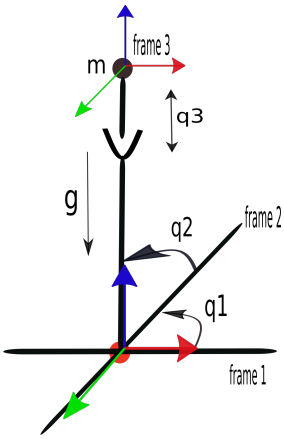

Figure B.3: Initial configuration with frames

Considering an initial configuration as shown in Figure B.3, the prismatic joint carrying the end effector slides along the (z-axis) direction of the global coordinate frame. Hence, $q = [q_1\, q_2\, q_3]^T = [0\, 0\, mg]^T$. The robotic leg is treated with a point mass and its center of mass is located at the end effector point. Therefore, masses of the first and second links are zeros respectively while the third link has a mass value of one. The gravity g of course acts along the z-axis direction of the sliding prismatic joint.

1. Declare some global and symbolic variables in Matlab using the command sym. For a 2R1P manipulator, you can write.

```
global Param; % Structure with all geoemtric and dynamic
   robot parameters
global Chain; % Structure with all temporal data
global n; % DOF, number of joints
global g_vector; % gravity vector
global ee; % end effector configuration
syms q1 q2 q3 real % Generalised position vector components
syms dq1 dq2 dq3 real % Generalised velocity vector
   components
syms ddq1 ddq2 ddq3 real % Generalised acceleration vector
   components
syms g % gravity
syms pi % symbolic treatment of pi (saves you from numerical
    issues)
g_vector = [0,0,g];
% mass and Moment of Inertia properties
syms m1 c1x c1y c1z I1 I1xx I1xy I1xz I1yy I1yz I1zz real
syms m2 c2x c2y c2z I2 I2xx I2xy I2xz I2yy I2yz I2zz real
syms m3 c3x c3y c3z I3 I3xx I3xy I3xz I3yy I3yz I3zz real
```

2. Input Denavit-Hartenberg (DH) parameter table using the modified DH convention.

```
%%The DH-table for the 2R1P robotic leg is a 3x3 matrix
   dimension with the parameters defined column-wise as thus
   ;
```

sigma (σ), alpha (α), d, theta (θ) and r representing revolute or prismatic joint, link twist,

link length, joint angle and joint offset respectively.

```
dh_table = [0, pi/2, 0, -pi/2, 0;
        0, -pi/2, 0, -pi/2, 0;
        1, pi/2, 0, pi/2, 0];
Param = dhToScrewCoord(dh_table); %% Function builds the
   screw coordinate paramters.
```

3. End-effector configuration w.r.t the last link body fixed frame in the chain.

```
re = [0;0;0];
ee = [eye(3),re;[0,0,0],[1]];
```

4. Mass, Inertia and Center of mass paramaters for the three joints.

```
m1   = 0.00000;
c1x  = 0.00000;
c1y  = 0.00000;
c1z  = 0.00000;
I1xx = 0.00000;
I1xy = 0.00000;
I1xz = 0.00000;
I1yy = 0.00000;
I1yz = 0.00000;
I1zz = 0.00000;

m2   = 0.00000;
c2x  = 0.00000;
c2y  = 0.00000;
c2z  = 0.00000;
I2xx = 0.00000;
I2xy = 0.00000;
I2xz = 0.00000;
I2yy = 0.00000;
I2yz = 0.00000;
I2zz = 0.00000;

m3   = 0.00000;
c3x  = 0.00000;
c3y  = 0.00000;
c3z  = 0.00000;
I3xx = 0.00000;
```

```
I3xy = 0.00000;
I3xz = 0.00000;
I3yy = 0.00000;
I3yz = 0.00000;
I3zz = 0.00000;
```

5. Function builds mass-inertia matrix in SE(3) from the mass, inertia and center of mass data.

```
Param(1).Mb = MassMatrixMixedData(m1, ...
InertiaMatrix(I1xx, I1xy, I1xz, I1yy, I1yz, I1zz), ...
[c1x, c1y, c1z]);
Param(2).Mb = MassMatrixMixedData(m2, ...
InertiaMatrix(I2xx, I2xy, I2xz, I2yy, I2yz, I2zz), ...
[c2x, c2y, c2z]);
Param(3).Mb = MassMatrixMixedData(m3, ...
InertiaMatrix(I3xx, I3xy, I3xz, I3yy, I3yz, I3zz), ...
[c3x, c3y, c3z]);
```

6. Iteration of the loop describing the chain

```
for i=1:n
    Chain(i).V = zeros(n,1);
    Chain(i).Vd = zeros(n,1);
    Chain(i).f = zeros(4,4);
    Chain(i).C = zeros(4,4);
    Chain(i).Crel = zeros(4,4); % C_i,i-1
    Chain(i).AdCrel = zeros(6,6);
    Chain(i).adX = zeros(6,6);
    Chain(i).W = zeros(6,1);   % interbody wrench
    Chain(i).Q = 0;
end
```

7. Define a generalised trajectory vector for position, velocity and acceleration as follows;

```
q = [q1 q2 q3];
qd = [dq1 dq2 dq3];
q2d = [ddq1 ddq2 ddq3];
n = length(q);
WEE = zeros(6,1);
```

8. Call the matlab function *ClosedFormKinematics_BodyFixed(q,qd,q2d)*. The function below returns the position and orientation of the end effector generally referred to as forward kinematics.

```
[T] = ClosedFormKinematics_BodyFixed(q',qd',q2d');
```

9. Call the matlab function *ClosedFormInvDyn_BodyFixed(q,qd,q2d)*. This returns the equations of motion for the generalised forces and torque vector as a result of the function below.

```
[Q] = ClosedFormInvDyn_BodyFixed(q',qd',q2d');
Q_simplified = simplify(Q) %% simplified version for the
   equations of motion.
```

From the above simulation, the forward kinematics and inverse dynamics are both computed. However, the Jacobian matrix, mass-inertia matrix, gravity matrix, and coriolis-centrifugal matrix are also derived analytically from the generated Matlab equations. The symbolic expressions of these matrices are listed below.

1. **Forward Kinematics:**

$$E_{xyz} = \begin{bmatrix} \cos(q_1) & -\sin(q_1)\sin(q_2) & -\sin(q_1)\cos(q_2) & -q_3\, sin(q_1)\cos(q_2) \\ 0 & \cos(q_2) & -\sin(q_2) & -q_3\sin(q_2) \\ \sin(q_1) & \cos(q_1)\sin(q_2) & \cos(q_1)\cos(q_2) & q_3\, cos(q_1)\cos(q_2) \\ 0 & 0 & 0 & 1 \end{bmatrix} \tag{B.1}$$

2. **Jacobian matrix:** The jacobian matrix is analytically computed from the partial derivative of the end effector positional vector with respect to its joint coordinates q_1, q_2, and q_3. Generally, it is the velocity of the end-effector $(\dot{E}_{xyz})$ in terms of the joint velocities $(\dot{q})$. The first three rows of the jacobian matrix (6x3) are associated with the linear velocities (rate of change of positions) of the end effector while the last three forms the angular velocities (rate of change of orientation).

$$\begin{bmatrix} \dot{x} \\ \dot{y} \\ \dot{z} \\ w_x \\ w_y \\ w_z \end{bmatrix} = \begin{bmatrix} -q_3\cos(q_1)\cos(q_2) & q_3\sin(q_1)\sin(q_2) & -\sin(q_1)\cos(q_2)) \\ 0 & -q_3\cos(q_2) & -\sin(q_2) \\ q_3\sin(q_1)\cos(q_2) & -q_3\cos(q_1)\sin(q_2) & \cos(q_1)\cos(q_2)) \\ 0 & 0 & 0 \\ 0 & 0 & 0 \\ 1 & 1 & 0 \end{bmatrix} \begin{bmatrix} \dot{q}_1 \\ \dot{q}_2 \\ \dot{q}_3 \end{bmatrix} \tag{B.2}$$

```
%% Extracting only the Linear velocity part of the
   Jacobian matrix as shown below.
```

$$\mathbf{J_{sys}} = \begin{bmatrix} -q_3\cos(q_1)\cos(q_2) & q_3\sin(q_1)\sin(q_2) & -\sin(q_1)\cos(q_2)) \\ 0 & -q_3\cos(q_2) & -\sin(q_2) \\ -q_3\sin(q_1)\cos(q_2) & -q_3\cos(q_1)\sin(q_2) & \cos(q_1)\cos(q_2)) \\ 1 & 1 & 0 \end{bmatrix} \tag{B.3}$$

In order to understand the Jacobian matrix and how it affects the velocity of the end effector, we can multiply each row of the jacobian matrix by the corresponding joint velocity. This defines the joint speed that controls the end effector velocity in the zero configuration. However, the entries of the jacobian matrix with zero row values indicates nomatter what we do with the joints, we can not get the end effector to rotate about and the axes of the zero configuration. Therefore, the manipulability of a robot describes its ability to move freely in all directons of its workspace by reaching set positions as well as to change orientation at a given configuration.

3. **Generalized Mass-inertia matrix $\mathbf{M}(\mathbf{q})$:**

$$\mathbf{M} = \begin{bmatrix} 0.25 + q_3\cos\left(q_2^2\right) + q_2^2\cos\left(q_2^2\right) \\ 0.25 + q_3 + {q_3}^2 \\ 1 \end{bmatrix} \tag{B.4}$$

4. **Coriolis-centrifugal matrix $\mathbf{C}(\mathbf{q},\dot{\mathbf{q}})$:**

$$\mathbf{C} = \begin{bmatrix} (\cos\left(q_2^2\right) + 2q_3\cos\left(q_2^2\right))\,\mathrm{dq}_1\,\mathrm{dq}_3 - (q_3\sin(2q_2) + q_3^2\sin(2q_2))(\mathrm{dq}_1\,\mathrm{dq}_2) \\ (1+2q_3)\mathrm{dq}_2\,\mathrm{dq}_3 + ((0.5q_3\sin(2q_2) + 0.5q_3^2\sin\left(2q_2\right))\mathrm{dq}_1^2) \\ -(0.5\cos\left(q_2^2\right) + q_3\cos\left(q_2^2\right))\mathrm{dq}_2^2 - (0.5+q_3)\mathrm{dq}_2^2 \end{bmatrix} \tag{B.5}$$

5. **Gravity matrix $\mathbf{G}(\mathbf{q})$:**

$$\mathbf{G} = \begin{bmatrix} -(0.5\sin(q_1)\cos(q_2) + q_3\sin(q_1)\cos(q_2)) \\ -(0.5\cos(q_1)\sin(q_2) + q_3\cos(q_1)\sin(q_2)) \\ \cos(q_1)\cos(q_2) \end{bmatrix} \tag{B.6}$$

Therefore, the above equations were extracted from the below symbolic computed equations of motion;

$$\begin{aligned} \phi_1 = {} & 0.25\,\mathrm{ddq}_1 + \mathrm{dq}_1\,\mathrm{dq}_3\cos\left(q_2^2\right) + \mathrm{ddq}_1\,q_3\cos\left(q_2^2\right) - 0.5\,g\sin(q_1)\cos(q_2) \\ & + \mathrm{ddq}_1\,q_3^2\cos\left(q_2^2\right) - 1.0\,\mathrm{dq}_1\,\mathrm{dq}_2\,q_3\sin(2q_2) - \mathrm{dq}_1\,\mathrm{dq}_2\,q_3^2\sin(2q_2) \\ & + 2\,\mathrm{dq}_1\,\mathrm{dq}_3\,q_3\cos\left(q_2^2\right) - q_3\,g\sin(q_1)\cos(q_2)) \end{aligned} \tag{B.7}$$

$$\begin{aligned}\phi_2 = 0.25\,\mathrm{ddq}_2 + \mathrm{dq}_2\,\mathrm{dq}_3 + \mathrm{ddq}_2\,q_3 + \mathrm{ddq}_2\,q_3^2 + 0.5\,\mathrm{dq}_1^2\,q_3\,\sin(2q_2) + 0.5\,\mathrm{dq}_1^2\,q_3^2\,\sin(2q_2) \\ - 0.5\,g\cos(q_1)\sin(q_2) + 2\,\mathrm{dq}_2\,\mathrm{dq}_3\,q_3 - q_3\,g\cos(q_1)\sin(q_2))\end{aligned} \tag{B.8}$$

$$\phi_3 = \mathrm{ddq}_3 - 0.5\,\mathrm{dq}_1^2\cos\left(q_2^2\right) - q_3\,\mathrm{dq}_2^2 - 0.5\,\mathrm{dq}_2^2 + g\cos(q_1)\cos(q_2) - \mathrm{dq}_1\,q_3\cos\left(q_2^2\right) \tag{B.9}$$

$$\tau = \begin{bmatrix}\tau_1 \\ \tau_2 \\ \tau_3\end{bmatrix} \tag{B.10}$$

This is how we can derive the equations of motion symbolically using this tool.

List of Figures

Figure 1.1 Various mobility aids for individuals with mobility disorder 2
Figure 1.2 Wearable and platform-based exoskeleton 3
Figure 1.3 Thesis Organization 7
Figure 2.1 Medical application exoskeletons 14
Figure 2.4 Classification of exoskeleton robots based on applications. 20
Figure 2.5 Number of exoskeleton robots according to domain area. 21
Figure 2.6 Histogram of the publication years of the considered works. 21
Figure 2.7 Series-parallel (hybrid) exoskeleton design [101]. 24
Figure 3.1 ASPM ankle device [104] 42
Figure 3.2 Recupera-Reha full-body exoskeleton [101] 43
Figure 3.3 Feasible workspace configurations adapted in [104]. 43
Figure 3.4 Human and ASPM ankle complex 44
Figure 3.9 CAD prototype of the Recupera-Reha foot base 53
Figure 4.1 The Recupera-Reha exoskeleton robot in (1) sitting, (2) standing and (3) static walking mode 57
Figure 4.2 Recupera-Reha system and its topological graph 57
Figure 4.3 Leg in the Recupera-Reha exoskeleton [112] 59
Figure 5.1 Low-level Control Architecture for the Recupera-Reha exoskeleton . . 67
Figure 5.2 Integrating low-level control with HyRoDyn software([101]) 68
Figure 5.3 Overall Simulation and Experimental Pipeline 69
Figure 5.4 Joint space tracking in PyBullet simulator during four-steps static walk 70
Figure 5.5 Floating base motion in PyBullet simulator during four-steps static walk 71
Figure 5.6 The screenshot of the exoskeleton leg joints symmetric movements . . 72
Figure 5.7 Hip joint's ROM tracking 73
Figure 5.8 Prismatic Knee joint's ROM tracking 73

Figure 5.9 Ankle joint's ROM tracking . . . 74
Figure 5.10 The screenshot of the exoskeleton at initial standing, sitting, and final standing position, both in simulation and on the real system . . . 75
Figure 5.11 Sitting and standing motion of the prismatic knee joints . . . 75
Figure 5.12 Position of the hip joint motors during the sitting motion . . . 76
Figure 5.13 Position of the hip joint motors during the standing motion . . . 76
Figure 5.14 The Recupera exoskeleton four-steps static walking motion in simulation and on the real system . . . 77
Figure 5.15 Hip joint's position during four steps static walk motion . . . 78
Figure 5.16 Prismatic Knee joint's position tracking during four steps static walk motion . . . 78
Figure 5.17 Ankle joint's position tracking during four steps static walk motion . . . 79
Figure 5.18 Hip joint's position during sitting motion . . . 80
Figure 5.19 Prismatic Knee joint's position during sitting motion . . . 80
Figure 5.20 Ankle joint's position during sitting motion . . . 81
Figure 5.21 The screenshots of the Recupera exoskeleton in sitting, standing, and static walk during the experiment with a human . . . 82
Figure 5.22 Hip joint's position during four steps static walk motion with human wearer . . . 82
Figure 5.23 Prismatic Knee joint's position tracking during four steps static walk motion with human wearer . . . 83
Figure 5.24 Ankle joint's position tracking during four steps static walk motion with human wearer . . . 83
Figure A.1 Topology of spherical manipulators . . . 90
Figure A.2 kinematic architecture . . . 91
Figure A.3 Velocity analysis of 2R1P robotic leg . . . 94
Figure A.4 Acceleration analysis of 2R1P robotic leg . . . 95
Figure A.5 Inverse Dynamic analysis of 2R1P robotic leg . . . 97
Figure B.1 2R1P robotic leg . . . 98
Figure B.2 Global coordinate . . . 98
Figure B.3 Initial configuration with frames . . . 99

List of Tables

Table 2.1 Overview on medically-based biped exoskeleton robots for rehabilitation purposes. . . . 15
Table 2.2 Overview on medically-based biped exoskeleton robots assistive purposes. 15
Table 2.3 Overview on medically-based biped exoskeleton robots for power augmentation. . . . 16
Table 2.4 Overview on industrially-based biped exoskeleton robots (for walking assistance, load handling, pain or fatigue relief assistance) . . . 18
Table 2.5 Overview of companies pursuing bipedal walking exoskeleton . . . 22
Table 2.6 Review on hip joint . . . 26
Table 2.7 Review on knee joint . . . 27
Table 2.8 Review on ankle joint . . . 28
Table 2.9 Review on control methods and approaches for LEE. . . . 34
Table 3.1 Comparison between the human and existing ankle joint ROM . . . 45
Table 3.2 Ankle motion ranges with $\pm 25^\circ$ actuator constraint . . . 48
Table 3.3 Hip motion ranges with $\pm 25^\circ$ actuator constraint . . . 49
Table 3.4 Ankle motion ranges with $\pm 27^\circ$ actuator constraint . . . 51
Table 3.5 Hip motion ranges with $\pm 27^\circ$ actuator constraint . . . 52
Table 4.1 Loop closure constraints [49] . . . 58
Table 4.2 ROM for the Actuator Joints . . . 60
Table 4.3 ROM for the Independent Joints . . . 61
Table A.1 DH-parameters for 2R1P robotic leg . . . 92

LIST OF ACRONYMS

ASPM ALmost Spherical Parallel Mechanism

HYRODYN Hybrid Robot Dynamics

BLDC Brushless Direct Current

SEA Series Elastic Actuator

DOF Degree of Freedom

ROM Range of Motion

SCI Spinal Cord Injury

OA Osteoarthritis

ZMP Zero Moment Point

COP Center of Pressure

COM Center of Mass

EMG Electromyography

EEG Electroencephalography

CGA Clinical Gate Array

ERP Error Related Potential

FPGA Field-Programmable Gate Array

IMU Inertia Measurement Unit

PID Proportional–Integral–Derivative

NN Neural Network

PD Proportional–Derivative

ML Machine Learning

RL Reinforcement Learning

DL Deep Learning

DRL Deep Reinforcement Learning

LQR Linear Quadratic Regulator

TVLQR Time Varying Linear Quadratic Regulator

MPC Model Predictive Controller

AI Artificial Intelligence

XAI Explainable Artificial Intelligence

QDD Quasi-Direct Drives

HRI Human Robot Interaction

SOTA State of the Art

3D Three Dimension

2D Three Dimension

PM Parallel Manipulator

SPM Spherical Parallel Manipulator

DF-PF Dorsi-Flexion Plantar-Flexion

AD-AB Adduction-Abduction

EV-IN Eversion-Inversion

EE End-Effector

RIGM Rotative Inverse Geometric Method

CAD Computer Aided Design

OC Optimal Control

OCP Optimal Control Problem

WBC Whole Body Control

QP Quadratic program

DDP DIfferential Dynamic Programming

FDDP Feasibilty DIfferential Dynamic Programming

ALU Actuator Control Unit

PCB Printed Circuit Board

NDLCOM Node Data Link Communication

ALU Arithmetic Logic Unit

ROCK Robot Construction kit

CROCODDYL Contact RObot COntrol by Differential DYnamic Library

BIBLIOGRAPHY

[1] *AXO-SUIT: full-body exoskeleton*. https://www.axo-suit.eu/. [Accessed: 2021-07-03]. 2020.

[2] Gabriel Aguirre-Ollinger, J. Edward Colgate, Michael A. Peshkin, and Ambarish Goswami. "Active-Impedance Control of a Lower-Limb Assistive Exoskeleton." In: *2007 IEEE 10th International Conference on Rehabilitation Robotics*. 2007, pp. 188–195. DOI: 10.1109/ICORR.2007.4428426.

[3] Junhyeok Ahn, Donghyun Kim, Seung Hyeon Bang, Nick Paine, and Luis Sentis. "Control of a High Performance Bipedal Robot using Viscoelastic Liquid Cooled Actuators." In: Oct. 2019, pp. 146–153. DOI: 10.1109/Humanoids43949.2019.9035023.

[4] Hayder Al-Shuka, Mohammad Rahman, Steffen Leonhardt, Ileana Ciobanu, and Mihai Berteanu. "Biomechanics, actuation, and multi-level control strategies of power-augmentation lower extremity exoskeletons: an overview." In: *International Journal of Dynamics and Control* 7 (Dec. 2019). DOI: 10.1007/s40435-019-00517-w.

[5] Kristy Alexandratos, Fiona Barnett, and Yvonne Thomas. "The Impact of Exercise on the Mental Health and Quality of Life of People with Severe Mental Illness: A Critical Review." In: *British Journal of Occupational Therapy* 75 (Feb. 2012), pp. 48–60. DOI: 10.4276/030802212X13286281650956.

[6] Aaron D. Ames. "Human-Inspired Control of Bipedal Walking Robots." In: *IEEE Transactions on Automatic Control* 59.5 (2014), pp. 1115–1130. DOI: 10.1109/TAC.2014.2299342.

[7] Adae O. Amoako and George Guntur A. Pujalte. "Osteoarthritis in Young, Active, and Athletic Individuals." In: *Clinical Medicine Insights: Arthritis and Musculoskeletal Disorders* 7 (2014). PMID: 24899825, CMAMD.S14386. DOI: 10.4137/CMAMD.S14386. eprint: https://doi.org/10.4137/CMAMD.S14386. URL: https://doi.org/10.4137/CMAMD.S14386.

[8] *B-Temia Inc.: The New and Improved Version of Keeogo dermoskeleton*. https://b-temia.com/keeogo/. [Accessed: 2021-09-15].

[9] Erfan Shojaei Barjuei, M. Mahdi Ghazaei Ardakani, Darwin G. Caldwell, Marcello Sanguineti, and Jesús Ortiz. "Optimal Selection of Motors and Transmissions in Back-Support Exoskeleton Applications." In: *IEEE Transactions on Medical Robotics and Bionics* 2.3 (2020), pp. 320–330. DOI: 10.1109/TMRB.2020.3010611.

[10] Harrison L. Bartlett, Shane T. King, Michael Goldfarb, and Brian E. Lawson. "A Semi-Powered Ankle Prosthesis and Unified Controller for Level and Sloped Walking." In: *IEEE Transactions on Neural Systems and Rehabilitation Engineering* 29 (2021), pp. 320–329. DOI: 10.1109/TNSRE.2021.3049194.

[11] Romain Baud, Ali Manzoori, A.J. Ijspeert, and Mohamed Bouri. "Review of control strategies for lower-limb exoskeletons to assist gait." In: *Journal of NeuroEngineering and Rehabilitation* 18 (July 2021). DOI: 10.1186/s12984-021-00906-3.

[12] Jonas Beil, Gernot Perner, and Tamim Asfour. "Design and control of the lower limb exoskeleton KIT-EXO-1." In: *2015 IEEE International Conference on Rehabilitation Robotics (ICORR)* (2015), pp. 119–124.

[13] Oriol Bellmunt and Lucio Flavio Campanile. *Design Rules for Actuators in Active Mechanical Systems*. Jan. 2010. ISBN: 978-1-84882-613-7. DOI: 10.1007/978-1-84882-614-4.

[14] *Berkeley Bionics unveiled eLEGS (2010)*. https://bleex.me.berkeley.edu/research/exoskeleton/elegs/. [Accessed: 2020-10-17]. 2010.

[15] Pieter Beyl, Michaël Damme, Ronald Van Ham, Bram Vanderborght, and Dirk Lefeber. "Design and Control of a Lower Limb Exoskeleton for Robot-Assisted Gait Training." In: *Applied Bionics and Biomechanics* 6 (Apr. 2009), pp. 229–243. DOI: 10.1080/11762320902784393.

[16] Z. M. Bi. "Design of a spherical parallel kinematic machine for ankle rehabilitation." In: *Advanced Robotics* 27.2 (2013), pp. 121–132.

[17] German Bionic. *CrayX Exoskeleton*. https://www.germanbionic.com/en/cray-x-solution/. [Accessed: 2021-06-04]. 2018.

[18] Nick Birch, Jon Graham, Tom Priestley, Chris Heywood, Mohamed Sakel, Angela Gall, Andrew Nunn, and Nada Signal. "Results of the first interim analysis of the RAPPER II trial in patients with spinal cord injury: ambulation and functional exercise programs in the REX powered walking aid." In: *Journal of neuroengineering and rehabilitation* 14.1 (2017), pp. 1–10. DOI: 10.1186/s12984-017-0274-6.

[19] R. H. Bishop. *The Mechatronics Handbook - 2 Volume Set (2nd ed.). CRC Press*. https://www.perlego.com/book/1575680/the-mechatronics-handbook-2-volume-set-pdf. 2008. DOI: https://doi.org/10.1201/b16086.

[20] Melya Boukheddimi, Rohit Kumar, Shivesh Kumar, Justin Carpentier, and Frank Kirchner. "Investigations into Exploiting the Full Capabilities of a Series-Parallel Hybrid Humanoid Using Whole Body Trajectory Optimization." In: *2023 IEEE/RSJ International Conference on Intelligent Robots and Systems (IROS)*. 2023, pp. 10433–10439. DOI: 10.1109/IROS55552.2023.10341784.

[21] Jurgen Broeren, Mark Dixon, Katharina Stibrant Sunnerhagen, and Martin Rydmark. "Rehabilitation after Stroke using Virtual Reality, Haptics (force feedback) and Telemedicine." In: *Studies in health technology and informatics* 124 (2006), pp. 51–6.

[22] Maxime Brunet, Marine Pétriaux, Florent Di Meglio, and Nicolas Petit. *Enabling safe walking rehabilitation on the exoskeleton Atalante: experimental results*. 2023. arXiv: 2304.08091 [cs.RO].

[23] Rohan Budhiraja, Justin Carpentier, Carlos Mastalli, and Nicolas Mansard. "Differential Dynamic Programming for Multi-Phase Rigid Contact Dynamics." In: *IEEE-RAS Humanoids 2018*. Beijing, China, 2018.

[24] Di Carlo, Wensing Jared, M. Patrick, Benjamin Katz, Gerardo Bledt, and Sangbae Kim. "Dynamic Locomotion in the MIT Cheetah 3 Through Convex Model-Predictive Control." In: *2018 IEEE/RSJ International Conference on Intelligent Robots and Systems (IROS)*. 2018, pp. 1–9. DOI: 10.1109/IROS.2018.8594448.

[25] Justin Carpentier, Guilhem Saurel, Gabriele Buondonno, Joseph Mirabel, Florent Lamiraux, Olivier Stasse, and Nicolas Mansard. "The Pinocchio C++ library – A fast and flexible implementation of rigid body dynamics algorithms and their analytical derivatives." In: *SII*. IEEE. 2019.

[26] Ronnapee Chaichaowarat, Sarunpat Prakthong, and Siri Thitipankul. "Transformable Wheelchair Exoskeleton Hybrid Robot for Assisting Human Locomotion." In: *Robotics* 12.1 (2023). ISSN: 2218-6581. DOI: 10.3390/robotics12010016. URL: https://www.mdpi.com/2218-6581/12/1/16.

[27] R. Sarah Chang, Rudi Kobetic, Musa L. Audu, Roger D. Quinn, and Ronald J. Triolo. "Powered Lower-Limb Exoskeletons to Restore Gait for Individuals with Paraplegia - a Review." In: *Case orthopaedic journal,* 12.75-80 (2015). URL: https://pubmed.ncbi.nlm.nih.gov/28004009/.

[28] Bing Chen, Hao Ma, Lai-Yin Qin, Fei Gao, Kai-Ming Chan, Sheung-Wai Law, Ling Qin, and Wei-Hsin Liao. "Recent developments and challenges of lower extremity exoskeletons." In: *Journal of Orthopaedic Translation* 5 (2016). Special Issue: Orthopaedic Biomaterials and Devices, pp. 26–37. ISSN: 2214-031X. DOI: https://doi.org/10.1016/j.jot.2015.09.007. URL: https://www.sciencedirect.com/science/article/pii/S2214031X15000716.

[29] Simon Christensen, Shaoping Bai, Sajid Rafique, Magnus Isaksson, Leonard O'Sullivan, Valerie Power, and Gurvinder Virk. "AXO-SUIT - A Modular Full-Body Exoskeleton for Physical Assistance: Proceedings of the 4th IFToMM Symposium on Mechanism Design for Robotics." In: Jan. 2019, pp. 443–450. ISBN: 978-3-030-00364-7. DOI: 10.1007/978-3-030-00365-4_52.

[30] Gery Colombo, Matthias Jörg, R Schreier, and Volker Dietz. "Treadmill training of paraplegic patients using a robotic orthosis." In: *Journal of rehabilitation research and development* 37 (Nov. 2000), pp. 693–700.

[31] Erwin Coumans and Yunfei Bai. *PyBullet, a Python module for physics simulation for games, robotics and machine learning*. http://pybullet.org. 2016–2021.

[32] *DART (Dynamic Animation and Robotics Toolkit)*. https://dartsim.github.io/. [Accessed: 2021-12-30].

[33] Ashwin P. Dani, Iman Salehi, Ghananeel Rotithor, Daniel Trombetta, and Harish Ravichandar. "Human-in-the-Loop Robot Control for Human-Robot Collaboration: Human Intention Estimation and Safe Trajectory Tracking Control for Collaborative Tasks." In: *IEEE Control Systems Magazine* 40.6 (2020), pp. 29–56. DOI: 10.1109/MCS.2020.3019725.

[34] Scott L. Delp, Frank C. Anderson, Allison S. Arnold, Peter Loan, Ayman Habib, Chand T. John, Eran Guendelman, and Darryl G. Thelen. "OpenSim: Open-Source Software to Create and Analyze Dynamic Simulations of Movement." In: *IEEE Transactions on Biomedical Engineering* 54.11 (2007), pp. 1940–1950. DOI: 10.1109/TBME.2007.901024.

[35] Scott L. Delp, Frank C. Anderson, Allison S. Arnold, Peter Loan, Ayman Habib, Chand T. John, Eran Guendelman, and Darryl G. Thelen. "OpenSim: Open-Source Software to Create and Analyze Dynamic Simulations of Movement." In: *IEEE Transactions on Biomedical Engineering* 54.11 (2007), pp. 1940–1950. DOI: 10.1109/TBME.2007.901024.

[36] Christian Di Natali et al. "Pneumatic Quasi-Passive Actuation for Soft Assistive Lower Limbs Exoskeleton." In: *Frontiers in Neurorobotics* 14 (2020). ISSN: 1662-5218. DOI: 10.3389/fnbot.2020.00031. URL: https://www.frontiersin.org/article/10.3389/fnbot.2020.00031.

[37] Moritz Diehl and Sébastien Gros. *Numerical Optimal Control (preliminary and incomplete draft)*. 2017.

[38] Mingjie Dong, Yu Zhou, Jianfeng Li, Xi Rong, Wenpei Fan, Xiaodong Zhou, and Yuan Kong. "State of the art in parallel ankle rehabilitation robot: a systematic review." In: *Journal of NeuroEngineering and Rehabilitation* 18 (Mar. 2021). DOI: 10.1186/s12984-021-00845-z.

[39] Anirvan Dutta, Durgesh Haribhau Salunkhe, Shivesh Kumar, Arun Dayal Udai, and Suril V. Shah. "Sensorless full body active compliance in a 6 DOF parallel manipulator." In: *Robotics and Computer-Integrated Manufacturing* 59 (2019), pp. 278–290.

[40] Tong Duy Son, Ajinkya Bhave, Wouter Vandermeulen, Theo Geluk, Matthieu Worm, and Herman Van der Auweraer. "Model-based and Data-driven Learning Control for Safety and Comfort Autonomous Driving." In: (Nov. 2020). DOI: 10.13140/RG.2.2.13850.88003.

[41] Hyundai Medical EXoskeleton. *Hyundai Medical EXoskeleton: H-MEX*. https://exoskeletonreport.com/product/h-mex/. [Accessed: 2021-01-12]. 2017.

[42] Joan Edelstein. "36 - Canes, Crutches, and Walkers." In: *Atlas of Orthoses and Assistive Devices (Fifth Edition)*. Ed. by Joseph B. Webster and Douglas P. Murphy. Fifth Edition. Philadelphia: Elsevier, 2019, 377–382.e3. ISBN: 978-0-323-48323-0. DOI: https://doi.org/10.1016/B978-0-323-48323-0.00036-6. URL: https://www.sciencedirect.com/science/article/pii/B9780323483230000366.

[43] *Ekso Bionics: The leader in exoskeleton technology*. https://eksobionics.com/. [Accessed: 2021-07-11]. 2020.

[44] *Eksobionics: EksoNR EXoskeleton*. https://eksobionics.com/eksonr-2/. [Accessed: 2021-11-30].

[45] A. Kirchner Elsa, N. Will, M. Simnofske, L. M. V. Benitez, J. D. G. Fernández, P. Kampmann, and F. Kirchner. "Exoskelette und künstliche Intelligenz in der klinischen Rehabilitation, Digitale Transformation von Dienstleistungen im Gesundheitswesen V: Impulse für die Rehabilitation." In: ed. by P. Da-Cruz M. A. Pfannstiel and H. Mehlich. 2019, pp. 413–435. ISBN: 978-3-658-23986-2. DOI: https://doi.org/10.1007/978-3-658-23987-9_21.

[46] Johannes Englsberger et al. "Overview of the torque-controlled humanoid robot TORO." In: *2014 IEEE-RAS International Conference on Humanoid Robots*. 2014, pp. 916–923. DOI: 10.1109/HUMANOIDS.2014.7041473.

[47] Julian Eßer, Shivesh Kumar, Heiner Peters, Vinzenz Bargsten, Jose de Gea Fernandez, Carlos Mastalli, Olivier Stasse, and Frank Kirchner. "Design, analysis and control of the series-parallel hybrid RH5 humanoid robot." In: *2020 IEEE-RAS 20th International Conference on Humanoid Robots (Humanoids)*. 2021, pp. 400–407. DOI: 10.1109/HUMANOIDS47582.2021.9555770.

[48] Bin Fang, Quan Zhou, Fuchun Sun, Jianhua Shan, Ming Wang, Cheng Xiang, and Qin Zhang. "Gait Neural Network for Human-Exoskeleton Interaction." In: *Frontiers in Neurorobotics* 14 (2020). ISSN: 1662-5218. DOI: 10.3389/fnbot.2020.00058. URL: https://www.frontiersin.org/article/10.3389/fnbot.2020.00058.

[49] Roy Featherstone. *Rigid body dynamics algorithms*. Springer, 2014.

[50] Stefano Federici, Fabio Meloni, Marco Bracalenti, and Maria Laura De Filippis. "The effectiveness of powered, active lower limb exoskeletons in neurorehabilitation: A systematic review." In: *NeuroRehabilitation* 37.3 (2015). ISSN: 1053-8135URL = https://doi.org/10.3233/NRE-151265. DOI: 10.3233/nre-151265.

[51] Martin L. Felis. "RBDL: an efficient rigid-body dynamics library using recursive algorithms." In: *Autonomous Robots* (2016), pp. 1–17. ISSN: 1573-7527. DOI: 10.1007/s10514-016-9574-0. URL: http://dx.doi.org/10.1007/s10514-016-9574-0.

[52] Martin Felis. "RBDL: an efficient rigid-body dynamics library using recursive algorithms." In: *Autonomous Robots* 41 (Feb. 2017), pp. 495–511. DOI: 10.1007/s10514-016-9574-0.

[53] Larry Forrester, Anindo Roy, Ronald Goodman, Jeremy Rietschel, Joseph Barton, Hermano Krebs, and Richard Macko. "Clinical application of a modular ankle robot for stroke rehabilitation." In: *NeuroRehabilitation* 33 (June 2013). DOI: 10.3233/NRE-130931.

[54] *GOGOA: Belk system exoskeleton*. https://www.belkproject.eu/product. [Accessed: 2021-10-21].

[55] Jaime Gallardo-Alvarado, Ramon Rodriguez-Castro, Luciano Perez-Gonzalez, and Carlos R. Aguilar-Najera. "Kinematics of the 3(RPSP)-S Fully Spherical Parallel Manipulator by Means of Screw Theory." In: *Robotics* 7.2 (2018). DOI: 10.3390/robotics7020029.

[56] José de Gea Fernández and Frank Kirchner. "Predictive compliance for interaction control of robot manipulators." In: *2011 IEEE/RSJ International Conference on Intelligent Robots and Systems*. 2011, pp. 4134–4140. DOI: 10.1109/IROS.2011.6094476.

[57] David Gealy et al. "Quasi-Direct Drive for Low-Cost Compliant Robotic Manipulation." In: May 2019, pp. 437–443. DOI: 10.1109/ICRA.2019.8794236.

[58] *Global status report on road safety*. https://www.who.int/violence_injury_prevention/road_safety_status/2018/en/. [Accessed: 2020-06-17]. 2018.

[59] noonee germany GmbH. *German Noonee (Chairless chair)*. http://www.sechang-kr.com/download/5_noonee_en.pdf. [Accessed: 2021-12-30]. 2017.

[60] Anthony Goo, Curt A. Laubscher, Ryan J. Farris, and Jerzy T. Sawicki. "Design and Evaluation of a Pediatric Lower-Limb Exoskeleton Joint Actuator." In: *Actuators* 9.4 (2020). ISSN: 2076-0825. DOI: 10.3390/act9040138. URL: https://www.mdpi.com/2076-0825/9/4/138.

[61] Ashraf Gorgey. "Robotic exoskeletons: The current pros and cons." In: *World Journal of Orthopedics* 9 (Sept. 2018), pp. 112–119. DOI: 10.5312/wjo.v9.i9.112.

[62] Clément Gosselin, Éric St.-Pierre, and J. A. Martin Gagné. "On the development of the Agile Eye." In: *IEEE Robotics Autom. Mag.* 3.4 (1996), pp. 29–37. DOI: 10.1109/100.556480.

[63] C Grefkes and GR Fink. "Recovery from stroke: current concepts and future perspectives." In: *Neurological research and practice* 2 (2020), p. 17. DOI: 10.1186/s42466-020-00060-6.

[64] Mélanie Gréaux, Maria Moro, Kaloyan Kamenov, Amy Russell, Darryl Barrett, and Alarcos Cieza. "Health equity for persons with disabilities: a global scoping review on barriers and interventions in healthcare services." In: *International Journal for Equity in Health* 22 (Nov. 2023). DOI: 10.1186/s12939-023-02035-w.

[65] Qing Guo, Li Songjing, and Dan Jiang. "A Lower Extremity Exoskeleton: Human-Machine Coupled Modeling, Robust Control Design, Simulation, and Overload-Carrying Experiment." In: *Mathematical Problems in Engineering* 2015 (Sept. 2015), pp. 1–15. DOI: 10.1155/2015/905761.

[66] Thomas Gurriet, Sylvain Finet, Guilhem Boeris, Alexis Duburcq, Ayonga Hereid, Omar Harib, Matthieu Masselin, Jessy Grizzle, and Aaron D Ames. "Towards restoring locomotion for paraplegics: Realizing dynamically stable walking on exoskeletons." In: *2018 IEEE International Conference on Robotics and Automation (ICRA)*. IEEE. 2018, pp. 2804–2811. URL: http://ames.caltech.edu/exo-icra_2018.pdf.

[67] *HULC: Human Universal Load Carrier*. https://www.army-technology.com/projects/human-universal-load-carrier-hulc/. [Accessed: 2021-12-23].

[68] Omar Harib, Ayonga Hereid, Ayush Agrawal, Thomas Gurriet, Sylvain Finet, Guilhem Boeris, Alexis Duburcq, M Eva Mungai, Mattieu Masselin, Aaron D Ames, et al. "Feedback control of an exoskeleton for paraplegics: Toward robustly stable, hands-free dynamic walking." In: *IEEE Control Systems Magazine* 38.6 (2018), pp. 61–87.

[69] Omar Harib et al. "Feedback Control of an Exoskeleton for Paraplegics: Toward Robustly Stable, Hands-Free Dynamic Walking." In: *IEEE Control Systems* 38 (2018), pp. 61–87.

[70] H. He and K. Kiguchi. "A Study on EMG-Based Control of Exoskeleton Robots for Human Lower-limb Motion Assist." In: *2007 6th International Special Topic Conference on Information Technology Applications in Biomedicine*. 2007, pp. 292–295. DOI: 10.1109/ITAB.2007.4407405.

[71] A. Hemami, M. G. Mehrabi, and R. M. H. Cheng. "Synthesis of an Optimal Control Law for Path Tracking in Mobile Robots." In: *Automatica* 28.2 (1992), pp. 383–87. ISSN: 0005-1098. DOI: 10.1016/0005-1098(92)90123-W. URL: https://doi.org/10.1016/0005-1098(92)90123-W.

[72] Masato Hirose and Kenichi Ogawa. "Honda humanoid robots development." In: *Philosophical transactions. Series A, Mathematical, physical, and engineering sciences* 365 (Feb. 2007), pp. 11–9. DOI: 10.1098/rsta.2006.1917.

[73] A.L. Hof, M.G.J. Gazendam, and W.E. Sinke. "The condition for dynamic stability." In: *Journal of Biomechanics* 38.1 (2005), pp. 1–8. ISSN: 0021-9290. DOI: https://doi.org/10.1016/j.jbiomech.2004.03.025. URL: https://www.sciencedirect.com/science/article/pii/S0021929004001642.

[74] Britta Husemann, Friedemann Müller, Carmen Krewer, Silke Heller, and Eberhard Koenig. "Effects of Locomotion Training With Assistance of a Robot-Driven Gait Orthosis in Hemiparetic Patients After Stroke: A Randomized Controlled Pilot Study." In: *Stroke* 38 (2007), pp. 349–354. URL: https://api.semanticscholar.org/CorpusID:6647101.

[75] Oliver Jansen, Dennis Grasmuecke, Renate C. Meindl, Martin Tegenthoff, Peter Schwenkreis, Matthias Sczesny-Kaiser, Martin Wessling, Thomas A. Schildhauer, Christian Fisahn, and Mirko Aach. "Hybrid Assistive Limb Exoskeleton HAL in the Rehabilitation of Chronic Spinal Cord Injury: Proof of Concept; the Results in 21 Patients." In: *World Neurosurgery* 110 (2018), e73–e78. ISSN: 1878-8750. DOI: https://doi.org/10.

1016/j.wneu.2017.10.080. URL: https://www.sciencedirect.com/science/article/pii/S1878875017318089.

[76] Sylvain Joyeux. *Rock: the robot construction kit*. 2013.

[77] Jun-Young Jung, Wonho Heo, Hyundae Yang, and Hyunsub Park. "A Neural Network-Based Gait Phase Classification Method Using Sensors Equipped on Lower Limb Exoskeleton Robots." In: *Sensors* 15.11 (2015), pp. 27738–27759. ISSN: 1424-8220. DOI: 10.3390/s151127738. URL: https://www.mdpi.com/1424-8220/15/11/27738.

[78] S. Kajita, O. Matsumoto, and M. Saigo. "Real-time 3D walking pattern generation for a biped robot with telescopic legs." In: *Proceedings 2001 ICRA. IEEE International Conference on Robotics and Automation (Cat. No.01CH37164)*. Vol. 3. 2001, pp. 2299–2306. DOI: 10.1109/ROBOT.2001.932965.

[79] Peter Kampmann and Frank Kirchner. "Towards a fine-manipulation system with tactile feedback for deep-sea environments." In: *Robotics and Autonomous Systems* 67 (2015). Advances in Autonomous Underwater Robotics, pp. 115–121. ISSN: 0921-8890. DOI: https://doi.org/10.1016/j.robot.2014.09.033. URL: https://www.sciencedirect.com/science/article/pii/S0921889014002188.

[80] Jacques Kerdraon, Jean Gabriel Previnaire, Maegan Tucker, Pauline Coignard, Willy Allègre, Emmanuel Knappen, and A. Ames. "Evaluation of safety and performance of the self balancing walking system Atalante in patients with complete motor spinal cord injury." In: *Spinal Cord Series and Cases* 7 (2021). URL: https://api.semanticscholar.org/CorpusID:236920767.

[81] Yusuf M Khalid, Darwin Gouwanda, and Subramanian Parasuraman. "A review on the mechanical design elements of ankle rehabilitation robot." In: *Proceedings of the Institution of Mechanical Engineers, Part H: Journal of Engineering in Medicine* 229.6 (2015). PMID: 25979442, pp. 452–463. DOI: 10.1177/0954411915585597. eprint: https://doi.org/10.1177/0954411915585597. URL: https://doi.org/10.1177/0954411915585597.

[82] W Khalil and E Dombre. "Chapter 3 - Direct geometric model of serial robots." In: *Modeling, Identification and Control of Robots*. Ed. by W Khalil and E Dombre. Oxford: Butterworth-Heinemann, 2002, pp. 35–55. ISBN: 978-1-903996-66-9. DOI: https://doi.org/10.1016/B978-190399666-9/50003-8. URL: https://www.sciencedirect.com/science/article/pii/B9781903996669500038.

[83] W Khalil and E Dombre. "Chapter 9 - Dynamic modeling of serial robots." In: *Modeling, Identification and Control of Robots*. Ed. by W Khalil and E Dombre. Oxford: Butterworth-Heinemann, 2002, pp. 191–233. ISBN: 978-1-903996-66-9. DOI: https://doi.org/10.1016/B978-190399666-9/50009-9. URL: https://www.sciencedirect.com/science/article/pii/B9781903996669500099.

[84] Wisama Khalil and Etienne Dombre. *Modeling, identification and control of robots*. Jan. 2004.

[85] Maryam Khamar, Mehdi Edrisi, and Mohsen Zahiri. "Human-exoskeleton control simulation, kinetic and kinematic modeling and parameters extraction." In: *MethodsX* 6 (2019), pp. 1838–1846. ISSN: 2215-0161. DOI: https://doi.org/10.1016/j.mex.2019.08.014. URL: https://www.sciencedirect.com/science/article/pii/S2215016119302171.

[86] Jung-Hoon Kim, Jong Hyun Choi, and Baek-Kyu Cho. "Walking Pattern Generation for a Biped Walking Robot Using Convolution Sum." In: *Advanced Robotics* 25.9-10 (2011), pp. 1115–1137. DOI: 10.1163/016918611X574632.

[87] Jung-Hoon Kim, Jeong Woo Han, Deog Young Kim, and Yoon Su Baek. "Design of a Walking Assistance Lower Limb Exoskeleton for Paraplegic Patients and Hardware Validation Using CoP." In: *International Journal of Advanced Robotic Systems* 10.2 (2013), p. 113. DOI: 10.5772/55336.

[88] Su-Kyoung Kim, Elsa Kirchner, Arne Stefes, and Frank Kirchner. "Intrinsic interactive reinforcement learning – Using error-related potentials for real world human-robot interaction." In: *Scientific Reports* 7 (Dec. 2017). DOI: 10.1038/s41598-017-17682-7.

[89] Elsa A. Kirchner and Su Kyoung Kim. "Multi-Tasking and Choice of Training Data Influencing Parietal ERP Expression and Single-Trial Detection—Relevance for Neuroscience and Clinical Applications." In: *Frontiers in Neuroscience* 12 (2018). ISSN: 1662-453X. DOI: 10.3389/fnins.2018.00188. URL: https://www.frontiersin.org/article/10.3389/fnins.2018.00188.

[90] Elsa Andrea Kirchner, Jan Christian Albiez, Anett Seeland, Mathias Jordan, and Frank Kirchner. "Towards Assistive Robotics for Home Rehabilitation." In: *BIODEVICES*. 2013.

[91] Elsa Andrea Kirchner, Stephen Fairclough, and Frank Kirchner. "Embedded Multimodal Interfaces in Robotics: Applications, Future Trends, and Societal Implications." In: *The Handbook of Multimodal-Multisensor Interfaces*. Ed. by S. Oviatt, B. Schuller, P. Cohen, D. Sonntag, G. Potamianos, and A. Krueger. Vol. 3. Morgan & Claypool Publishers, 2019. Chap. 13, pp. 523–576. ISBN: e-book: 978-1-97000-173-0, hardcover: 978-1-97000-175-4, paperback: 978-1-97000-172-3, ePub: 978-1-97000-174-7.

[92] Elsa Andrea Kirchner, Su Kyoung Kim, Sirko Straube, Anett Seeland, Hendrik Wöhrle, Mario Michael Krell, Marc Tabie, and Manfred Fahle. "On the Applicability of Brain Reading for Predictive Human-Machine Interfaces in Robotics." In: *PLOS ONE* 8 (Dec. 2013), pp. 1–19. DOI: 10.1371/journal.pone.0081732. URL: https://doi.org/10.1371/journal.pone.0081732.

[93] Elsa Andrea Kirchner and Marc Tabie. "Closing the gap: combined EEG and EMG analysis for early movement prediction in exoskeleton based rehabilitation." In: *Proceedings of the 4th European Conference on Technically Assisted Rehabilitation-TAR 2013*. 2013.

[94] Elsa Andrea Kirchner, Marc Tabie, and Anett Seeland. "Multimodal Movement Prediction - Towards an Individual Assistance of Patients." In: *PLOS ONE* 9.1 (Jan. 2014), pp. 1–9. DOI: 10.1371/journal.pone.0085060. URL: https://doi.org/10.1371/journal.pone.0085060.

[95] Elsa Andrea Kirchner, Niels Will, Marc Simnofske, Luis Manuel Vaca Benitez, Bertold Bongardt, Mario Michael Krell, Shivesh Kumar, Martin Mallwitz, Anett Seeland, Marc Tabie, et al. "Recupera-Reha: Exoskeleton Technology with Integrated Biosignal Analysis for Sensorimotor Rehabilitation." In: 2016.

[96] Sebastien Kleff, Avadesh Meduri, Rohan Budhiraja, Nicolas Mansard, and Ludovic Righetti. "High-Frequency Nonlinear Model Predictive Control of a Manipulator." In: *2021 IEEE International Conference on Robotics and Automation (ICRA)*. 2021, pp. 7330–7336. DOI: 10.1109/ICRA48506.2021.9560990.

[97] Natasa Koceska, Saso Koceski, Francesco Durante, Pierluigi Beomonte Zobel, and Terenziano Raparelli. "Control Architecture of a 10 DOF Lower Limbs Exoskeleton for Gait Rehabilitation." In: *International Journal of Advanced Robotic Systems* 10.1 (2013), p. 68. DOI: 10.5772/55032. eprint: https://doi.org/10.5772/55032. URL: https://doi.org/10.5772/55032.

[98] Matthias Kreil, Georg Ogris, and Paul Lukowicz. "Muscle activity evaluation using force sensitive resistors." In: *2008 5th International Summer School and Symposium on Medical Devices and Biosensors*. 2008, pp. 107–110. DOI: 10.1109/ISSMDBS.2008.4575029.

[99] Scott Kuindersma, Robin Deits, Maurice Fallon, Andrés Valenzuela, Hongkai Dai, Frank Permenter, Twan Koolen, Pat Marion, and Russ Tedrake. "Optimization-based locomotion planning, estimation, and control design for the atlas humanoid robot." English. In: *Autonomous Robots* 40.3 (2016), pp. 429–455. ISSN: 0929-5593. DOI: 10.1007/s10514-015-9479-3.

[100] Rohit Kumar, Shivesh Kumar, Andreas Müller, and Frank Kirchner. "Modular and Hybrid Numerical-Analytical Approach - A Case Study on Improving Computational Efficiency for Series-Parallel Hybrid Robots." In: *2022 IEEE/RSJ International Conference on Intelligent Robots and Systems (IROS)*. 2022, pp. 3476–3483. DOI: 10.1109/IROS47612.2022.9981474.

[101] Shivesh Kumar. "Modular and Analytical Methods for Solving Kinematics and Dynamics of Series-Parallel Hybrid Robots." PhD thesis. Universität Bremen, 2019.

[102] Shivesh Kumar. "Modular and Analytical Methods for Solving Kinematics and Dynamics of Series-Parallel Hybrid Robots." PhD thesis. Jan. 2019.

[103] Shivesh Kumar, Bertold Bongardt, Marc Simnofske, and Frank Kirchner. "Task space controller for the novel Active Ankle mechanism." In: 2016. DOI: 10.13140/RG.2.2.30022.11845.

[104] Shivesh Kumar, Bertold Bongardt, Marc Simnofske, and Frank Kirchner. "Design and Kinematic Analysis of the Novel Almost Spherical Parallel Mechanism Active Ankle." In: *Journal of Intelligent & Robotic Systems* 94 (May 2019), pp. 303–325.

[105] Shivesh Kumar and Andreas Mueller. "An Analytical and Modular Software Workbench for Solving Kinematics and Dynamics of Series-Parallel Hybrid Robots." In: vol. 12. 2. Feb. 2020. DOI: 10.1115/1.4045941.

[106] Shivesh Kumar, Abhilash Nayak, Bertold Bongardt, Andreas Mueller, and Frank Kirchner. "Kinematic Analysis of Active Ankle Using Computational Algebraic Geometry." In: *Computational Kinematics*. Cham: Springer International Publishing, 2018, pp. 117–125.

[107] Shivesh Kumar, Valerie Renaudin, Yannick Aoustin, Eric Le-Carpentier, and Christophe Combettes. "Model-based and experimental analysis of the symmetry in human walking in different device carrying modes." In: *2016 6th IEEE International Conference on Biomedical Robotics and Biomechatronics (BioRob)*. 2016, pp. 1172–1179. DOI: 10.1109/BIOROB.2016.7523790.

[108] Shivesh Kumar, Marc Simnofske, Bertold Bongardt, Andreas Müller, and Frank Kirchner. "Integrating Mimic Joints into Dynamics Algorithms: Exemplified by the Hybrid Recupera Exoskeleton." In: New York, NY, USA: Association for Computing Machinery, 2017. ISBN: 9781450352949. DOI: 10.1145/3132446.3134891. URL: https://doi.org/10.1145/3132446.3134891.

[109] Shivesh Kumar, Kai Alexander von Szadkowski, Andreas Mueller, and Frank Kirchner. "An Analytical and Modular Software Workbench for Solving Kinematics and Dynamics of Series-Parallel Hybrid Robots." In: *Journal of Mechanisms and Robotics* 12.2 (Feb. 2020). 021114. ISSN: 1942-4302. DOI: 10.1115/1.4045941. eprint: https://asmedigitalcollection.asme.org/mechanismsrobotics/article-pdf/12/2/021114/6648769/jmr_12_2_021114.pdf. URL: https://doi.org/10.1115/1.4045941.

[110] Shivesh Kumar, Hendrik Woehrle, José Fernández, Andreas Mueller, and Frank Kirchner. "A Survey on Modularity and Distributivity in Series-Parallel Hybrid Robots." In: *Mechatronics* 68 (Apr. 2020). DOI: 10.1016/j.mechatronics.2020.102367.

[111] Shivesh Kumar, Hendrik Wöhrle, José de Gea Fernández, Andreas Müller, and Frank Kirchner. "A survey on modularity and distributivity in series-parallel hybrid robots." In: *Mechatronics* 68 (2020), p. 102367.

[112] Shivesh Kumar, Hendrik Wöhrle, Mathias Trampler, Marc Simnofske, Heiner Peters, Martin Mallwitz, Elsa Andrea Kirchner, and Frank Kirchner. "Modular Design and Decentralized Control of the Recupera Exoskeleton for Stroke Rehabilitation." In: *Applied Sciences* 9.4 (2019). ISSN: 2076-3417. DOI: 10.3390/app9040626. URL: https://www.mdpi.com/2076-3417/9/4/626.

[113] Arthur D. Kuo and J. Maxwell Donelan. "Dynamic Principles of Gait and Their Clinical Implications." In: *Physical Therapy* 90.2 (Feb. 2010), pp. 157–174. ISSN: 0031-9023. DOI: 10.2522/ptj.20090125. eprint: https://academic.oup.com/ptj/article-pdf/90/2/157/31643241/ptj0157.pdf. URL: https://doi.org/10.2522/ptj.20090125.

[114] Justin Lam. *Hyundai ChairlessExoskeleton (H-CEX)*. https:/www.trendhunter.com/trends/hcex. [Accessed: 2021-05-10]. 2018.

[115] Jeongseok Lee, Michael X. Grey, Sehoon Ha, Tobias Kunz, Sumit Jain, Yuting Ye, Siddhartha S. Srinivasa, Mike Stilman, and C. Karen Liu. "DART: Dynamic Animation and Robotics Toolkit." In: *Journal of Open Source Software* 3.22 (2018), p. 500. DOI: 10.21105/joss.00500. URL: https://doi.org/10.21105/joss.00500.

[116] *Legal requirements for medical devices in Europe: The new Medical Device Regulation (MDR)*. https://senetics.de/veranstaltungen/gesetzliche-vorgaben-fuer-medizinprodukte-in-der. [Accessed: 2020-09-15].

[117] Zhang Leiyu, Jianfeng Li, Mingjie Dong, Bin Fang, Ying Cui, Shiping Zuo, and Kai Zhang. "Design and Workspace Analysis of a Parallel Ankle Rehabilitation Robot (PARR)." In: *Journal of Healthcare Engineering* 2019 (Mar. 2019), pp. 1–10. DOI: 10.1155/2019/4164790.

[118] Johannes Lemburg, José de Gea Fernández, Markus Eich, Dennis Mronga, Peter Kampmann, Andreas Vogt, Achint Aggarwal, Yuping Shi, and Frank Kirchner. "AILA - design of an autonomous mobile dual-arm robot." In: *2011 IEEE International Conference on Robotics and Automation*. 2011, pp. 5147–5153. DOI: 10.1109/ICRA.2011.5979775.

[119] Chun-Ting Li, Yao-Te Peng, Yen-Ting Tseng, Yen-Nien Chen, and Kuen-Horng Tsai. "Comparing the effects of different dynamic sitting strategies in wheelchair seating on lumbar-pelvic angle." In: *BMC Musculoskeletal Disorders* 17 (Dec. 2016). DOI: 10.1186/s12891-016-1358-3.

[120] Yang Li, Cheng Xu, Xiaorong Guan, and Zhong Li. "Optimization of the control scheme for human extremity exoskeleton." In: *Journal of Vibroengineering* 18 (Dec. 2016), pp. 5432–5439. DOI: 10.21595/jve.2016.17397.

[121] Andreas Liampas, Panayiota Neophytou, Maria Sokratous, Giustino Varrassi, Christiana Ioannou, Georgios Hadjigeorgiou, and Panagiotis Zis. "Musculoskeletal Pain Due to Wheelchair Use: A Systematic Review and Meta-Analysis." In: *Pain and Therapy* 10 (Aug. 2021). DOI: 10.1007/s40122-021-00294-5.

[122] Chujun Liu, Musa L. Audu, Ronald J. Triolo, and Roger D. Quinn. "Neural Networks Trained via Reinforcement Learning Stabilize Walking of a Three-Dimensional Biped Model With Exoskeleton Applications." In: *Frontiers in Robotics and AI* 8 (2021). ISSN: 2296-9144. DOI: 10.3389/frobt.2021.710999. URL: https://www.frontiersin.org/article/10.3389/frobt.2021.710999.

[123] *Lockheed Martin Industrial: ONYX exoskeleton*. https://www.lockheedmartin.com/en-us/products/exoskeleton-technologies/first-responder.html. [Accessed: 2021-09-15].

[124] Sebastian Lohmeier, Thomas Buschmann, Heinz Ulbrich, and Friedrich Pfeiffer. "Modular Joint Design for Performance Enhanced Humanoid Robot LOLA." In: vol. 2006. Jan. 2006, pp. 88–93. DOI: 10.1109/ROBOT.2006.1641166.

[125] Chiara Lucarotti, Calogero Maria Oddo, Nicola Vitiello, and Maria Chiara Carrozza. "Synthetic and Bio-Artificial Tactile Sensing: A Review." In: *Sensors* 13.2 (2013), pp. 1435–1466. ISSN: 1424-8220. DOI: 10.3390/s130201435. URL: https://www.mdpi.com/1424-8220/13/2/1435.

[126] Shuzhen Luo, Ghaith Androwis, Sergei Adamovich, Hao Su, Erick Nunez, and Xianlian Zhou. "Reinforcement Learning and Control of a Lower Extremity Exoskeleton for Squat Assistance." In: *Frontiers in Robotics and AI* 8 (2021). ISSN: 2296-9144. DOI: 10.3389/frobt.2021.702845. URL: https://www.frontiersin.org/article/10.3389/frobt.2021.702845.

[127] Martin Mallwitz, Niels Will, Johannes Teiwes, and Elsa Andrea Kirchner. "THE CAPIO ACTIVE UPPER BODY EXOSKELETON AND ITS APPLICATION FOR TELEOPERATION." In: 2015.

[128] Matteo Malosio, Simone Negri, Nicola Pedrocchi, Federico Vicentini, Marco Caimmi, and Lorenzo Molinari Tosatti. "A spherical parallel 3 degrees-of-freedom robot for ankle-foot neuro-rehabilitation." In: *IEEE Engr. in Med. & Bio. Society Conf.* 2012 (2012), pp. 3356–3359.

[129] Nicolas Mansard. *Feasibility-prone Differential Dynamic Programming Is DDP a Multiple Shooting Algorithm?)* 2019. URL: https://gepgitlab.laas.fr/loco-3d/crocoddyl.

[130] Simnofske Marc, Kumar Shivesh, Bongardt Bertold, and Kirchner Frank. "Active Ankle - an Almost-Spherical Parallel Mechanism." In: *Proceedings of ISR 2016: 47st International Symposium on Robotics*. 2016, pp. 1–6.

[131] Lockheed Martin. *FORTIS® industrial exoskeleton*. https://www.lockheedmartin.com/en-us/products/exoskeleton-technologies/industrial.html. [Accessed: 2021-09-15]. 2018.

[132] Uriel Martinez-Hernandez, Sina Firouzy, Pouyan Mehryar, Lin Meng, Craig Childs, Arjan Buis, and Abbas A. Dehghani-Sanij. "Human-in-the-loop layered architecture for control of a wearable ankle–foot robot." In: *Robotics and Autonomous Systems* 161 (2023), p. 104353. ISSN: 0921-8890. DOI: https://doi.org/10.1016/j.robot.2022.104353. URL: https://www.sciencedirect.com/science/article/pii/S0921889022002421.

[133] Carlos Mastalli, Rohan Budhiraja, Wolfgang Merkt, Guilhem Saurel, Bilal Hammoud, Maximilien Naveau, Justin Carpentier, Ludovic Righetti, Sethu Vijayakumar, and Nicolas Mansard. "Crocoddyl: An Efficient and Versatile Framework for Multi-Contact Optimal Control." In: (2020).

[134] Takamitsu Matsubara, Akimasa Uchikata, and Jun Morimoto. "Full-body exoskeleton robot control for walking assistance by style-phase adaptive pattern generation." In: *2012 IEEE/RSJ International Conference on Intelligent Robots and Systems*. 2012, pp. 3914–3920. DOI: 10.1109/IROS.2012.6385528.

[135] Pauline Maurice et al. "Evaluation of PAEXO, a novel passive exoskeleton for overhead work." In: *Computer Methods in Biomechanics and Biomedical Engineering* 22 (Oct. 2019), S448–S450. DOI: 10.1080/10255842.2020.1714977.

[136] C. Meijneke et al. "Symbitron Exoskeleton: Design, Control, and Evaluation of a Modular Exoskeleton for Incomplete and Complete Spinal Cord Injured Individuals." In: *IEEE Transactions on Neural Systems and Rehabilitation Engineering* 29 (2021), pp. 330–339. DOI: 10.1109/TNSRE.2021.3049960.

[137] Qiaoling Meng, Bolei Kong, Qingxin Zeng, Cuizhi Fei, and Hongliu Yu. "Concept design of hybrid-actuated lower limb exoskeleton to reduce the metabolic cost of walking with heavy loads." In: *PLOS ONE* 18.5 (May 2023), pp. 1–19. DOI: 10.1371/journal.pone.0282800. URL: https://doi.org/10.1371/journal.pone.0282800.

[138] Y. Meng, Y. Wang, Q. Gu, and Guoxing Bai. "LQR-GA Path Tracking Control of Articulated Vehicle Based on Predictive Information." In: *Nongye Jixie Xuebao/Transactions of the Chinese Society for Agricultural Machinery* 49 (June 2018), pp. 375–384. DOI: 10.6041/j.issn.1000-1298.2018.06.045.

[139] Qing Miao, Mingming Zhang, Congzhe Wang, and Hongsheng Li. "Towards Optimal Platform-Based Robot Design for Ankle Rehabilitation: The State of the Art and Future Prospects." In: *Journal of Healthcare Engineering* 2018 (Mar. 2018), pp. 1–9. DOI: 10.1155/2018/1534247.

[140] Luis I. Minchala, Fabian Astudillo-Salinas, Kenneth Palacio-Baus, and Andrés Vázquez-Rodas. "Mechatronic Design of a Lower Limb Exoskeleton." In: 2017.

[141] Vukobratovic Miomir, Borovac Branislav, Surla Dusan, and Stokic Dragan. "Biped Locomotion." In: *Dynamics, Stability, Control and Application*. Vol. 7. 1. Springer, Berlin, Heidelberg, 1990. DOI: 10.1115/1.4024736. URL: https://doi.org/10.1007/978-3-642-83006-8.

[142] *Mitsubishi Heavy Industries: Power Assist Suit (PAS)*. https://www.mhi.com/news/1512011943.html. [Accessed: 2021-02-30]. 2018.

[143] Ralph S. Mosher. *Handyman to Hardiman, SAE Technical Paper 670088*. 1967. DOI: https://doi.org/10.4271/670088.

[144] Dennis Mronga, Shivesh Kumar, and Frank Kirchner. "Whole-Body Control of Series-Parallel Hybrid Robots." In: *2022 International Conference on Robotics and Automation (ICRA)*. 2022, pp. 228–234. DOI: 10.1109/ICRA46639.2022.9811616.

[145] Jiamin Mu, Hongzhou Jiang, Yuxiang Hua, Jie Zhao, and Yanhe Zhu. "Design and Implementation of a Lightweight Lower Extremity Exoskeleton." In: *MATEC Web of Conferences* 291 (Jan. 2019), p. 02010. DOI: 10.1051/matecconf/201929102010.

[146] Andreas Müller. "Dynamics of parallel manipulators with hybrid complex limbs — Modular modeling and parallel computing." In: *Mechanism and Machine Theory* 167 (2022), p. 104549. ISSN: 0094-114X. DOI: https://doi.org/10.1016/j.mechmachtheory.2021.104549. URL: https://www.sciencedirect.com/science/article/pii/S0094114X21002962.

[147] Sabrina M. Neuman, Twan Koolen, Jules Drean, Jason E. Miller, and Srinivas Devadas. "Benchmarking and Workload Analysis of Robot Dynamics Algorithms." In: *2019 IEEE/RSJ International Conference on Intelligent Robots and Systems (IROS)*. 2019, pp. 5235–5242. DOI: 10.1109/IROS40897.2019.8967694.

[148] Siobhan O'Connor. "Exoskeletons in Nursing and Healthcare: A Bionic Future." In: *Clinical Nursing Research* 30 (Aug. 2021). DOI: 10.1177/10547738211038365.

[149] Georg Ogris, Matthias Kreil, and Paul Lukowicz. "Using FSR based muscule activity monitoring to recognize manipulative arm gestures." In: *2007 11th IEEE International Symposium on Wearable Computers*. 2007, pp. 45–48. DOI: 10.1109/ISWC.2007.4373776.

[150] U. Onen, F. M. Botsal, M. Kalyoncu, Y. Sahin, and M. Tinkir. "Design and Motion Control of a Lower Limb Robotic Exoskeleton." In: *Design, Control and Applications of Mechatronic Systems in Engineering*. 2017, pp. 135–152.

[151] Gelu Onose, Vladimir Cárdei, Stefan T. Cráciunoiu, Valeriu Avramescu, Ioan Opris, Mikhail A. Lebedev, and Marian Vladimir Constantinescu. "Mechatronic Wearable Exoskeletons for Bionic Bipedal Standing and Walking: A New Synthetic Approach." In: *Frontiers in Neuroscience* 10 (2016). DOI: 10.3389/fnins.2016.00343. URL: https://www.frontiersin.org/article/10.3389/fnins.2016.00343.

[152] World Health Organization. *Global report on health equity for persons with disabilities: executive summary*. World Health Organization, 2022. ISBN: 9789240063624. URL: https://books.google.de/books?id=7HwOEQAAQBAJ.

[153] *Ottobock Industrials: Passive Exoskeleton (PAEXO)*. https://paexo.com/?lang=en. [Accessed: 2021-05-15].

[154] H. Peters, P. Kampmann, and M. Simnofske. *Konstruktion eines zweibeinigen humanoiden roboters 2. VDI Fachkonferenz humanoide roboter*. 2017.

[155] *Phoenix SuitX: robotic exoskeleton help a paralyzed man walk*. https://www.youtube.com/watch?v=AYVZped_Qh4. [Accessed: 2020-06-30]. 2020.

[156] Minerva V. Pillai, Logan Van Engelhoven, and Homayoon Kazerooni. "Evaluation of a Lower Leg Support Exoskeleton on Floor and Below Hip Height Panel Work." In: *Human Factors* 62.3 (2020). PMID: 32150477, pp. 489–500. DOI: 10.1177/0018720820907752.

[157] *Pinocchio: A fast and flexible implementation of Rigid Body Dynamics algorithms and their analytical derivatives*. https://gepettoweb.laas.fr/doc/stack-of-tasks/pinocchio/master/doxygen-html/. [Accessed: 2021-12-12].

[158] R. R. Playter and M. H. Raibert. "Control Of A Biped Somersault In 3D." In: *Proceedings of the IEEE/RSJ International Conference on Intelligent Robots and Systems*. Vol. 1. 1992, pp. 582–589. DOI: 10.1109/IROS.1992.587396.

[159] year = 2008-month = mar day = 5 doi = 10.1002/9780470987667 language = English (US) isbn = 9780470512944 publisher = John Wiley and Sons Pons Jose L. *Wearable Robots: Biomechatronic Exoskeletons*.

[160] G.A. Pratt and M.M. Williamson. "Series elastic actuators." In: *Proceedings 1995 IEEE/RSJ International Conference on Intelligent Robots and Systems. Human Robot Interaction and Cooperative Robots*. Vol. 1. 1995, 399–406 vol.1. DOI: 10.1109/IROS.1995.525827.

[161] J. Pratt, P. Dilworth, and G. Pratt. "Virtual model control of a bipedal walking robot." In: *Proceedings of International Conference on Robotics and Automation*. Vol. 1. 1997, 193–198 vol.1. DOI: 10.1109/ROBOT.1997.620037.

[162] Jerry Pratt and Ben Krupp. "Design of a bipedal walking robot." In: *Unmanned Systems Technology X*. Ed. by Grant R. Gerhart, Douglas W. Gage, and Charles M. Shoemaker. Vol. 6962. International Society for Optics and Photonics. SPIE, 2008, pp. 480 –492. DOI: 10.1117/12.777973. URL: https://doi.org/10.1117/12.777973.

[163] Agustinus Purna Irawan, Didi Utama, Enru Affandi, Michael, and Herlambang Suteja. "Product design of chairless chair based on local components to provide support for active workers." In: *IOP Conference Series: Materials Science and Engineering* 508 (May 2019), p. 012054. DOI: 10.1088/1757-899X/508/1/012054.

[164] Carlos Pérez Díaz, Ignacio Muñoz Planelles, Daniel Martin Hernandez, Carlos Zuluaga, Ivan Torres-Rodriguez, Jordi Marsa, Daniel Sanz Merodio, and Miguel López Estévez. "Design and Experimental Characterisation of a Novel Quasi-Direct Drive Actuator for Highly Dynamic Robotic Applications." In: May 2024.

[165] *RBDyn: Rigid body dynamics*. https://jrl-umi3218.github.io/RBDyn/doxygen/HEAD/index.html. [Accessed: 2021-01-24].

[166] Marc H. Raibert, Jr H. Benjamin Brown, and Michael Chepponis. "Experiments in Balance with a 3D One-Legged Hopping Machine." In: *The International Journal of Robotics Research* 3.2 (1984), pp. 75–92. DOI: 10.1177/027836498400300207. eprint: https://doi.org/10.1177/027836498400300207. URL: https://doi.org/10.1177/027836498400300207.

[167] Fatemeh Rasouli and Kyle B. Reed. "Walking assistance using crutches: A state of the art review." In: *Journal of Biomechanics* 98 (2020), p. 109489. ISSN: 0021-9290. DOI: https://doi.org/10.1016/j.jbiomech.2019.109489. URL: https://www.sciencedirect.com/science/article/pii/S0021929019307390.

[168] *Raytheon XOS Exoskeleton: Second-Generation Robotics Suit*. https://www.army-technology.com/projects/raytheon-xos-2-exoskeleton-us/. [Accessed: 2020-06-30]. 2020.

[169] L. Righetti and Auke Jan Ijspeert. "Programmable central pattern generators: an application to biped locomotion control." In: *Proceedings 2006 IEEE International Conference on Robotics and Automation, 2006. ICRA 2006.* 2006, pp. 1585–1590. DOI: 10.1109/ROBOT.2006.1641933.

[170] *Robot Assisted Gait Training System: WalkBot*. http://walkbot.co.kr/. [Accessed: 2021-09-15].

[171] Baltej Singh Rupala, Ashish Singla, and Gurvinder S. Virk. "Lower Limb Exoskeletons: A Brief Review." In: *International Journal for Scientific Research and Development* (2016), pp. 18–24.

[172] *SDF (Simulation Description Format)*. http://sdformat.org/. [Accessed: 2021-11-15].

[173] *SIFAC 2020 Germany: Machine Learning meets Model-based Control*. https://www.ifac2020.org/program/workshops/machine-learning-meets-model-based-control/.

[174] Tariq Samad. "Human-in-the-Loop Control: Applications and Categorization." In: *IFAC-PapersOnLine* 53.5 (2020). 3rd IFAC Workshop on Cyber-Physical & Human Systems CPHS 2020, pp. 311–317. ISSN: 2405-8963. DOI: https://doi.org/10.1016/j.ifacol.2021.04.108. URL: https://www.sciencedirect.com/science/article/pii/S2405896321002093.

[175] Yoshiyuki Sankai. "Leading Edge of Cybernics: Robot Suit HAL." In: *2006 SICE-ICASE International Joint Conference*. 2006, pp. 1–2. DOI: 10.1109/SICE.2006.314982.

[176] *Sarcos Robotics: Guardian XO Alpha prototype powered exoskeleton*. https://www.bing.com/videos/search?q=Guardian+XO+Alpha-+&&view=detail&mid=A93D9225F2B5FE64660AA93D9225F2B5FE64660A&&FORM=VDRVSR. [Accessed: 2020-12-10]. 2019.

[177] Matthias Sczesny-Kaiser, Rebecca Kowalewski, Thomas Schildhauer, Mirko Aach, Oliver Jansen, Dennis Grasmücke, Anne-K Güttsches, Matthias Vorgerd, and Martin Tegenthoff. "Treadmill Training with HAL Exoskeleton—A Novel Approach for Symptomatic Therapy in Patients with Limb-Girdle Muscular Dystrophy—Preliminary Study." In: *Frontiers in Neuroscience* 11 (Aug. 2017). DOI: 10.3389/fnins.2017.00449.

[178] Anett Seeland, Marc Tabie, Su Kyoung Kim, Frank Kirchner, and Elsa Andrea Kirchner. "Adaptive multimodal biosignal control for exoskeleton supported stroke rehabilitation." In: *2017 IEEE International Conference on Systems, Man, and Cybernetics (SMC)*. 2017, pp. 2431–2436. DOI: 10.1109/SMC.2017.8122987.

[179] Émélie Séguin and Marc Doumit. "Review and Assessment of Walking Assist Exoskeleton Knee Joints." In: *2020 IEEE International Conference on Systems, Man, and Cybernetics (SMC)*. 2020, pp. 1230–1235. DOI: 10.1109/SMC42975.2020.9283152.

[180] A. Seireg and J. Grundmann. "Design of a Multitask Exoskeletal Walking Device for Paraplegics." In: 1981.

[181] Anusha Sethuraman. *The Next Generation of AI: Explainable AI*. https://www.datanami.com/2020/01/29/the-next-generation-of-ai-explainable-ai/. [Accessed: 2021-12-17]. 2020.

[182] Ahmadreza Shahrokhshahi, Majid Khadiv, Ali Taherifar, Saeed Mansouri, Edward J. Park, and Siamak Arzanpour. "Sample-Efficient Policy Adaptation for Exoskeletons Under Variations in the Users and the Environment." In: *IEEE Robotics and Automation Letters* 7.4 (2022), pp. 9020–9027. DOI: 10.1109/LRA.2022.3187262.

[183] Di Shi, Wuxiang Zhang, Wei Zhang, and Xilun Ding. "A Review on Lower Limb Rehabilitation Exoskeleton Robots." In: *Chinese Journal of Mechanical Engineering* 32 (2019), pp. 1–11.

[184] Jonah Siekmann, Kevin Green, John Warila, Alan Fern, and Jonathan Hurst. *Blind Bipedal Stair Traversal via Sim-to-Real Reinforcement Learning*. 2021. eprint: 2105.08328.

[185] Vishram Singh. "Textbook of anatomy." In: *Textbook of Anatomy (Regional and Clinical) Abdomen and Lower Limb*. 2014.

[186] The Royal Society. *Explainable AI, The Royal Society, the basics Policy briefng Issue*. https://ec.europa.eu/futurium/en/system/files/ged/ai-and-interpretability-policy-briefing_creative_commons.pdf. [Accessed: 2021-07-11]. 2019.

[187] R. Arun Srivatsan, Sandipan Bandyopadhyay, and Ashitava Ghosal. "Analysis of the degrees-of-freedom of spatial parallel manipulators in regular and singular configurations." In: *Mechanism and Machine Theory* 69 (2013), pp. 127–141. ISSN: 0094-114X. DOI: https://doi.org/10.1016/j.mechmachtheory.2013.04.016. URL: https://www.sciencedirect.com/science/article/pii/S0094114X13000979.

[188] Olivier Stasse et al. "TALOS: A new humanoid research platform targeted for industrial applications." In: Nov. 2017, pp. 689–695. DOI: 10.1109/HUMANOIDS.2017.8246947.

[189] R. N. Stauffer and & Brewster-R. C. Chao E. Y. "Force and motion analysis of the normal, diseased, and prosthetic ankle joint." In: vol. 127. 1977, pp. 189–196.

[190] D. Stewart. "A Platform with Six Degrees of Freedom." In: *Proceedings of the Institution of Mechanical Engineers* 180.1 (1965), pp. 371–386. DOI: 10.1243/PIME_PROC_1965_180_029_02. eprint: https://doi.org/10.1243/PIME_PROC_1965_180_029_02.

[191] *SuitX: BoostX*. https://www.suitx.com/boostknee. [Accessed: 2021-09-15].

[192] *SuitX: LegX Exoskeleton*. https://www.suitx.com/legx. [Accessed: 2021-09-15].

[193] Nahla Tabti, Mohamad Kardofaki, Samer Alfayad, Yacine Chitour, Fathi Ben Ouezdou, and Eric Dychus. "A Brief Review of the Electronics, Control System Architecture, and Human Interface for Commercial Lower Limb Medical Exoskeletons Stabilized by Aid of Crutches." In: *2019 28th IEEE International Conference on Robot and Human Interactive Communication (RO-MAN)*. 2019, pp. 1–6. DOI: 10.1109/RO-MAN46459.2019.8956311.

[194] Jiaoyan Tang, Qunfei Zhao, and Jie Huang. "Application of "human-in-the-loop" control to a biped walking-chair robot." In: *2007 IEEE International Conference on Systems, Man and Cybernetics*. 2007, pp. 2431–2436. DOI: 10.1109/ICSMC.2007.4413944.

[195] *Technaid: Exo-H3*. https://www.technaid.com/products/robotic-exoskeleton-exo-exoesqueleto-h3/. [Accessed: 2021-09-15].

[196] Russ Tedrake. *Underactuated Robotics: Algorithms for Walking, Running, Swimming, Flying, and Manipulation (Course Notes for MIT 6.832)*. http://underactuated.mit.edu/. [Accessed: 2021-06-12]. 2021.

[197] Russ Tedrake and the Drake Development Team. *Drake: Model-based design and verification for robotics*. Accessed: 2021-08-05. 2019. URL: "https://www.orocos.org/rtt.

[198] *The ReWalk Personal 6.0 System*. https://youtu.be/gGTYXxc7aVA. [Accessed: 2021-07-09]. 2015.

[199] Dingkui Tian, Wentao Li, Jinke Li, Feng Li, Ziqiang Chen, Yong He, Jianquan Sun, and Xinyu Wu. "Self-Balancing Exoskeleton Robots Designed to Facilitate Multiple Rehabilitation Training Movements." In: *IEEE Transactions on Neural Systems and Rehabilitation Engineering* PP (Jan. 2024), pp. 1–1. DOI: 10.1109/TNSRE.2023.3348985.

[200] Ibrahim Tijjani. "Finding Optimal Placement of the Almost Spherical Parallel Mechanism in the Recupera-Reha Lower Extremity Exoskeleton for Enhanced Workspace." In: *Advances in Service and Industrial Robotics*. Ed. by Andreas Müller and Mathias Brandstötter. Cham: Springer International Publishing, 2022, pp. 536–544. ISBN: 978-3-031-04870-8.

[201] Ibrahim Tijjani, Shivesh Kumar, and Melya Boukheddimi. "A survey on design and control of lower extremity exoskeletons for bipedal walking." In: *Applied Sciences* 12.5 (2022), p. 2395.

[202] Matt Turek. *Explainable Artificial Intelligence (XAI), The U.S. Defense Advanced Research Projects Agency (DARPA). (link resides outside IBM)*. https://www.darpa.mil/program/explainable-artificial-intelligence. [Accessed: 2021-12-17].

[203] *UC Berkeley: BLEEX*. https://www.wevolver.com/wevolver.staff/bleex. [Accessed: 2021-07-11]. 2005.

[204] *Vanderbilt exoskeleton (Indego)*. https://news.vanderbilt.edu/2012/10/30/exoskeleton/. [Accessed: 2021-05-09].

[205] Jan F. Veneman, Rik Kruidhof, Edsko E. G. Hekman, Ralf Ekkelenkamp, Edwin H. F. Van Asseldonk, and Herman van der Kooij. "Design and Evaluation of the LOPES Exoskeleton Robot for Interactive Gait Rehabilitation." In: *IEEE Transactions on Neural Systems and Rehabilitation Engineering* 15.3 (2007), pp. 379–386. DOI: 10.1109/TNSRE.2007.903919.

[206] M. Vukobratovic, D. Hristic, and Z. Stojiljkovic. "Development of active anthropomorphic exoskeletons." In: *Medical and biological engineering* 12.1 (1974), pp. 66–80.

[207] *Walk Again: Paraplegic in robotic suit kicks off World Cup*. https://www.walkagainproject.organdhttps://www.google.com/search?q=WM+2014+by+a+patient+with+paraplegia. [Accessed: 2021-05-15]. 2014.

[208] Congzhe Wang, Yuefa Fang, Sheng Guo, and Yaqiong Chen. "Design and Kinematical Performance Analysis of a 3-RUS/RRR Redundantly Actuated Parallel Mechanism for Ankle Rehabilitation." In: *Journal of Mechanisms and Robotics* 5.4 (2013). DOI: 10.1115/1.4024736.

[209] Shiqian Wang et al. "Design and Control of the MINDWALKER Exoskeleton." In: *IEEE Transactions on Neural Systems and Rehabilitation Engineering* 23.2 (2015), pp. 277–286. DOI: 10.1109/TNSRE.2014.2365697.

[210] Michael F. Wehner, Brendan T. Quinlivan, Patrick M. Aubin, Ernesto C. Martinez-Villalpando, Michael Baumann, Leia A. Stirling, Kenneth G. Holt, Robert J. Wood, and Conor James Walsh. "A lightweight soft exosuit for gait assistance." In: *2013 IEEE International Conference on Robotics and Automation* (2013), pp. 3362–3369.

[211] Niels Will, Elsa Andrea Kirchner, and Frank Kirchner. "Künstliche Intelligenz und robotergestützte Rehabilitation." In: *Künstliche Intelligenz, Robotik und autonome Systeme in der Gesundheitsversorgung*. Ed. by Heinrich Hanika. Schriften zu Gesundheitsökonomie / Gesundheitsmanagement. Hrsg. Manfred Erbsland und Evelin Häusler. Wissenschaft & Praxis, 2019, pp. 101–128. ISBN: 978-3-89673-759-5.

[212] Hanseung Woo, Kyoungchul Kong, and Dong-Wook Rha. "Lower-Limb-Assisting Robotic Exoskeleton Reduces Energy Consumption in Healthy Young Persons during Stair Climbing." In: *Applied bionics and biomechanics* 2021 (Apr. 2021), p. 8833461. DOI: 10.1155/2021/8833461.

[213] Fitri Yakub and Yasuchika Mori. "Comparative study of autonomous path-following vehicle control via model predictive control and linear quadratic control." In: *Proceedings of the Institution of Mechanical Engineers Part D Journal of Automobile Engineering* 229 (Jan. 2015). DOI: 10.1177/0954407014566031.

[214] Tingfang Yan, Marco Cempini, Calogero Maria Oddo, and Nicola Vitiello. "Review of assistive strategies in powered lower-limb orthoses and exoskeletons." In: *Robotics and Autonomous Systems* 64 (2015), pp. 120–136. ISSN: 0921-8890. DOI: https://doi.org/10.1016/j.robot.2014.09.032. URL: https://www.sciencedirect.com/science/article/pii/S0921889014002176.

[215] Xiong Yang, Haotian She, Haojian Lu, Toshio Fukuda, and Yajing Shen. "State of the Art: Bipedal Robots for Lower Limb Rehabilitation." In: *Applied Sciences* 7.11 (2017). ISSN: 2076-3417. DOI: 10.3390/app7111182. URL: https://www.mdpi.com/2076-3417/7/11/1182.

[216] Ekrem Yavuz, Yavuz Senol, Merih Ozcelik, and Huseyin Aydin. "Design of a String-Encoder and IMU Based 6D Pose Measurement System." In: June 2019, pp. 1–6. DOI: 10.1109/ECAI46879.2019.9042021.

[217] Wei Ye and Qinchuan Li. "Type Synthesis of Lower Mobility Parallel Mechanisms: A Review." In: *Chinese Journal of Mechanical Engineering* 32 (Dec. 2019). DOI: 10.1186/s10033-019-0350-x.

[218] Lingzhou Yu, Harun Leto, and Shaoping Bai. "Design and Gait Control of an Active Lower Limb Exoskeleton for Walking Assistance." In: *Machines* 11.9 (2023). ISSN: 2075-1702. DOI: 10.3390/machines11090864. URL: https://www.mdpi.com/2075-1702/11/9/864.

[219] Shuangyue Yu, Tzu-Hao Huang, Xiaolong Yang, Chunhai Jiao, Jianfu Yang, Yue Chen, Jingang Yi, and Hao Su. "Quasi-Direct Drive Actuation for a Lightweight Hip Exoskeleton With High Backdrivability and High Bandwidth." In: *IEEE/ASME Transactions on Mechatronics* 25.4 (2020), pp. 1794–1802. DOI: 10.1109/TMECH.2020.2995134.

[220] Tochigi Yuki. "Effect of Arch Supports on Ankle—Subtalar Complex Instability: A Biomechanical Experimental Study." In: *Foot & Ankle International* 24.8 (2003), pp. 634–639. DOI: 10.1177/107110070302400811.

[221] Gabi Zeilig, Harold Weingarden, Manuel Zwecker, Israel Dudkiewicz, Ayala Bloch, and Alberto Esquenazi. "Safety and tolerance of the ReWalk™ exoskeleton suit for ambulation by people with complete spinal cord injury: A pilot study." In: *The Journal of Spinal Cord Medicine* 35.2 (2012). PMID: 22333043, pp. 96–101. DOI: 10.1179/2045772312Y.0000000003. eprint: https://doi.org/10.1179/

2045772312Y.0000000003. URL: https://doi.org/10.1179/2045772312Y.0000000003.

[222] Ting Zhang and He Huang. "Design and Control of a Series Elastic Actuator With Clutch for Hip Exoskeleton for Precise Assistive Magnitude and Timing Control and Improved Mechanical Safety." In: *IEEE/ASME Transactions on Mechatronics* 24.5 (2019), pp. 2215–2226. DOI: 10.1109/TMECH.2019.2932312.

[223] Jinman Zhou, Shuo Yang, and Qiang Xue. "Lower limb rehabilitation exoskeleton robot: A review." In: *Advances in Mechanical Engineering* 13.4 (2021), p. 16878140211011862. DOI: 10.1177/16878140211011862. eprint: https://doi.org/10.1177/16878140211011862. URL: https://doi.org/10.1177/16878140211011862.

[224] A.B. Zoss, H. Kazerooni, and A. Chu. "Biomechanical design of the Berkeley lower extremity exoskeleton (BLEEX)." In: *IEEE/ASME Transactions on Mechatronics* 11.2 (2006), pp. 128–138. DOI: 10.1109/TMECH.2006.871087.

[225] Adam Zoss and H. Kazerooni. "Design of an electrically actuated lower extremity exoskeleton." In: *Advanced Robotics* 20.9 (2006), pp. 967–988. DOI: 10.1163/156855306778394030.

[226] Shiping Zuo, Jianfeng Li, Mingjie Dong, Xiaodong Zhou, Wenpei Fan, and Yuan Kong. "Design and Performance Evaluation of a Novel Wearable Parallel Mechanism for Ankle Rehabilitation." In: *Frontiers in Neurorobotics* 14 (2020), p. 9. DOI: 10.3389/fnbot.2020.00009.